Expression von immunreaktiven NKG2DL in der gesunden und malignen Hämatopoese

Inauguraldissertation

zur

Erlangung der Würde eines Doktors der Philosophie

vorgelegt der

Philosophisch-Naturwissenschaftlichen Fakultät

der Universität Basel

von

Henrik Landerer

2024

Genehmigt von der Philosophisch-Naturwissenschaftlichen Fakultät

auf Antrag von

Erstbetreuerin:	Prof. Dr. Claudia Lengerke
Zweitbetreuer:	Prof. Dr. Markus Affolter
Externer Experte:	Prof. Dr. Klaus Schulze-Osthoff

Basel, den 27.02.2024

Prof. Dr. Marcel Mayor

Dekan der Philosophisch

Naturwissenschaftlichen Fakultät

Abbreviations

7-AAD	7-Aminoactinomycin
µl (unit)	Microliter
µM (unit)	Micromolar
A (amino acid)	Alanine
A (nucleobase)	Adenine
A (unit)	Area
ACK	Ammonium-chloride-potassium)
ADP	Adenosine diphosphate
AML	Acute myeloid leukemia
ALL	Acute lymphoid leukemia
Amp	Ampicillin
APC	Allophycocyanin
ATM	Ataxia-telangiectasia mutated
ATR	Ataxia telangiectasia and Rad3-related
BCL-2	B-cell lymphoma 2
BCR	Breakpoint cluster region
BRCA	Breast cancer gene
bp	Base pairs
BM	Bone marrow
BSA	Bovine serum albumin
BV	BrilliantViolet
C (nucleobase)	Cytosine
Cas	CRISPR-associated protein
Cas9	CRISPR-associated endonuclease 9
CBMC	Cord blood mononuclear cell
CD	Cluster of differentiation
CFU	Colony forming unit
CHK	Checkpoint kinases
CLL	Chronic lymphocytic leukemia
CLP	Common lymphoid progenitor
CML	Chronic myeloid leukemia
CMP	Common myeloid progenitor
CRISPR	Clustered regularly interspaced short palindromic repeats
CRK	CDK-related kinase
CSC	Cancer stem cell
COL	Cell of leukemia origin
ddH_2O	Double-distilled water
DAP10	DNAX activating protein 10
DAPI	4',6-Diamidino-2-phenylindol
DMSO	Dimethyl sulfoxide
DNA	Deoxyribonucleic acid
DNMT3	DNA methyltransferase 3 alpha
DPBS	Dulbecco's phosphate-buffered saline

DOT1L	Disruptor of telomeric silencing 1-like
DTT	Dithiothreitol
E. coli	Escherichia coli
e.g.	For example
EDTA	Ethylenediaminetetraacetic acid
eGFP	enhanced GFP
ELISA	Enzyme-linked immunosorbent assay
ELN	European Leukemia Net
ER	Endoplasmic reticulum
ERC	Endoplasmic reticulum-resident calcium-binding protein
F (unit)	Farad
FACS	Fluorescence-activated single cell sorting
FBS	Fetal bovine serum
FcR	Fc receptor
FCS	Fetal calf serum
Fiji	Fiji is just ImageJ
FISH	Fluorescence-in-situ-hybridization
FITC	Fluorescein
FLT-3	FMS-like receptor tyrosine kinase-3
FLT-3-L	FMS-like receptor tyrosine kinase-3 ligand
FP	Forward primer
G (nucleobase)	Guanine
GAPDH	Glycerinaldehyd-3-phosphat-Dehydrogenase
GATA2	GATA-binding factor 2
G-CSF	Granulocyte colony-stimulating factor
GFP	Green fluorescent protein
GMP	Granulocyte-macrophage progenitor
GPI	Glycophosphatidylinositol
Grb2	Receptor-bound protein 2
gRNA	Guide RNA
GS	Glycine-serine
h (unit)	Hour
h (species)	Human
HEPES	4-(2-hydroxyethyl)-1-piperazineethanesulfonic acid
HOXA9	Homeobox A9, is a protein-coding
HSC	Hematopoietic stem cell
HSF1	Heat shock transcription factor 1
HSP	Heat shock protein
HSPC	Hematopoietic stem and progenitor cell
Hsp	Heat shock protein
IC_{50}	Half maximal inhibitory concentration
i.e.	For example
IDH	Isocitrate dehydrogenase
IgG	immunoglobulin G
IL	Interleukin

IF	Immunofluorescence
IFN γ	Interferon γ
kb	Kilobase
KIRL	Killer Cell Immunoglobulin-like receptors ligands
KMT2A	Lysin-methyltransferase 2A
KMT2A-r	KMT2A-rearranged
KSHV	Kaposi's sarcoma-associated herpesvirus
l (unit)	Liter
LB	Lysogeny broth
LSC	leukemic stem cell(s)
M (unit)	Molar
m	Murine
MACS	Magnetic activated cell sorting
MAPK	Mitogen-Activated Protein Kinase
MEP	Megakaryocyte-erythroid progenitor
MHC	major histocompatibility complexM
MIC	MHC class I polypeptide-related sequence
min (unit)	Minute
ml (unit)	Milliliter
MLL	Mixed lineage leukemia/ myeloid lymphoid leukemia
MLL^C	C-terminal MLL
MLL^N	N-terminal MLL
MLLr	KMT2A-rearranged
MLLT1	MLLT1 super elongation complex subunit, ENL
MLLT3	MLLT3 super elongation complex subunit, AF9
MPP	Multipotent progenitor cells
MRC2	Mannose Receptor C Type 2
NAD	Nicotinamide adenine dinucleotide
NFkB	nuclear factor-kappa B
NP-40	Nonidet-40
ng (unit)	Nanogram
NGS	next generation sequencing
NK	Natural killer
NKG2DL	Natural killer group 2, member D ligands
NKG2DR	Natural killer group 2, member D receptor
NSD1	Nuclear receptor binding SET domain protein 1
NSG	NOD-Scid-Gamma
ORC	Origin recognition complex
pH	Pondus hydrogenii
P53	Tumor protein 53
PARP1	Poly (ADP-ribose) polymerase 1
PCR	Polymerase chain reaction
PE	Phycoerythrin
PerCP	Peridinin-Chlorophyll-Protein
pH	Potentia hydrogenii
PI3K	Phosphoinositide 3-kinase

POI	Protein of interest
PTD	Partial tandem duplication
qPCR	Quantitative polymerase chain reaction
RAF	Rapidly accelerated fibrosarcoma
RAS	Rat sarcoma
s	Soluable
sg	Safe guide
SCF	Stem cell factor
SDS-PAGE	Sodium dodecyl sulfate polyacrylamide gel electrophoresis
P/S	Penicillin-Streptomycin
PBMC	Peripheral blood mononuclear cells
PBS	Phosphate-buffered saline
PCR	Polymerase chain reaction
Pol	Polymerase
RBC	Red blood cell
RIPA	Radioimmunoprecipitation assay
RNA	Ribonucleic acid
ROI	Region of interest
RP	Reverse primer
RPMI medium	Roswell Park Memorial Institute medium
RT	Room temperature or real time
SCF	Stem cell factor
SD	Standard deviation
SDS	Sodium dodecyl sulfate polyacrylamide
sec (unit)	Second
sgRNA	Single guide RNA
siRNA	Small interfering RNA
SR-1	StemRegenin 1
T (nucleobase)	Thymine
t	Translocation
t(4;9)	MLL-AF4, Intron 9
t(4;11)	MLL-AF4, Intron 11
t(9;9)	MLL-AF9, Intron 9
t(9;11)	MLL-AF9, Intron 11
TAE	Tris-acetate-EDTA
TALEN	Transcription activator-like effector nuclease
TAP	Transporter associated with antigen processing
TBS	Tris-buffered saline
TE	Tris-EDTA
TEMED	Tetraacetylethylenediamine
TET2	Ten-Eleven Translocation 2
TP53	Tumor protein 53
TPO	Thyroperoxidase
TRIS	Tris(hydroxymethyl)-aminomethane
µg (unit)	µ gram

ULBP	UL16 binding proteins
UTR	Untranslated region
UV	Ultraviolet
V (unit)	Volt
w/v	Weight per volume
WT	Wild type
Y (amino acid)	Tyrosine
YINM	Tyrosine-based motif
ZF	Zink finger
ZFA	Zink-finger-nuclease

Summary

Natural killer group 2, member D ligands (NKG2DL) are known immunogenic molecules, whose cell surface presentation is absent in healthy cells but is induced following cellular stress or malignant transformation, thereby rendering cells susceptible to immune surveillance by NKG2D receptor (NKG2DR) expressing NK and cytotoxic T cells. Absence of NKG2DL on the cell surface enables immune evasion and is reported in various cancers including acute myeloid leukemia (AML), where our laboratory could previously show that reduced NKG2DL expression is a feature of leukemic stem cells (LSC). Here I aim to investigate the intracellular mechanisms inducing NKG2DL surface presentation in both malignant and healthy cells.

Using RT-qPCR, western blotting, ELISA, image, and conventional flow cytometry, I analyzed NKG2DL expression on mRNA and protein levels and determined the intracellular localization, surface presentation and shedding of NKG2DL in AML cells, healthy hematopoietic cells from cord blood (CB) or adult peripheral blood, as well as genetically modified CB HSPC expressing mixed lineage leukemia (MLL) fusion proteins.

I show for the first time that NKG2DL are expressed intracellularly with or without subsequent released into the extracellular fluids in malignant and healthy hematopoietic cells. Interestingly, similar levels of NKG2DL mRNA and protein were detected in healthy HSPC, MLL rearranged (MLLr) CB HSPC, and AML cell lines, indicating a mechanism controlling the intracellular retention of NKG2DL that could importantly contribute to the regulation of NKG2DL surface expression.

Surprisingly, when compared to MLL1 gene breakpoints at intron 9, breakpoint localization at intron 11 did not, or only partially allow NKG2DL surface presentation. Absence of NKG2DL in MLL-AF4 (Intron 11) subpopulations coincided with an increased clonogenic potential similar to previous reports in primary AML. Additionally, I show that current AML and potential future therapies (PARP1 and GATA2 inhibition) do not affect NKG2DL surface presentation in healthy cells while treatment with IFN γ increases NKG2DL cell surface expression of MLL-AF4 (Intron 11) cord blood derived cells.

Here, I present an approach to systematically characterize NKG2DL presentation in both healthy and malignant hematopoietic cells, showing for the first time that NKG2DL are robustly expressed in healthy hematopoietic cells, but retained intracellularly. Mechanisms regulating intracellular NKG2DL retention may enable rapid induction of NKG2DL surface expression and thereby immediate immune clearance of damaged cells. Crucially, an improved understanding of NKG2DL presentation and retention in these malignant cells could lead to novel strategies for targeting therapy resistant cancer cells such as AML LSC.

Table of Contents

Table of Tables

Table of Figures

List of publications, manuscripts in preparation and contributions

Publication:

Two Flow Cytometric Approaches of NKG2D Ligand Surface Detection to Distinguish Stem Cells from Bulk Subpopulations in Acute Myeloid Leukemia

Henrik Landerer[#], Marlon Arnone[#], Ronja Wieboldt, Elsa Goersch, Anna MP Stanger, Martina Konantz, Claudia Lengerke

J Vis Exp2021 Feb 21:(168). doi: 10.3791/61803.

Contribution: I designed the project, performed experiments, analyzed and interpreted data, generated tables, figures and assisted manuscript writing and filming of the video article

Manuscript in preparation:

Immunogenic NKG2DL are present in healthy hematopoietic cells and translocation of the MLL1 gene affects NKG2DL surface phenotypes

Henrik Landerer, Saskia Rudat, Rahel Fitzel, Estelle Erkner, Anna Maria Paczulla Stanger, Janine Schneider, Hildegard Keppeler, Corina Schneidawind Claudia Lengerke

Contribution: I contributed to the design of the project, performed experiments, analyzed and interpreted data, generated tables, figures and wrote the first version of the manuscript.

Introduction

Human hematopoiesis

Identification of human hematopoietic cell types

Scientific discoveries, such as antibiotics, anesthetics, or plastic, are often made during times of crisis or accidents. The study of human hematopoiesis was similarly boosted by an accident.

The concept of a long-lived hematopoietic stem cell population that can both self-renew and give rise to different, more differentiated blood cells was first postulated by the Russian biologist A. Maximow in 1908. Maximow proposed that hematopoiesis is organized as a cellular hierarchy derived from a common precursor, known as human hematopoietic stem cells (HSC). Stem cells were believed to have the potential to differentiate into all types of blood cells, encompassing all stages of development [1].

However, the first evidence supporting this theory came during the atomic era, when countless people were exposed to lethal radiation and died partly as a result of bone marrow (BM) failure. First observations showed that in some cases hematopoiesis could be restored by injecting spleen or marrow cells from healthy, unirradiated donors [2]. This confirmed a portion of A. Maximow's theory by demonstrating the existence of blood-forming progenitor cells. However, it did not provide clear evidence of a common precursor cell at the top of the human hematopoiesis hierarchy.

In 1961, canadian researchers at the University of Toronto were the first to functionally identify HSC. Inspired by the rescue of human hematopoiesis, they performed the first clonal *in vivo* repopulation assays by sub-lethally irradiating mice and consecutively transplanting human marrow cells. They observed a clonal repopulation of the – at the time assumed – three primary blood cell lineages: red blood cells, white blood cells, and platelets. This discovery demonstrated the existence of a common hematopoietic progenitor, leading to the first description of HSC [3, 4].

These findings established the basis for the current knowledge of human hematopoiesis and have over time been improved through *in vivo* repopulation assays, as well as the identification of selected cellular subpopulations by advancements in the fields of cell surface antibodies and flow cytometry. Together, these techniques have provided a baseline for today’s finely detailed view of the hierarchy of the human hematopoietic system [5].

Due to the technical difficulties of functional *in vitro* cultivation of hematopoietic cells and ethical barriers that prevent human *in vivo* experiments, our current understanding of human hematopoiesis was largely gained from *in vivo*

experiments using humanized mouse models. Through the use of xenotransplantation, *in vitro* clonal assays, and refined flow cytometry sorting strategies, a comprehensive understanding of human hematopoiesis has been developed [6-8].

The hierarchy of human hematopoiesis starts with the hematopoietic stem cell, which is identified by the cell surface presentation of the cluster of differentiation (CD) proteins CD34, a cell-cell adhesion factor involved in the attachment of HSC with the bone marrow matrix [9], CD49f [10], CD229 [11], as well as high surface levels of CD99 [12], and CD150 [13] and the absence of CD38, an ectoenzyme catalyzing the synthesis of adenosine diphosphate (ADP) and cyclic ADP-ribose from nicotinamide adenine dinucleotide (NAD+), and CD45RA [14]. This cell has the ability to self-renew and differentiate into all blood types, thus providing lifelong blood production. The process of differentiation begins within an HSC, progressing from a long-term HSC (LT-HSC) to a short-term HSC (ST-HSC), marked by a decrease in CD90 and CD150 expression, which results in a lower capacity for reconstitution and self-renewal. ST-HSC then differentiate into multipotent progenitor cells (MPPs), which lose expression of stemness markers CD49 and CD90 and are no longer capable of self-renewal [15]. MPPs have the ability to differentiate into different types of fully differentiated hematopoietic cell types. During the differentiation stage, the MPP can develop into both common lymphoid and myeloid progenitors (CLP [16] and CMP [17]), which acquire differentiation markers such as CD38 [18] and lineage markers (CD123 for myeloid and CD10 for lymphoid), thereby determining their respective lineages. As differentiation continues, cells develop further lineage marker signatures that define different cell types and differentiation stages.

The myeloid lineage comprises granulocytes, monocytes, macrophages derived from monocytes, erythrocytes, and megakaryocytes, while the lymphoid lineage produces lymphocytes, such as T cells, B cells, and natural killer (NK) cells. The CMP gives rise to two progenitors: the megakaryocyte-erythroid progenitor (MEP) and the granulocyte-macrophage progenitor (GMP) [16]. The MEP produces megakaryocytes, the precursors for platelets and red blood cells (RBCs), while the GMP produces granulocytes (neutrophils, eosinophils, and basophils), monocytes, and macrophages. These cells are involved in functions such as innate and adaptive immunity [17].

The common lymphoid progenitors (CLPs) give rise to B cells (marked by CD19 /20 expression [19, 20]), T cells (marked by CD3 expression and further divided into helper (CD4 positive) and cytotoxic (CD8 positive) T cells) [21] and NK cells (marked by absence of CD3 and presence of CD56) cells [22], which play crucial roles in both the adaptive and innate immune systems. Notably, both the CLPs and the common myeloid progenitors (CMPs) can give rise to monocytes and dendritic cells, with dendritic cells representing a special group of antigen-

presenting cells that play a key role in signaling between the innate and adaptive immune systems [16].

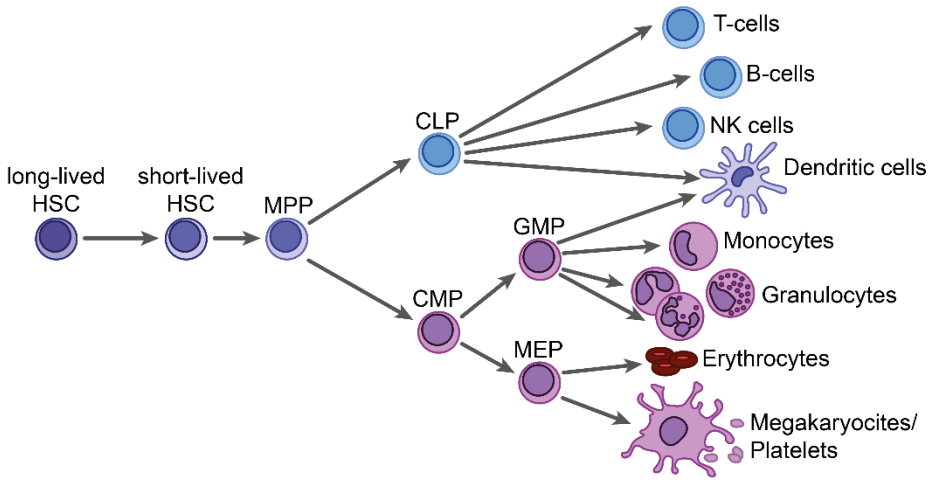

Figure 1 Schematic illustration of human hematopoiesis
The process begins with LT-HSC (dark blue) differentiating into ST-HSC and MPP successively. At this point, the lineage is committed, and cells differentiate into myeloid (violet) and lymphoid (light blue) progenitors before taking their final form. This Figure is adapted from [23]

Development of the immune system

The development of the human immune system is a complex and dynamic process that occurs from early prenatal life to adulthood. It involves a series of biological events that result in the establishment of a sophisticated and adaptable defense network. This process is crucial for individual survival and well-being, as it enables the body to recognize and respond to a variety of pathogens while maintaining tolerance to self-antigens [24].

The human immune system starts to develop during early embryogenesis through a process known as primitive hematopoiesis, or the first wave of hematopoiesis. This process involves the creation of erythroid and myeloid progenitor cells in the yolk sac [25]. The definitive hematopoiesis, also known as the second and third wave of hematopoiesis, involves the formation of erythroid-myeloid progenitors (second wave) and self-renewing HSC (third wave) from endothelial cells in the aorto-gonad-mesonephros region of the developing embryo [26]. During definitive hematopoiesis, the hematopoietic system develops alongside the embryo and transitions first to the fetal liver before finally settling in the bone marrow, which is the primary site of blood cell production throughout life [27].

The human immune system is composed of two closely intertwined branches: the innate and adaptive immune systems (Figure 2). At birth, the infant relies on the critical early protection provided by IgG antibodies that are transferred via the placenta or mother milk. At this point, the immune system, both innate and

adaptive, is relatively immature and undergoes significant maturation through exposure to pathogens, which allows for the acquisition of memory [28]. The first major exposure to various pathogens occurs at birth, as the infant travels through the birth canal and interacts with intestinal commensal bacteria. From this point onward the newborn is then continuously exposed to pathogens, which initiates the maturation and adaptation of the immune system [29]. The development of the human immune system into a more adaptive and responsive state is a lifelong process that is influenced by a complex interplay of genetic background and environmental factors, particularly in the early years of human life. Yet, at some point immune function begins to decline, with advanced age resulting in reduced pathogen recognition, antigen presentation, and immune cell function, which can ultimately lead to death through e.g., infections or cancer [24].

The innate immune system, also known as the nonspecific immune system, is comprised of granulocytes, monocytes, macrophages, dendritic and NK cells and serves as the body's initial defense against pathogens [30]. Upon detection of an infection or invasion of pathogens, pathogen-associated molecular patterns are recognized by immune cells such as macrophages or dendritic cells [31]. These cells then release cytokines, such as interferons and interleukins, to coordinate the immune response by initiating the proliferation of immune cells and mobilizing the adaptive immune system [32]. The adaptive immune system is slower to respond during first exposure to specific pathogens, but is the more specific component of our immune system. It complements the innate immune system by clearing pathogens or infections that cannot be controlled and cleared by the innate immune response. The adaptive immune system targets the specific type of pathogen causing the infection. It first identifies the pathogen by distinguishing between self and non-self-antigens and then adapts by generating pathogen-specific immunologic effector pathways to eliminate specific pathogens or pathogen-infected cells. Ultimately, this results in cellular memory of the pathogens for more efficient clearance during potential consecutive infections [33].

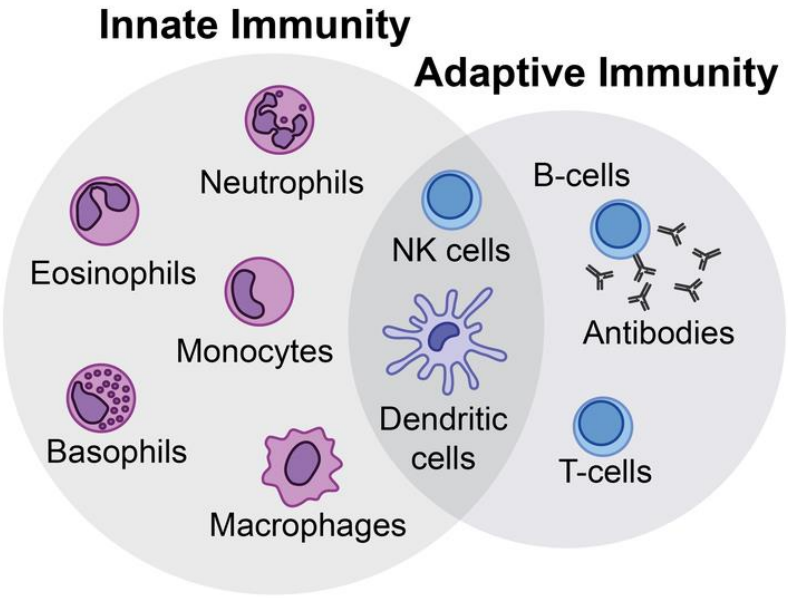

Figure 2 Basic schematic of the innate and adaptive immune systems.
The innate immune system (violet) consists of granulocytes (basophils, eosinophils, neutrophils), dendritic cells, macrophages, and NK cells. The adaptive immune system (blue) consists of B cells, NK cells, and T cells. This diagram was adapted from [34].

Leukemia

Cancer is a disease that is characterized by the uncontrolled growth and spread of abnormal cells in the body. Leukemia is a relatively rare type of cancer with a lifetime risk of approximately 1.6%. It is the seventh leading cause of cancer death, responsible for approximately 2.7 out of 100,000 deaths per year in the USA [35]. Leukemia is a condition characterized by the rapid production and accumulation of abnormal blood cells affecting hematopoietic tissues, such as the BM or lymphatic system, ultimately interfering with the production and function of normal, essential blood cells. Consequently, symptoms of this disease are a higher risk of infections, anemia and insufficient oxygen transport resulting in fatigue, and reduced healing due to interference with blood clotting [36].

There are various forms of leukemia, which can be broadly grouped by their progression speed into acute or chronic and by lineage into myeloid or lymphoid in origin. The most common forms of leukemia include acute myeloid leukemia (AML), acute lymphocytic leukemia (ALL), chronic lymphocytic leukemia (CLL), chronic myeloid leukemia (CML), and a special form of leukemia that can have both myeloid and lymphoid phenotypes, known as mixed lineage or myeloid lymphoid leukemia (MLL) [37]. The disease can occur in individuals of various ages but is most commonly found in either pediatric patients (ALL, MLL) or in the

elderly (AML, CLL, CML). Several risk factors have been identified for leukemia, including exposure to radiation, certain chemicals, and genetic factors. The most common treatments for leukemia are chemotherapy, targeted therapy, radiation therapy, stem cell transplantation, and immunotherapy. Treatment is highly dependent on the specific type of leukemia [38].

Acute myeloid leukemia (AML)

AML is the most common type of acute leukemia in adults. The occurrence of AML increases with age, and the current average age at diagnosis is 68 years. Treatment of AML is challenging and depends on the patient's age, overall health, and genetic characteristics of the disease [39].

At diagnosis, AML usually presents with various leukemic subclones within the patient, and specific recurrent genome mutations increasing proliferation or survival advantage in leukemic cells e.g., Fms-like tyrosine kinase 3 (FLT-3) [40], additional sex combs-like 1 (ASXL1) [41], tumor protein 53 (TP53) [42], protein tyrosine phosphatase, non-receptor type 11 (PTPN11) [43], neuroblastoma rat sarcoma (RAS) viral (v-ras) oncogene homolog (NRAS) [44], Kirsten rat sarcoma viral oncogene homolog (KRAS) [45], or impairing their differentiation e.g., runt-related transcription factor 1 (RUNX1) [46], CCAAT/enhancer binding protein α (CEBPA) [47], GATA-binding factor 2 (GATA2) [48], Ten-Eleven Translocation 2 (TET2) [49], and DNA methyltransferase 3 alpha (DNMT3A) [50]. These mutations play a significant role in the pathogenesis of AML and have implications for prognosis and treatment strategies. Mutations causing AML can result from genetic and chromosomal changes. They may be acquired through exposure to radiation or chemicals, but also randomly with increased frequency with age. Treatment sensitivity varies between cells of different genetic backgrounds, and thus molecular analyses can guide treatment decisions [51]. Since single patients may exhibit multiple clones of varying genetic backgrounds, targeted elimination of certain clones may leave others unaffected [52]. Thus, untargeted therapies affecting all leukemic cells (e.g., chemotherapy) remain an important treatment backbone.

The European Leukemia Net (ELN) classifies AML into favorable, intermediate, and adverse risk groups using molecular and cytogenic criteria. This classification is an essential tool for diagnosis, prognosis, and treatment decision-making in clinical practice and accurately reflects treatment outcomes. There is a significant difference in survival rates between young and elderly patients within the same ELN risk groups. This difference is likely due to patient-related factors such as ability to tolerate intensive treatments and higher overall co-morbidities but also to biologic differences in leukemic cells themselves occurring in young versus older individuals [53].

The World Health Organization (WHO) and International Consensus Classification (ICC) are further classification systems, which emphasize the integration of clinical, molecular/genetic, morphologic, and immunophenotypic parameters to provide evidence-based classification of AML, facilitating precision diagnosis and prognostication, and improving treatment. The ICC 2022 introduced a new major category of AML, AML with mutated TP53, and made changes to the blast count used to define AML, allowing patients previously diagnosed as high blast count myelodysplastic syndromes (MDS, 10-19 % blasts) to now be defined as low-blast count AML and access treatment approaches for this entity [54].

In addition to standard chemotherapy and allogenic hematopoietic stem cell transplantation, AML has evolved to include targeted therapies. These targeted therapies can be classified into Isocitrate dehydrogenase (IDH) inhibitors (vosidenib, enasidenib, and olutasidenib), FLT-3 inhibitors (gilteritinib, midostaurin, and quizartinib), B-cell lymphoma 2 (BCL-2) inhibitors (venetoclax), hypomethylating agents (azacitidine and decitabine) and CPX-351 (cytarabine and daunorubicin) [55].

IDH plays a crucial role in cellular metabolism by catalyzing the oxidative decarboxylation of isocitrate to produce alpha-ketoglutarate. This process involves the reduction of NAD(P)+ to NAD(P)H, which is essential for energy production [56]. In cancer, mutations can lead to the production of the oncometabolite D-2-hydroxglutarate. This oncometabolite contributes to tumorigenesis by affecting histone methylation, hypoxia signaling, DNA repair, and redox homeostasis [57]. FLT-3 is a crucial factor in hematopoiesis as it auto-phosphorylates signaling pathways, such as JAK/STAT, that regulate cell survival, proliferation, and differentiation of hematopoietic progenitors [58]. It is the most frequent (30%) genetic alteration in AML, and mutations can cause constitutive activation of the FLT-3, leading to uncontrolled cell proliferation and tumorigenesis [59]. Recently, the treatment of AML has made significant progress by inhibiting BCL-2 with venetoclax, achieving high response rates [60]. BCL-2 is an anti-apoptotic protein that shifts the balance of apoptosis by inactivating pro-apoptotic proteins BX and BAK, enabling cancer cell survival [61]. However, it has also been shown to play a role in healthy cells by affecting mitochondrial dynamics and calcium influx [62]. Hypomethylating agents act as inhibitors of DNA methyltransferase, inducing hypomethylation by incorporating into DNA/RNA of highly proliferating cells, such as cancer cells, and depleting DNMT1. This depletion allows for the re-expression of tumor suppressor genes [63]. CPX-351 is a dual drug liposomal encapsulation that enables the simultaneous delivery of cytarabine and daunorubicin at a fixed molecular ratio [64]. Cytarabine affects cells during the S-Phase of the cell cycle by disrupting the function of DNA polymerases, resulting in the inhibition of DNA replication and repair, and ultimately leading to cell death. Daunorubicin inhibits DNA and RNA synthesis by

intercalating between DNA base pairs, causing uncoiling of the DNA double helix and inhibiting topoisomerase II [65].

These therapies can achieve remission in around 60% of patients. Remission is characterized by the absence or minimal occurrence of AML blasts (<5%) in blood and BM [66]. However, relapse remains a significant concern in AML. The risk of relapse increases with age, with a mean relapse rate of approximately 45% [67]. Several factors, including age, pretreatment cytogenetics, molecular abnormalities, and the number of chemotherapy induction cycles, influence the risk of relapse. It is worth noting that relapse typically occurs within the first year after remission and risk decreases over time, with only 3% of cases of relapse occurring at 5 years post-remission [68].

Relapse in cancer is often associated with the cancer stem cell theory, which proposes that tumor initiation and relapse are both driven by so-called cancer stem cells (CSC) [69, 70]. These cells are believed to possess similar characteristics to healthy stem cells, especially the ability to self-renew and differentiate into various more mature cancer cells. In AML CSC are termed leukemia stem cells (LSC) [71]. LSC show enhanced resistance and are considered the cause of the commonly occurring relapses in AML [72].

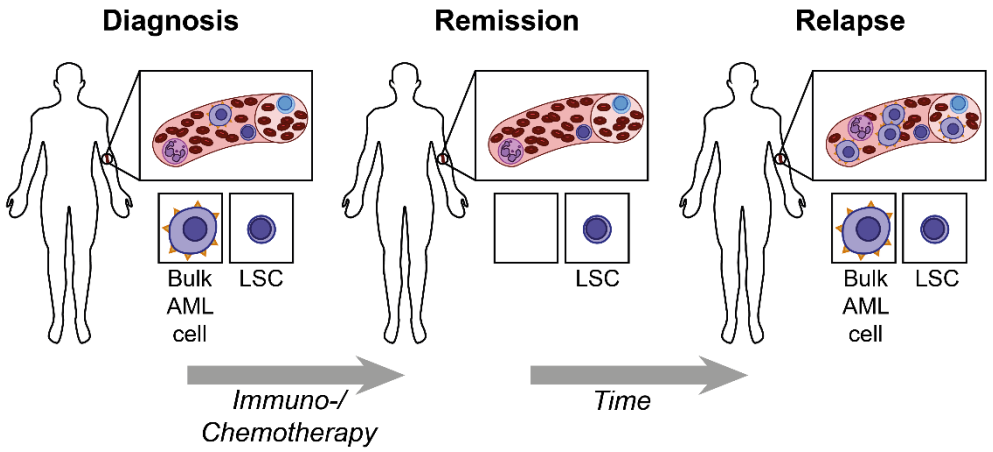

Figure 3 Illustration of AML disease progression
Patients diagnosed with AML are treated with immuno-/chemotherapy and reach remission, but relapse over time due to therapy resistant LSC.

LSC were defined by their ability to induce leukemia in immunosuppressed mice [73]. Our understanding of LSC biology, especially of the cell of origin in leukemia (COL), and of LSC-targeted treatment remains very poor. Two major theories to the emergence of LSC exist: (I) LSC to originate from an HSC that underwent malignant transformation and (II) LSC to originate from a progenitor cell, that regained stem like potential through mutations [74]. LSC biology is very heterogeneous between patients and while most reported evidence suggests that

AML originates from a transformed HSC other studies show indications of more complex scenarios where AML arises from a broader range of progenitor cells [75]. It is very conceivable that both scenarios can indeed exist in different patients.

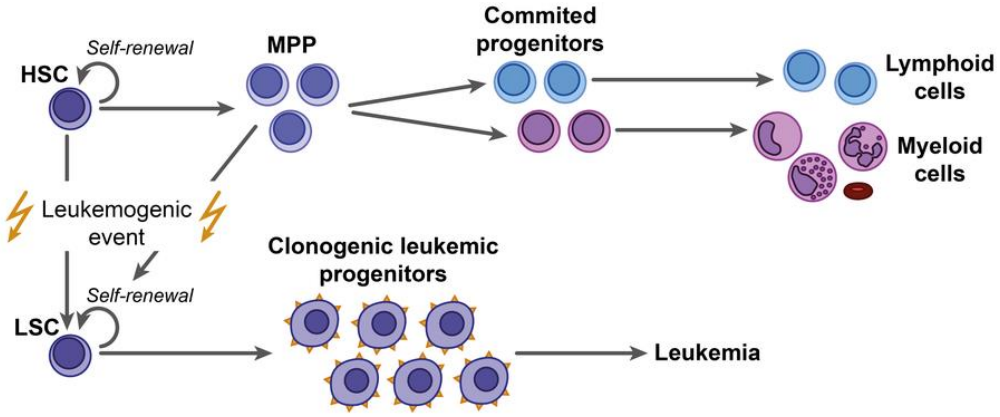

Figure 4 Schematic of the COL theory
HSC undergoes a leukemogenic event and transforms into an LSC, which differentiates into leukemic progenitors and initiates leukemia. This Figure was adapted from [76]

Identification of LSC

In theory, LSC can be identified functionally by their capacity to induce leukemia when injected into immunodeficient mice. However, this method is inefficient for diagnostic purposes due to the long incubation time in mice. Numerous studies have been conducted to identify LSC or other CSCs using alternative methods, such as cell identification via cell surface marker expression or metabolic signatures. Identifying LSC in AML is challenging due to the broad expression of LSC surface antigens on various mesenchymal and healthy hematopoietic stem and progenitor cells. Although flow cytometry has improved LSC identification, a definitive harmonized description of LSC is still unavailable. Currently, LSC are commonly identified using a panel of markers such as CD34, CD38, CD117, and GPR56 [75].

More recently, Paczulla *et al*. have identified a more functional LSC marker: the absence of natural killer group 2D ligands (NKG2DL). The absence of NKG2DLs was shown to identify subsets of leukemic cells with leukemia-initiation as well as chemotherapy resistance properties in AML [73].

Natural killer group 2D Ligands (NKG2DL)

The NKG2D receptor (NKG2DR) is a crucial activating receptor involved in immune recognition and elimination of abnormal cells by NK cells and T lymphocytes [77, 78]. It recognizes NKG2DL, which are stress-induced ligands upregulated by various forms of cellular stress, including viral infection, oxidative

damage, ionizing radiation, DNA damage and chromatin modulations and plays a vital role in cancer [79]. They are upregulated during excessive proliferation and have been associated with TP53 [80] (ataxia-telangiectasia mutated (ATM) [81]/ ataxia telangiectasia and Rad3-related (ATR) [82]) and Phosphoinositide 3-kinase (PI3K)/ Protein Kinase B (PKB) [83] and RAS/ rapidly accelerated fibrosarcoma (RAF) pathways [84]. NKG2DLs are self-molecules located at the cell surface similar to major histocompatibility complex (MHC) class-I that are biochemically highly diverse. The human genome encodes eight functional NKG2DL, which are separated into two subclasses. The MHC class I polypeptide-related sequence (MIC) family includes MICA and MICB, and the UL16 binding proteins (ULBP) family includes ULBP1-6 (also known as RAET1I, RAET1H, RAET1N, RAET1E, RAET1G, and RAET1L, respectively) [85].

In contrast, in mice, NKG2DL can be divided into three subgroups: five different isoforms of the Rae1 family (α-ε), three isoforms of H60 (a, b, and c), and MULT1. All NKG2DL are distant MHC class I-like molecules, but do not associate with β2 macroglobulin [86].

NKG2DLs exhibit significant polymorphism in humans, second only to major histocompatibility complex (MHC) molecules. This high polymorphism is primarily caused by genetic variations and adaptations during an individual's lifecycle. Currently, there are a total of 100 known alleles for MICA, while 40 alleles are known for MICB and only three variants are known for ULBP1 [87]. Several structurally diverse NKG2DL variants have been reported, but most of them share similarities with the structure of MHC class I proteins. MICA and MICB consist of three α domains, while all ULBP family proteins contain two α domains. The outer part of the molecule is formed by α1, which interacts with the NKG2DR. α2 binds peptides similar to MHC class I molecules, but it does not bind to peptides derived from intracellular proteins e.g., HLA-A2 for presentation to T cells. Finally, the α3 domain, which is exclusive to MICA and MICB, anchors the molecules to the cell membrane through a membrane-spanning domain. While the α1 and α2 domains are highly polymorphic, the α3 domain is highly conserved. In the absence of an α3 domain, some members of the ULBP family (ULBP 1/2/3/5/6) possess a transmembrane region that anchors ULBP to the cell membrane via a glycophosphatidylinositol (GPI) motif. ULBP4 and certain variants of ULBP2 and ULBP5 use a transmembrane domain for membrane anchoring, similar to proteins of the MIC family, instead of the GPI anchor [88]. The variability of NKG2DL variants is crucial in determining their expression levels, recognition by the immune system, and susceptibility to various diseases e.g., MICA007 has been linked to inflammatory diseases such as arthritis. Initially associated with viral infections, NKG2DL's high polymorphism is believed to be a result of adaptation to viral evolution. NKG2DLs are not typically present on the cell surface of healthy cells at a steady state [89]. However, NKG2DL surface expression has been reported in healthy cells in association with cellular stress during e.g.,

hyperproliferation, such as embryogenesis or wound healing [90]. Inflammation-induced NKG2DL surface expression has also been reported in otherwise healthy cells in autoimmune disease settings and has been shown to be upregulated in senescent cells [91] and in T cells during immune response [92]. However, in these cases, NKG2DL surface expression is not directly associated with cell clearance as ligands for inhibitory receptors on NK cells are still present on the NKG2DL-positive cell. Of note, NKG2DL-mediated killing via NK or CD8 T cells is a delicate balance of activating (NKG2DL) and inhibiting signals (NKG2A and Killer Cell Immunoglobulin-like receptors ligands (KIRL)). The activation state of an NK cell results from the balance of these signals, and activation can occur when inhibitory signaling is lost or when activating receptor signaling overwhelms inhibitory signaling [93].

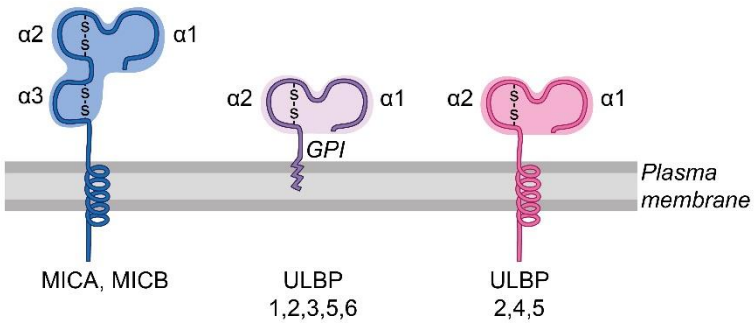

Figure 5 Schematic illustration of NKG2DL protein structures
MICA and MICB (blue) comprise of three α domains anchored to the cell by a transmembrane domain. ULBP1-6 comprise of 2 α domains. ULBP1,2,3,5,6 (violet) are anchored to the cell membrane through a GPI motif, whereas ULBP2,4,5 (magenta) are anchored through a transmembrane domain. Adapted from [94]

Regulation of NKG2DL expression

The regulation of NKG2DL is a complex process that involves transcriptional, post-transcriptional, and post-translational mechanisms. While transcriptional induction and presentation of NKG2DL are well-characterized, intracellular mechanisms remain poorly understood.

NKG2DL mRNA transcription is activated by various types of stress, such as heat shock, DNA damage, activation of p53, hyperproliferation during early tumorigenesis through activation of E2F transcription factors by entry into the cell cycle, and PI3K by enhancing proliferation and infections [83, 90]. In addition to heat shock, the heat shock pathway and heat shock proteins (HSP) are upregulated in various cellular conditions, including cell quiescence in overly confluent cells, infections, and cancer cells. This upregulation has been shown to increase the expression of MICA and MICB through direct activation of the heat shock transcription factor 1 (HSF1) or downstream effects of inhibiting apoptotic signaling [95]. Upregulation of NKG2DL mRNA through DNA damage is

associated with the ATR and ATM pathways detecting collapsed replication forks and resulting DNA breaks. These pathways initiate a protein kinase cascade with downstream targets, such as checkpoint kinases 1 and 2 (CHK1 and CHK2) and TP53. This upregulation of NKG2DL mRNA leads to its presentation on the cell surface [82]. NKG2DL is observed to be upregulated on mRNA levels and presented on the cell surface through hyperproliferation in both healthy and malignant cells during wound healing or early tumorigenesis. Hyperproliferation is often associated with DNA damage and activation of p53. However, cell cycle entry also requires the activation of E2F transcription factors, which are associated with upregulation of NKG2DL mRNA. In addition, infections such as CMV have been shown to induce degradation of MICA mRNA via microRNA, thereby reducing susceptibility to the immune response, while initiating presentation of MICB and ULBP1 on the cell surface [96, 97].

Regulation of NKG2DL on the protein level is not well understood. However, regulators for specific NKG2DL have been reported. MICA and MICB are presented on the cell surface of a T cell leukemia cell line through N-linked glycosylation [98]. Meanwhile, MULT1 is susceptible to degradation through ubiquitylation or MARCH4 and MARCH9, as demonstrated in [99].

Paczulla *et al*. recently showed that absence of NKG2DL can be a marker for LSC and identified 22 genes e.g., GPR56, mannose Receptor C Type 2 (MRC2) that were differently regulated in NKG2DL presenting populations compared to non-presenting populations. One of these genes, poly (ADP-ribose) polymerase 1 (PARP1) has been shown to repress NKG2DL in LSC and that repression can be reversed by chemical or genetic inhibition of PARP1 [73]. PARP1 is a chromatin-associated enzyme responsible for poly(ADP)ribosylation of various nuclear proteins and plays a crucial role in DNA damage repair, chromatin remodeling, and stabilization of DNA replication forks [100]. The clinical relevance of PARP1 is demonstrated by the approval of PARP1 inhibitors in the treatment of breast cancers that display the BRCA mutation. Cells with BRCA mutations are unable to repair DNA damage through homologous recombination, making them dependent on PARP1 for DNA damage repair. However, inhibiting PARP1 results in synthetic lethality, a genetic interaction where cells remain viable with the loss of individual gene function, but not with the loss of combinatory gene function [101].

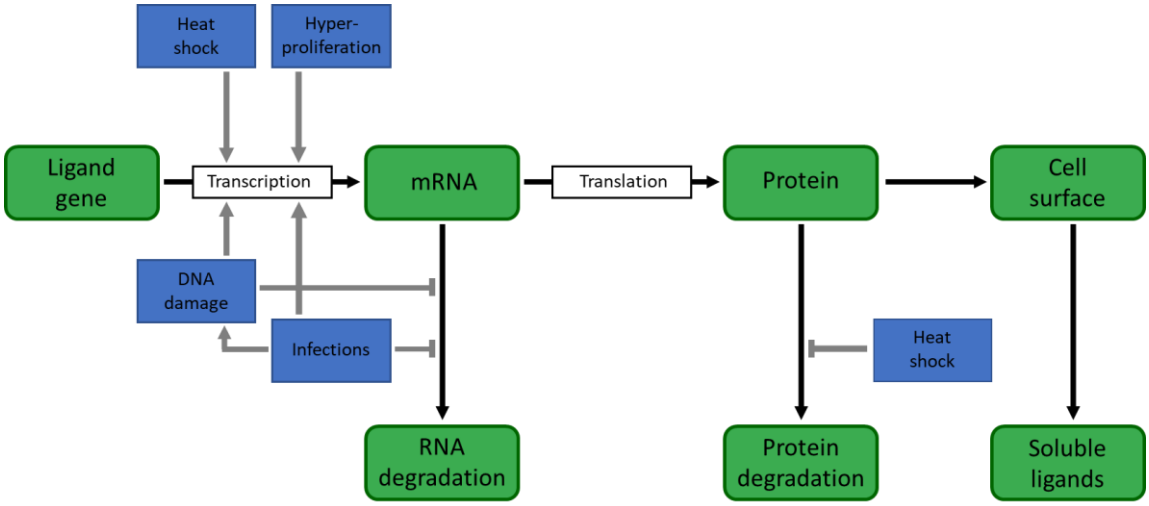

Figure 6 Schematic overview of NKG2DL regulation.

NKG2D receptor (NKG2DR) and NKG2DL/NKG2D-mediated cell killing

The NKG2DR is an activating immune receptor that belongs to the lectin-like type 2 transmembrane receptor family. It is encoded by the Klrk1 gene and is part of the NK gene complex on chromosome 12. NKG2DR is expressed on the cell surface of NK and cytotoxic (CD8) T cells [77]. There are two isoforms of NKG2D: NKG2D-long (NKG2D-L) and NKG2D-short (NKG2D-S), which are created by alternative splicing. Both isoforms can recognize and bind all reported NKG2DLs, including their variants, and activate NK and cytotoxic (CD8) T cells upon binding of NKG2DLs. Unlike T cells, in which NKG2DR acts as a co-stimulatory signal complementing the T cell receptor-induced cytotoxicity, it functions as an independent receptor in mature NK cells [102].

Upon recognition of NKG2DLs, NKG2DR forms a homodimer and associates with two transmembrane adaptors, DNAX activating protein 10 (DAP10) molecules, which contain a functional tyrosine-based motif (YINM). Ligand binding promotes the phosphorylation of the YINM domain, resulting in the recruitment and activation of the growth factor receptor-bound protein 2 (Grb2)/Vav1 complex, which activates the phosphatidylinositol-3-kinase (PI3K) to phosphorylate the YINM domain. The PI3K pathway results in the production of phosphatidylinositol 3,4,5-triphosphate (PIP3), which acts as a signaling molecule to activate downstream proteins, including nuclear factor-kappa B (NFkB) and Mitogen-activated protein kinase (MAPK). These proteins are involved in various cellular functions, such as cell survival, proliferation, and activation, ultimately leading to the activation of NK cell-mediated cell killing. The signaling cascades' precise details may vary between different cell types and can be influenced by the immune response's specific context [103].

When a virus-infected or cancerous cell is recognized by an NK cell through NKG2DL, an immunological synapse is formed between the NK cell and the target cell and apoptosis is induced through granule-mediated or death receptors mediated cytotoxicity [104]. The formation of the immunological synapse leads to the targeted release of lytic granules from the NK cell to the target cell. Granzymes then enter the target cells via, perforin pores in the plasma membrane or endocytosis and perforin-assisted escape from endosomes. This results in the induction of mitochondrial dysfunction by cleavage of Bid, resulting in a truncated form tBid that relocates to mitochondria to interact with the apoptotic proteins Bax and/or Bak [105, 106], or by activation of caspase activation via proteolytic processing or caspase-independent apoptosis [107]. During initial killing events, NK cells almost exclusively use the granule-mediated pathway, resulting in rapid and efficient elimination of target cells [108]. However, final killing events are dominated by death receptors such as the Fas ligand or TRAIL, which are expressed on the surface of NK cells and activated by binding to their respective receptors (TRAIL R and FAS). Binding, similar to granule-mediated cytotoxicity, results in the induction of mitochondrial dysfunction, induction of caspase activation or caspase-independent activation, and ultimately initiation of apoptosis [109, 110].

The cells are killed and metabolized in a conserved manner, which prevents the release of harmful molecules, such as viruses or viral particles [111].

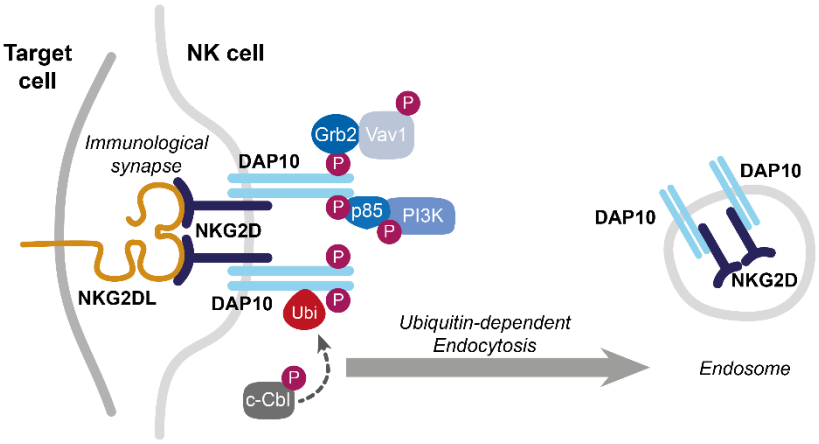

*Figure 7 Schematic of how NKG2DR (dark blue) recognizes NKG2DLs (orange) NKG2DLs are recognized by NKG2D, which causes DAP10 (light blue) to homo-dimerize. This, in turn, activates the PI3K and c-Cbl pathways, leading to the activation of the NK cell and the endosomal degradation of NKG2D. Adapted from **[112]**.*

NKG2D/NKG2DL-axis in cancer and evasion mechanisms

Malignant transformation often leads to the expression of NKG2DLs, which makes cancer cells susceptible to immune clearance. However, cancer cells frequently downregulate NKG2DLs through mechanisms such as shedding, transcriptional mutations, epigenetic silencing, and post-transcriptional inhibition via microRNA.

Shedding occurs when NKG2DLs are cleaved from the cell surface and released into the extracellular fluids through a complex process known as ectodomain shedding. This process is mediated by metalloproteases (adam9/10/17) in humans. The process starts with the substrate (NKG2DL) binding to the active site of the metalloprotease, followed by cleavage at a specific sequence [113].

Shedding is a mechanism primarily associated with the advanced stages of cancer progression and is predominantly used by tumor cells to evade the immune response [114]. The impaired immune recognition and escape from immune surveillance and elimination by cancer cells are caused by two factors: (I) the reduction of NKG2DL molecules at the cell surface [115] and (II) the binding, and thereby blocking, of sNKG2DL to the NKG2DR and its subsequent endocytosis [116]. While metalloproteases mediated shedding is the primary mechanism for the release of sNKG2DL, it can also be released through an alternative mechanism known as exosome release [117]. Cancer cells often use exosome release to funnel immunosuppressive molecules into the tumor microenvironment, promoting tumor evasion [118].

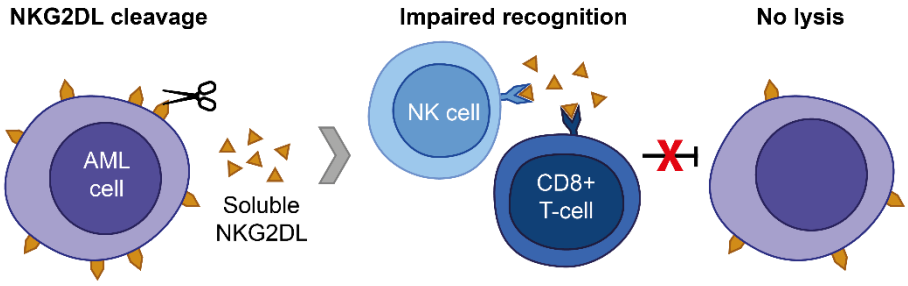

Figure 8 Schematic of NKG2DL shedding
Metalloproteases cleave NKG2DL (orange) from the cell surface, releasing them into extracellular fluids as sNKG2DL. sNKG2DL can bind to NKG2DR located at NK and CD8 T cells (blue), resulting in impaired recognition and reduction of NKG2DL at the surface of AML cells.

Although controlled recognition of NKG2DLs represents a danger signal sufficient to activated NK cell mediated damaged cell killing chronic exposure, e.g., through high levels of shedded soluble NKG2DLs by cancer cells, which leads to activation of the ubiquitin ligase c-Cbl, which promotes DAP10 ubiquitination resulting in NKG2DR internalization and lysosomal degradation and thereby hyporesponsiveness towards NKG2DL recognition [116].

Mixed lineage leukemia (MLL)

MLL is a group of aggressive leukemias that can initiate acute leukemia of both the lymphoid and myeloid lineages and mainly affects pediatric patients. The disease is characterized by the rearrangement of the mixed lineage leukemia 1 (MLL1) gene, also commonly known as lysine (K)-specific methyltransferase 2 (KMT2A) [119]. MLL1 is a histone methyltransferase that regulates Histone H3 Lysine 4 (H3K4) and plays a key role in gene transcription during embryonic development, especially for Hox genes. The MLL1 gene is a large protein consisting of 3969 amino acid residues and several conserved domains. The protein is post-translationally cleaved into two fragments, MLL-C and MLL-N, and their association is necessary for full activity [120]. MLL is caused by a double-strand break at the breakpoint in the MLL-N fragment, specifically in the breakpoint cluster (BCR) region spanning from intron 8 to 13 [121, 122].

There are currently 82 known MLL fusion patterns. The most common patterns are MLL- ALL-1-fused gene from chromosome (AF) 4, MLL-AF9, MLL- Eleven-Nineteen Leukemia (ENL), and MLL-AF10, which account for 92% of MLL cases [123].

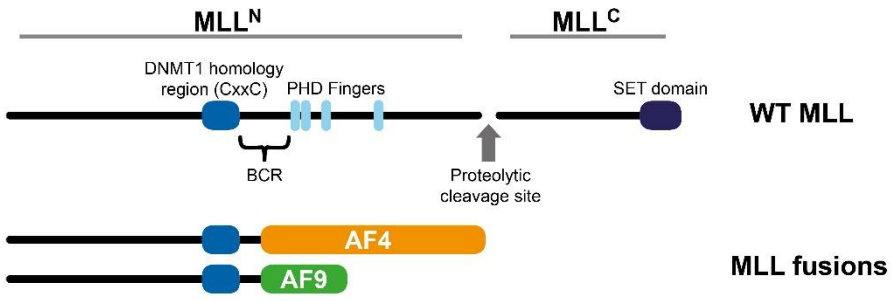

Figure 9 Schematic of the MLL1 gene and MLL fusion proteins AF4 and AF9
MLL1 is composed of two fragments, MLL-C and MLL-N, each with key domains (DNMT1, BCR, PhD, SET) illustrated. Breakpoints can occur at the BCR, resulting in the recruitment of common fusion partners such as AF4 and AF9 to form an MLL fusion protein. This information was adapted from [119].

Gene fusion can occur at any of the BCR spanning regions, but breakpoint hotspots are known to predominantly occur at intron 9 and intron 11, which have a direct impact on the clinical implication. While both breakpoint hotspots have a very poor disease prognosis, intron 11 MLLs presents a more aggressive phenotype resulting in an average lifespan of only 12 months in patients [122]. Disease progression, especially in lineage commitment, is also affected by the MLL fusion partners, with fusion partners AF4 and AF9 playing central roles. MLL-AF4 fusions are the most occurring (34% of cases) fusion partners for ALL-like MLLs. In contrast fusions of MLL-AF9 have been associated primarily with an AML-like phenotype (33%) but are also the 3rd most occurring fusion partner for an ALL-like phenotype (18%) [124, 125].

The rearrangement of the MLL1 gene not only creates a novel fusion protein but also directly affects its function in terms of complex formation and downstream signaling pathways. MLL fusion genes have an increased interactome and can recruit proteins such as positive transcription elongation factor (P-TEFb) [126], nuclear factor kappa B subunit 1 (NFkB1) [127], disruptor of telomeric silencing 1-like (DOT1L) histone lysine methyltransferase [128], and nuclear receptor binding SET domain protein 1 (NSD1) [129]. These new partners share the ability to directly bind and activate RNA polymerase II (RNAPII) [130], resulting in transcriptional activity. Furthermore, histone methyltransferases (DOT1L, NSD1) interact with the SET domain of the MLL fusion protein, leading to an altered methylation pattern. This activation of silent chromatin regions halts differentiation, expresses stem cell genes, and creates an oncological potential that initiates leukemia [131].

Furthermore, MLL fusion genes bind to transcriptional genes forming heterodimeric transcription factor complexes, such as homeobox A9, which is a protein-coding (HOXA9)/MEIS1 [132, 133]. These transcription factors are associated with the dysregulation of gene expression, enhanced proliferation, and the blocking of myeloid differentiation of hematopoietic cells, leading to their pathological accumulation. The transcription factor HOXA9 especially plays a key role in HSC expansion and has been associated with malignant transformation from healthy hematopoietic cells to LSC [42, 134].

MLL can be induced in hematopoietic stem and progenitor cells (HSPC) derived from cord blood through an efficient CRISPR/Cas9-based MLL1 model. The HSPC cells are induced to undergo malignant transformation by introducing plasmid- and virus-free single guide (sg) RNAs for the genes MLL, as well as AF4 or AF9, together with the Cas9 protein, which leads to successful inductions of the MLL rearrangements MLL-AF4 (Intron 9/11) and MLL-AF9 (Intron 9/11). After the introduction of all components of the system, the cells are cultured in a liquid medium supplemented with cytokines and chemokines optimized for the growth of MLL rearranged (MLLr) cells. Successful transformation induction is subsequently demonstrated through PCR analysis of genomic DNA [135-137].

Human NKG2DL expression is not reported in MLLr cells. However, previous studies have shown that MLL rearrangements have a direct impact on NKG2DL surface expression in mice. Partial murine NKG2DLs (mNKG2DL) expression has been reported for murine MLL-ENL and MLL- partial tandem duplication (PTD)/FLT-3-ITD, but MLL-AF9 did not allow surface NKG2DL expression [73].

Aim of the thesis

AML remains a deadly cancer despite considerable efforts and remarkable progress. Patients often achieve remission, but relapse frequently due to the persistence of therapy resistant LSC. Our laboratory recently identified the absence of NKG2DL as a marker for LSC.

NKG2DL are immunogenic molecules that are not present on the surface of healthy cells but are induced following cellular stress or malignant transformation. This renders cells susceptible to immune surveillance by NK and cytotoxic T cells that express the NKG2DR. Although many regulators of NKG2DL mRNA and surface presentation have been identified, our knowledge of their potential intracellular presence and protein processing is limited.

The purpose of this study is to systematically characterize the expression of NKG2DL in malignant cell lines, including AML and MLLr cells, as well as healthy hematopoietic cells, including HSPC, at a steady state. To achieve this, we utilized qPCR, western blotting, ELISA, and immunofluorescence assays to analyze NKG2DL expression on both mRNA and protein levels. Additionally, we determined potential intracellular localization, surface presentation, and shedding of NKG2DL.

As primary AML is notoriously difficult to culture *in vitro*, I will additionally investigate the potential surrogate system of MLLr cord blood transformed cells to study AML biology *in vitro*. Therefore, I will phenotype for AML and LSC surface markers, such as CD33, CD34, and NKG2DL, to determine if they exhibit a similar phenotype as AML and will investigate clonogenic activity based on their NKG2DL surface expression.

Additionally, I aim to investigate how current, and potentially novel therapies, such as PARP1-inhibitors, as well as LPS and IFN γ mimicking infection or immune responses, may affect NKG2DL expression.

Materials and methods

Materials

Laboratory Equipment

General equipment

Table 1 Laboratory Equipment.

Equipment	Name	Company
Agarose gel electrophoresis equipment	Bioanalyzer 2100	Agilent Technologies Inc (Santa Clara, USA)
	E831	Consort (Turnhout, Belgium)
	Mini-PROTEAN Tetra Cell	Bio-Rad Laboratories, Inc. (Hercules, USA)
	PerfectBlue Horizontal Mini Gel System	Peqlab Biotechnologie GmbH (Erlangen, Germany)
Autoclave	VX-150	Systec (Puchheim, Germany)
Balances	AT261 Delta range fact (d = 0,01 mg)	Mettler-Toledo GmbH (Gießen, Germany)
	M-prove (d = 0,01 g)	Sartorius AG (Göttingen, Germany)
Cell culture	Counting Chamber according to Neubauer	Neolab (Sydney, Australia)
	Heracell 240i	Thermo Fisher Scientific Inc. (Waltham, USA)
	Hera Safe HS12-ICN2	Thermo Fisher Scientific Inc. (Waltham, USA)
	Köttermann Typ 3044 water Bath	Köttermann GmbH (Uetze, Germany)
	MCO-230AICUV Incubator	Phcbi (Wood Dale, USA)
	Vacusafe	Integra Biosciences (Princeton, USA)
Centrifuges	5810	Eppendorf AG (Hamburg, Germany)
	5810R	Eppendorf AG (Hamburg, Germany)
	5415R	Eppendorf AG (Hamburg, Germany)
	Epredia CYTOSPIN 4	Thermo Fisher Scientific Inc. (Waltham, USA)
Electroporation devices	Consort EV2310	Consort bvba (Turnhout, Belgium)
	Lonza 4D-Nucleofector	Lonza Group AG (Basel, Switzerland)
FACS devices	Cell Sorter ARIAIIIu	BD Biosciences, (Franklin Lakes, USA)
	Cell Sorter MA900	Sony (Tokyo, Japan)
	LSRFortessa	BD Biosciences, (Franklin Lakes, USA)
	LSRFortessa + HTS	BD Biosciences, (Franklin Lakes, USA)
Fridges and freezers	Liebherr CN 4335-21	Liebherr-Hausgeräte GmbH (Ochsenhausen, Germany)
	Liebherr Comfort	Liebherr-Hausgeräte GmbH (Ochsenhausen, Germany)
	Lovibond KKExv	Tintometer GmbH (Dortmund, Germany)
Fume cupboard	Airflow Controller AC3	WALDNER Holding SE & Co. KG (Wangen im Allgäu, Germany)
Heating blocks	TS basic	CellMedia (Zeitz, Germany)
	RCT basic	IKA®-Werke GmbH & CO. KG (Staufen, Germany)
Bacterial Incubators	Heraeus chamber BK 6160 Kelvitron KP	Thermo Fisher Scientific Inc. (Waltham, USA)
Plate reader	Infinite M200 Pro	TECAN (Männedorf, Switzerland)
Pipets	Microliter pipet 0.2-2,5 µl	Eppendorf AG (Hamburg, Germany)
	Microliter pipet 0.5-10 µl	Eppendorf AG (Hamburg, Germany)
	12 channel Multipet 0.5-10 µl	Eppendorf AG (Hamburg, Germany)
	12 channel Multipet 10-100 µl	Eppendorf AG (Hamburg, Germany)

	Microliter pipet 2-20 µl	Eppendorf AG (Hamburg, Germany)
	Microliter pipet 20-200 µl	Eppendorf AG (Hamburg, Germany)
	12 channel Multipet 30-300 µl	Eppendorf AG (Hamburg, Germany)
	Microliter pipet 100-1000 µl	Eppendorf AG (Hamburg, Germany)
Pipetman	MultipetteE3	Eppendorf AG (Hamburg, Germany)
	Pipetboy	Integra Biosciences (Zizers, Switzerland)
Shakers and mixers	neoLabLine Vortex Mixer	neoLab Migge GmbH (Heidelberg, Germany)
	Titramax 100	Heidolph Instruments (Schwabach, Germany)
Spectrophotometer	Nanodrop One	Thermo Fisher Scientific Inc. (Waltham, USA)
Pure water dispenser	TKA GenPure	TKA Wasseraufbereitungssysteme GmbH (Niederelbert, Germany)
Thermal cyclers	LightCycler® 480 Instrument II	Hoffmann-La Roche AG (Basel, Switzerland)
	Mastercycler X50	Eppendorf AG (Hamburg, Germany)
SDS PAGE	Standard Power Pack P25 T	Analytik Jena GmbH (Jena, Germany)
Western Blot	Mini-PROTEAN Tetra Cell	Bio-Rad Laboratories (Hercules, USA)
	PowerPac™ Basic Power Supply	Bio-Rad Laboratories (Hercules, USA)
	Trans-Blot Turbo	Bio-Rad Laboratories (Hercules, USA)
Other	Heating plate and magnetic stirrer RH basic 2	IKA-Werke GmbH & CO. KG (Staufen, Germany)
	Heat-stir CB162	Stuart Pharmaceutical Company (Pasadena, USA)
	HMT75M451 (Microwave)	Bosch (Gerlingen, Germany)
	Ice Dispenser	Hubbard Systems Inc., (Great Blakenham, UK)
	Ultrasonic- Cleaning Device USC-TH	VWR (Radnor, USA)

Microscopes

Table 2 Microscopes

Instrument	Specifications	Company
Incucyte S3	**General:** Environment control, (CO_2, O_2, temperature, humidity) **Objectives**: 5x/10x/20x Air **Lasers:** Dual Color Module 4614 (488nm, 561nm)	Satorius (Göttingen, Germany)
Leica SP8 TCS DLS	**General:** Environment control (CO_2, temperature, humidity), resonant scanner, Adaptive Focus Control, spectral detection, acusto-optical beam splitter, HyD detectors, **Objectives**: 63x/1.4 HC PL Apo CS2 Oil, 63x/1.3 HC PL Apo CORR CS2 Gycerol, 20x/0.75 HC PL Apo IMM CORR CS2 H_2O, Glycerol, Oil **Lasers:** UV (50mW) – 405nm, Argon (65mW) – 458, 476, 488, 496, 514nm,	Leica Microsystems GmbH (Wetzlar, Germany)

	DPSS Yellow (20mW) – 561nm, HeNe (10mW) – 633nm	
Olympus IX2-SP	**General:** Basic light micrsocpe **Objectives**: 5x/10x/20x Air	Olympus (Tokyo, Japan)
Zeiss Airyscan 2 LSM900	**General:** Environment control, (CO_2, O_2, temperature, humidity), Variable Dichroics, Definite Focus 2, GaAsP – PMTs, Airyscan 2 with 4xMPLX **Objectives**: Plan-Apochromat 20x/0,8, Plan-Apochromat 40x/1,3 Oil DIC, Plan-Apochromat 63x/1,4 Oil DIC, LD LCI Plan-Apochromat 40x/1,2 Imm Korr DIC, Water, silicon oil or glycerol immersion **Lasers:** Diodenlaser 405nm, 5mW, Diodenlaser 488nm, 10mW, Diodenlaser (SHG) 561nm, 10mW, Diodenlaser 640nm, 5mW	Carl Zeiss AG (Oberkochen, Germany)

Consumables and reagents

Consumables

Table 3 Consumables

#	Company
Aluminum foil	Böttcher AG (Zöllnitz, Germany)
Cell culture dishes (10 cm, 20 nm)	Greiner Bio-One GmbH (Frickenhausen, Germany)
Cell culture plates (6-well, 24-well, 96-well)	Greiner Bio-One GmbH (Frickenhausen, Germany)
Cell culture flasks (25, 75, 175 cm^2)	Corning Incorporated (New York, USA)
Cryogenic vials (2 ml)	Greiner Bio-One GmbH (Frickenhausen, Germany)
Falcon tubes (15 ml, 50 ml)	Greiner Bio-One GmbH (Frickenhausen, Germany)
Filter paper	Thermo Fisher Scientific Inc. (Waltham, USA)
Filter tips (10 µl, 20 µl, 100 µl, 200 µl, 1000 µl)	Sorenson Bioscience Inc. (Salt Lake City, USA)
Glass slides	Thermo Fisher Scientific Inc. (Waltham, USA)
Gloves (M, L)	Braun Vasco (Kronberg, Germany)
Ibidi microscopy dishes (glass bottom 8-well, 8-well ibidi treat, 35 mm glass bottom round dishes)	Ibidi (Fitchburg, USA)
Immobilon-FL PVDF	Merck KgaA (Darmstadt, Germany)
LS Column	Miltenyi Biotec (Bergisch Gladbach, Germany)
Mini-PROTEAN TGX Precast Gels	Bio-Rad Laboratories, Inc. (Hercules, USA)
MS Column	Miltenyi Biotec (Bergisch Gladbach, Germany)
Needles (0.3 mm, 0.4 mm)	BD (Eysins, Switzerland)
Parafilm M	Bemis (Neenah, USA)
PAP-Pen	Merck KgaA (Darmstadt, Germany)
PCR tubes (single tubes, 8-strips)	Biozym Scientific GmbH (Hessisch Oldendorf, Germany)
Petri dishes	Greiner Bio-One GmbH (Frickenhausen, Germany)
Pipette tips (unfiltered) (10 µl, 20 µl, 200 µl, 1000 µl)	Steinbrenner Laborsysteme GmbH (Wiesenbach, Germany)
Precision wipes (KIM wipes)	Kimberley-Clark Professional (Irving, USA)
Protein LoBind Tubes (1.5 ml)	Eppendorf AG (Hamburg, Germany)
Reaction tubes (1.5 ml, 2 ml)	SARSTEDT AG & Co. KG (Nümbrecht, Germany)

Thermo Scientific™ Shandon™ TPX Single Sample Chamber, Caps, and Filter Cards	Thermo Fisher Scientific Inc. (Waltham, USA)
Serological pipettes (5 ml, 10 ml, 25 ml, 50 ml)	Greiner Bio-One GmbH (Frickenhausen, Germany)
SepMate™-50 (IVD)	Stemcell Technologies (Vancouver, Canada)
SuperFrost slides	R. Langenbrinck GmbH (Emmendingen, Germany)
SuperFrost Plus cover slides	R. Langenbrinck GmbH (Emmendingen, Germany)
Spin-Away Filter	Zymo Research (Irvine, USA)
Syringes (1 ml, 5ml, 10ml, 50 ml)	BD (Eysins, Switzerland)
Vivaspin 20	Merck KgaA (Darmstadt, Germany)

Chemicals and reagents

Table 4 Chemicals and reagents

Product	Company
2-Mercaptoethanol	Carl Roth GmbH + Co. KG (Karlsruhe, Germany)
2-Propanol	Carl Roth GmbH + Co. KG (Karlsruhe, Germany)
Acetone (anhydrous)	Sigma-Aldrich, Inc. (St. Louis, USA)
AG 14361 (in DMSO)	Selleckchem (Houston, USA)
Agarose NEEO ultra-quality EEO = 0,05-0,13	Carl Roth GmbH + Co. KG (Karlsruhe, Germany)
Ampicillin	Sigma-Aldrich, Inc. (St. Louis, USA)
Azazitidine (in DMSO)	Thermo Fisher Scientific Inc. (Waltham, USA)
Bambanker Serum Free Cell Freezing Medium	VWR (Radnor, USA)
Bovine serum albumin (BSA)	Carl Roth GmbH + Co. KG (Karlsruhe, Germany)
Blasticidin, solution (ant-bl-1)	InvivoGen (San Diego, USA)
Cell lysis buffer	Cell Signaling Technology (Danver, USA)
Cutsmart buffer	New England Biolabs (Ipswich, USA)
Cytarabine (in DMSO)	Thermo Fisher Scientific Inc. (Waltham, USA)
DMSO	Honeywell (Seelze, Germany)
Donkey Serum	Sigma-Aldrich, Inc. (St. Louis, USA)
DTT	GERBU Biotechnik GmbH (Heidelberg, Germany)
Dulbecco's Phosphate Buffered Saline (DPBS)	Gibco by life technologies (Paisley, UK)
ECL™ Prime Western Blotting System	Sigma-Aldrich, Inc. (St. Louis, USA)
EDTA	Sigma-Aldrich, Inc. (St. Louis, USA)
Ethanol	Sigma-Aldrich, Inc. (St. Louis, USA)
FBS	Gibco by life technologies (Paisley, UK)
Glycerol	AppliChem GmbH (Darmstadt, Germany)
Glycine	Labochem international (Heidelberg, Germany)
HEPES (H4034)	Sigma-Aldrich, Inc. (St. Louis, USA)
Histopaque®-1077	Merck KgaA (Darmstadt, Germany)
Human G-CSF, premium grade	Miltenyi Biotec (Bergisch Gladbach, Germany)
Human Hematopoietic Stem Cell Expansion Cytokine Package	Peprotech (New Jersey, USA)
IgG huma serum	Sigma-Aldrich, Inc. (St. Louis, USA)
Interferon γ (in PBS)	Thermo Fisher Scientific Inc. (Waltham, USA)
K-7147 (in H_2O)	MedChemExpress (New Jersey, USA)
Laemmli Sample Buffer	Bio-Rad Laboratories, Inc. (Hercules, USA)
Lentivirus Titration XpressCard	Antikörperonline.de
LB Broth	Carl Roth GmbH + Co. KG (Karlsruhe, Germany)
Lipofectamine™ 2000 Transfection Reagent	Thermo Fisher Scientific Inc. (Waltham, USA)
LPS (in PBS)	Thermo Fisher Scientific Inc. (Waltham, USA)
Maxima SYBR Green qPCR Master Mix (2X), with separate ROX vial	Thermo Fisher Scientific Inc. (Waltham, USA)

Methanol	Zentralbereich Neuenheimer Feld (Heidelberg, Germany)
MethoCult™ H4434 Classic	Stemcell Technologies (Vancouver, Canada)
Midori Green	Nippon Genetics Co., Ltd.(Tokyo, Japan)
Milk, powdered	Carl Roth GmbH + Co. KG (Karlsruhe, Germany)
Mowiol	Carl Roth GmbH + Co. KG (Karlsruhe, Germany)
NaCl	Sigma-Aldrich, Inc. (St. Louis, USA)
Nonidet P-40 (NP-40)	AppliChem GmbH (Darmstadt, Germany)
Paraformaldehyde (PFA) EM-grade	Electron Microscopy Sciences (Hatfield, Pennsylvania)
Pen streptomycin 5X	Sigma-Aldrich, Inc. (St. Louis, USA)
Phosphate-buffered saline (PBS)	Thermo Fisher Scientific Inc. (Waltham, USA)
Polybrene Infection / Transfection Reagent	Merck KgaA (Darmstadt, Germany)
Ponceau S	VWR (Radnor, USA)
Purple loading dye	New England Biolabs (Ipswich, USA)
Protector Rnase-Inhibitor	Sigma-Aldrich, Inc. (St. Louis, USA)
Quick Coomassie Stain	SERVA Electrophoresis GmbH (Heidelberg, Germany)
Q5 Hifi polymerase	New England Biolabs (Ipswich, USA)
Recombinant Human IL-3	Peprotech (New Jersey, USA)
Recombinant Human IL-6	Peprotech (New Jersey, USA)
RPMI 1640 GlutaMAX, phenol-red (61870010)	Gibco by life technologies (Paisley, UK)
RPMI 1640, stable Glutamine, w/o phenol-red, 2 g/l $NaHCO_3$ (P04-16520)	PAN Biotech (Aidenbach, Germany)
SDS	Carl Roth GmbH + Co. KG (Karlsruhe, Germany)
SOC outgrowth medium	New England Biolabs (Ipswich, USA)
Sodium pyruvate solution	Sigma-Aldrich, Inc. (St. Louis, USA)
SuperSignal™ West Femto Maximum Sensitivity Substrate	Thermo Fisher Scientific Inc. (Waltham, USA)
StemMACS™ HSC Expansion Media XF, human	Miltenyi Biotec (Bergisch Gladbach, Germany)
StemRegenin 1	Stemcell Technologies (Vancouver, Canada)
T4 DNA ligase buffer (10x)	New England Biolabs (Ipswich, USA)
T4 PNK	
Taq Reaction Buffer	New England Biolabs (Ipswich, USA)
Trans-Blot Turbo Mini 0.2 µm Nitrocellulose Transfer Packs	Bio-Rad Laboratories (Hercules, USA)
Tris	Carl Roth GmbH + Co. KG (Karlsruhe, Germany)
Triton-X-100	Merck KgaA (Darmstadt, Germany)
Trypsin (0.05%)	Thermo Fisher Scientific Inc. (Waltham, USA)
Tryphan Blue	Thermo Fisher Scientific Inc. (Waltham, USA)
Tween-20	Carl Roth GmbH + Co. KG (Karlsruhe, Germany)
UM729	Stemcell Technologies (Vancouver, Canada)
UltraComp eBeads™ Plus Compensation Beads	Thermo Fisher Scientific Inc. (Waltham, USA)
Venetoclax (in DMSO)	Tocris bioscience (Bristol, UK)
X-VIVO 10 Serum-free Hematopoietic Cell Medium	Lonza Group AG (Basel, Switzerland)

Media, buffers and solutions

Table 5 Media, buffers and solutions

Name	Composition	Purpose
10x SDS Running buffer	250 mM Tris 1.92 M Glycine 1% SDS	Co-immunoprecipitation (SDS-PAGE)
10xTBS	24,2g Tris base 80g Nattriumchloride ad 1l pH 7,6	WB
4x Laemmli buffer	4x Laemmli Sample Buffer 1:10 2-Mercaptoethanol (freshly added)	Co-immunoprecipitation (SDS-PAGE)
50xTAE	242,2g Tris base, solve in 800µL ddH_2O 52,1mL acetic acid 100mL 0,5M EDTA pH 8 ad 1l ddH_2O	Agarose gels
ACK/RBC	8,3g Ammonium chloride 1g Potassium bicarbonate 200µl 0,5M EDTA ad 1l pH 7,2-7,4	PBMC isolation
FACS	500 mL PBS 27.5 mL FBS 2mL EDTA 0,02M	FACS
Freezing medium	70% RPMI 20% FBS 10% DMSO	Cell culture (Freezing)
HSC medium	X-VIVO 10 Serum-free Hematopoietic Cell Medium 100 ng/ml hTPO, SCF, FLT-3 Ligand 60 ng/ml IL-3	HSC cultivation
MACS	500 mL PBS 27.5 mL FBS 2mL EDTA 0,02M 0,5% BSA	MACS
MLL medium	89% StemMACS HSC Expansion Medium XF, human 10% FBS 1% P/S 50 ng/mL FLT-3-L, SCF, hTPO, G-CSF, IL-3, IL-6 0,75µM SR-1, UM729	Cell culture (MLL cells)
LB Agar plates	15 g Agar-Agar ad 1 L LB-Medium 100 µg/mL Ampicillin	Plates for Bacteria culture
LB	10 g LB-Medium (Lennox) ad 1 L H_2O 100 µg/mL Ampicillin	Bacteria culture medium
RIPA	50 mM Tris/HCl, pH 8 1 % Nonidet P-40 (NP-40) 0.5 % Sodium deoxycholate 0.1 % SDS 1 mM DTT (freshly added) 1x cOmlpete™, EDTA-free Protease Inhibitor Cocktail (freshly added)	Co-immunoprecipitation (Cell lysis)
0,5M Tris/HCl	7,88g Tris HCl ad 100mL	WB gels

	pH 6,8	
1,5M Tris/HCl	59,1 Tris HCl ad 250mL pH 8,8	WB gels
TBS-T	10 mM TRIS 150 mM NaCl 0,05 %Tween20 pH7,6	WB washing
TE	10 mM Tris-HCl, pH 7.5 1 mM EDTA pH 7.5	Transfection (DNA resuspension)
Transfer	43,58 mM TRIS 39 mM Glycin 20 %Methanol	WB transfer

Standard markers

Table 6 Standard markers

Name	Company	Product Number
GeneRuler 1 kb DNA Ladder	Thermo Fisher Scientific Inc. (Waltham, USA)	SM0314
GeneRuler Low Range DNA Ladder	Thermo Fisher Scientific Inc. (Waltham, USA)	SM1193
PageRuler Plus Prestained	Thermo Fisher Scientific Inc. (Waltham, USA)	26619

Antibodies and nanobodies

Table 7 Antibodies and nanobodies

Conjugated Antibodies								
Name	Clone	Host	Species Reactivity	Isotype	Conjugation	Application(s)	Company	Product. Nr.
CD3	Okt3	Mouse	Human	IgG2a, κ	BV605	FACS	BioLegend (San Diego, USA)	317322
CD3	Okt3	Mouse	Human	IgG2a, κ	PE/Dazzle	FACS	BD bioscience (New Jersey, USA)	300312
CD4	Okt4	Mouse	Human, Cynomolgus, Rhesus	IgG1, κ	Alexa Fluor 700	FACS	BioLegend (San Diego, USA)	317426
CD8	SK1	Mouse	Human	IgG1, κ	BV421	FACS	BioLegend (San Diego, USA)	344748
CD8	SK1	Mouse	Human	IgG1, κ	BV605	FACS	BioLegend (San Diego, USA)	344742
CD14	MϕP9	Mouse	Human	IgG2a, κ	PE-Cy7	FACS	BD bioscience (New Jersey, USA)	562698
CD16	3G8	Mouse	Human	IgG1, κ	APC	FACS	BioLegend (San Diego, USA)	302012

CD19	4G7	Mouse	Human	IgG1, κ	APC	FACS	BioLegend (San Diego, USA)	392504
CD19	SJ25 C1	Mouse	Human	IgG1, κ	Alexa Fluor 700	FACS	BioLegend (San Diego, USA)	363034
CD33	WM53	Mouse	Human	IgG1, κ	BV421	FACS	BD bioscience (New Jersey, USA)	562854
CD34	581	Mouse	Human	IgG1, κ	FITC	FACS	BD bioscience (New Jersey, USA)	555821
CD34	581	Mouse	Human	IgG2a, κ	APC	FACS	BioLegend (San Diego, USA)	555821
CD38	HIT-2	Mouse	Human	IgG1, κ	APC	FACS	BioLegend (San Diego, USA)	303510
CD38	HIT2	Mouse	Human	IgG1, κ	PE-Cy7	FACS	BD bioscience (New Jersey, USA)	560677
CD45RA	HI100	Mouse	Human	IgG2a, κ	PercP	FACS	BioLegend (San Diego, USA)	304155
CD56	MEM-188	Mouse	Human	IgG2a, κ	FITC	FACS	BD bioscience (New Jersey, USA)	304604
CD80	2D10	Mouse	Human	IgG1, κ	BV711	FACS	BD bioscience (New Jersey, USA)	751726
CD117	104D2	Mouse	Human	IgG1, κ	PE-Cy5	FACS	BioLegend (San Diego, USA)	313210
CD183	G025H7	Mouse	Human	IgG1, κ	AF647	FACS	BioLegend (San Diego, USA)	353712
HLA-DR	G46-6	Mouse	Human	IgG2a, κ	BV421	FACS	BD bioscience (New Jersey, USA)	562804
IgD	IA6-2	Mouse	Human	IgG2a, κ	PE-Cy7	FACS	BD bioscience (New Jersey, USA)	561314
LAG-3	T47-530	Mouse	Human	IgG1, κ	BV421	FACS	BD bioscience (New Jersey, USA)	565721
NKG2DR	REA797	recombinant	Human	IgG1, κ	PE-Vio615 (PE-Cy5)	FACS	Miltenyi Biotec (Bergisch Gladbach, Germany)	130-111-727
TIGIT	A15153G	Mouse	Human	IgG1, κ	APC/Fire 750	FACS	BioLegend (San Diego, USA)	372707
Unconjugated Antibodies unconjugated								
Anti-GM130	Polyclonal	Mouse	Human	IgG	-	WB, IF	Abcam (Cambridge, UK)	ab169276
Human ULBP-1	Polyclonal	Goat	Human	IgG	-	WB, FACS	R&D systems (Minneapolis, USA)	AF1380

Human ULBP 2/5/6	Polyclonal	Goat	Human	IgG	-	WB, IHC, FACS	R&D systems (Minneapolis, USA)	AF 1298
Human ULBP 3	Polyclonal	Goa	Human	IgG	-	WB, FACS	R&D systems (Minneapolis, USA)	AF1517
Histone H3	D1H2	Rabbit	Human, Mouse, Rat, Monkey	IgG	-	WB, IHC, IF, FACS	Cell Signaling Technology (Danver, USA)	4499
MICA	Polyclonal	Rabbit	Human	IgG	-	WB, IHC, IF, FACS	Thermo-Fisher Scientific (Waltham, USA)	PA5-35346
MICB	Polyclonal	Rabbit	Human	IgG	-	IF, FACS	Thermo-Fisher Scientific (Waltham, USA)	PA5-66698
MICB	102	Rabbit	Human	IgG	-	WB	Thermo-Fisher Scientific (Waltham, USA)	MA5-29423
Recombinant Human NKG2D Fc Chimera Protein	-	Mouse	Human	-	-	FACS	R&D systems (Minneapolis, USA)	1299-NK-MTO
Secondary antibodies								
Donkey anti-Mouse Alexa Fluor Plus 647	Polyclonal	Donkey	Mouse	IgG	Alexa Fluor 647	IHC, IF	Thermo-Fisher Scientific (Waltham, USA)	A-21448
IRDye 680RD Goat anti-Rabbit	Polyclonal	Goat	Rabbit	IgG	IRDye 680RD	WB	Li-Cor (Lincoln, USA)	926-68071
IRDye 680RD Donkey anti-Goat	Polyclonal	Donkey	Goat	IgG	IRDye 680RD	WV	Li-Cor (Lincoln, USA)	926-68074
IRDye 800CW Donkey anti-Goat	Polyclonal	Donkey	Goat	IgG	IRDye 800CW	WB	Li-Cor (Lincoln, USA)	926-32214
IRDye 800CW Goat anti-Rabbit	Polyclona	Goat	Rabbit	IgG	IRDye 800CW	WB	Li-Cor (Lincoln, USA)	926-32211
Goat anti-Mouse Alexa Fluor Plus 647	Polyclonal	Goat	Mouse	IgG	Alexa Fluor 647	WB, IF	Thermo-Fisher Scientific (Waltham, USA)	A32728

Goat anti-Mouse Alexa Fluor 750	Polyclonal	Goat	Mouse	IgG	Alexa Fluor 750	WV, IF, FACS	Thermo-Fisher Scientific (Waltham, USA)	A-21037
Goat anti-Rabbit alexa 488	Polyclonal	Rabbit	Goat	IgG	Alexa Fluor 488	IF, FACS	Thermo-Fisher Scientific (Waltham, USA)	A-11034
Goat anti-Rabbit Alexa Fluor 647	Polyclonal	Goat	Rabbit	IgG	Alexa Fluor 647	IHC, IF	Thermo-Fisher Scientific (Waltham, USA)	A-21245
Goat anti-Rat Alexa Fluor 546	Polyclonal	Goat	Rat	IgG	Alexa Fluor 546	WB, IHC, IF	Thermo-Fisher Scientific (Waltham, USA)	A-11081
Rabbit anti-Goat IgG Alex 488	Polyclonal	Rabbit	Goat	IgG	Alexa Fluor 488	IHC, IF	Thermo-Fisher Scientific (Waltham, USA)	A-11078
Rabbit anti-Goat Alexa Fluor 647	Polyclonal	Rabbit	Goat	IgG	Alexa Fluor 647	IHC, IF	Thermo-Fisher Scientific (Waltham, USA)	A-21446

Dyes

Table 8 Dyes

Name	Application	Dilution	Source/Company	Product Number
7-AAD	FACS	1:1000	Thermo-Fisher Scientific (Waltham, USA)	A1310
DAPI	FACS; IFA	1 µg/mL	Thermo-Fisher Scientific (Waltham, USA)	D1306
Streptavidin R PE	FACS	1:100	Thermo-Fisher Scientific (Waltham, USA)	S866
LIVE/DEAD™ Fixable Aqua Dead Cell Stain Kit, for 405 nm excitation	FACS	1:200	Thermo-Fisher Scientific (Waltham, USA)	L34966
Midori Green	Agarose gel electrophoresis	1:10000	Nippon Genetics Co., Ltd.(Tokyo, Japan)	MG04
SYBR Green I	Growth curves, qPCR	1:1000	Thermo-Fisher Scientific (Waltham, USA)	S7563

Enzymes

Table 9 Enzymes

Name	Company	Product Number
BbsI	New England Biolabs (Ipswich, USA)	R0117

Kits

Table 10 Kits

Name	Company	Product Number
CD34 MicroBead Kit, human	MACS Milenyi Biotech	130-046-702
DuoSet ELISA Ancillary Reagent Kit 2	R&D systems (Minneapolis, USA)	DY008
Fixation/Permeabilization Solution Kit	BD Biosciences	554714
High-Capacity cDNA Reverse Transcription Kit	Thermo-Fisher Scientific (Waltham, USA)	4368814
Human MICA DuoSet ELISA	R&D systems (Minneapolis, USA)	DY1300
Human MICB DuoSet ELISA	R&D systems (Minneapolis, USA)	DY1599
Human ULBP-1 DuoSet ELISA	R&D systems (Minneapolis, USA)	DY1380
Monarch DNA Gel Extraction Kit	New England Biolabs (Ipswich, USA)	T1020S
One step antibody biotinylation kit 1strip, 8reactions	Miltenyi Biotec (Bergisch Gladbach, Germany)	130-093-385
QIAGEN Plasmid Plus Maxi Kit (25)	Qiagen (Hilden, Germany)	12963
QIAprep Spin MiniprepKit	Qiagen (Hilden, Germany)	27106
QIAquick PCR & Gel Cleanup Kit	Qiagen (Hilden, Germany)	28506
Revert™ 700 Total Protein Stain and Wash Solution Kit	Li-Cor (Lincoln, USA)	926-11015
Revert™ 700 Total Protein Stain and Wash Solution Kit	Li-Cor (Lincoln, USA)	926-11015
Rneasy Mini Kit (50)	Qiagen (Hilden, Germany)	74104
SelectFX™ Alexa Fluor™ 488 Endoplasmic Reticulum Labeling Kit, for fixed cells	Thermo-Fisher Scientific (Waltham, USA)	S34200
Zero Blunt™ TOPO™ PCR Cloning Kit for Sequencing, without competent cells	Invitrogen (Waltham, USA)	450159

Cell lines

Table 11 Cell lines

Name	Cell type	Description	Source
Lenti-X™ 293T	Human embryonic kidney	“transformed with adenovirus type 5 DNA, that also expresses the SV40 large T antigen. The cell line was subcloned for high transfectability and high-titer virus production.”	Takara [138]
HNT-34	Acute myeloid leukaemia	“established in 1994 from the peripheral blood of a 47-year-old woman with acute myeloid leukemia (AML FAB M4) secondary to previous myelodysplastic syndromes (MDS), specifically chronic myelomonocytic leukemia	DSMZ [139]

		(CMML); described in the literature to carry the t(3;3)(q21;q26) leading to MECOM (EVI1) overexpression and the Philadelphia chromosome t(9;22) expressing both P190 and P210 BCR-ABL1 chimeric transcripts"	
Kasumi-1	Acute myeloid leukaemia	"established from the peripheral blood of a 7-year-old boy with acute myeloid leukemia (AML FAB M2) (in 2nd relapse after bone marrow transplantation) in 1989; cells carry the t(8;21) leading to RUNX1-RUNX1T1 (AML1-ETO) fusion gene; described in the literature to carry the KIT mutation N822."	DSMZ [140]
SKM-1	Acute myeloid leukaemia	"established from the peripheral blood of a 76-year-old man with acute monoblastic leukemia (AML M5) in 1989 following myelodysplastic syndromes (MDS)"	DSMZ [141]

Bacteria

Table 12 Bacteria

Name	Description	Source	Product number
NEB® 5-alpha F'Iq Competent *E. coli*	Chemically competent *E. coli* cells derived from DH5α	New England Biolabs (Ipswich, USA)	C2992
One Shot™ TOP10 Chemically Competent E. coli	Chemically competent *E. coli* cells derived from TOP10	Thermo-Fisher Scientific (Waltham, USA)	C404010

DNA

Oligonucleotides

Table 13 Oligonucleotides

Primer for NKG2DL knockout cloning	
Name	Sequence (5'→3')
MICA_1_FW	CACCGGCAGCTCCCGGAGGTGCAAA
MICA_1_RV	AAACTTTGCACCTCCGGGAGCTGCC
MICA_2_FW	CACCGATTCCTGACGTTCATGGCCA
MICA_2_RV	AAACTGGCCATGAACGTCAGGAAT
MICA_3_FW	CACCGGAACGTCAGGAATTTCTTGA
MICA_3_RV	AAACTCAAGAAATTCCTGACGTTCC
MICB_1_FW	CACCGAGAATGGGCAAGACCTCAGG
MICB_1_RV	AAACCCTGAGGTCTTGCCCATTCTC
MICB_2_FW	CACCGATTTGTGACGTTCATAGCCA
MICB_2_RV	AAACTGGCTATGAACGTCACAAATC
MICB_3_FW	CACCGGAACGTCACAAATTTCTGGA
MICB_3_RV	AAACTCCAGAAATTTGTGACGTTCC
MICB_4_FW	CACCGACAGCGATATCTGAAATCCG
MICB_4_RV	AAACCGGATTTCAGATATCGCTGTC
ULBP1_1_FW	CACCGGAAGCCCATGGACACGGCAG
ULBP1_1_RV	AAACCTGCCGTGTCCATGGGCTTCC
ULBP1_2_FW	CACCGTCTTCCAGAAGATTTCACTG
ULBP1_2_RV	AAACCAGTGAAATCTTCTGGAAGAC

ULBP1_3_FW	CACCGAAGATGATGAGAAGGCTCCA
ULBP1_3_RV	AAACTGGAGCCTTCTCATCATCTTC
ULBP1_4_FW	CACCGTGCCAGCTAGAATGAAGCAG
ULBP1_4_RV	AAACCTGCTTCATTCTAGCTGGCAC
qPCR Primer	
Name	Sequence (5'→3')
MICAFW	GGCGCCTAAAGTCTGAGAGA
MICA RV	AACCCTGACTGCACAGATCC
MICA Vari1 FW	CCCGGTCTTTCTGCTTCTG
MICA Vari1 RV	CCTCAGCAAGAAACCCTGAC
MICA Vari1-1 FW	GGCATCTTCCCTTTTGCAC
MICA Vari1-1 RV	GGACAGCACCGTGAGGTTAT
MICB Vari1 FW	CTGAGAAGGTGGCGACGTA
MICB Vari1 RV	CGAAGACTGTGGGGCTCA
MICB Vari2 FW	AGTGGCGCCTAAAGTCTGC
MICB Vari2 RV	GCACCATGAGGTTGTAACGA
MICB Vari3 FW	CTGAGAAGGTGGCGACGTA
MICB Vari3 RV	CGAAGACTGTGGGGCTCA
ULBP1 FW	ACTGGGAACAAATGCTGGAT
ULBP1 RV	GAGAAGGCTCCAGGGACTG
ULBP2 FW	CCGCTACCAAGATCCTTCTG
ULBP2 RV	GGGATGACGGTGATGTCATAG
ULBP3 FW	TCCCTGGCATCTGAGAAGAG
ULBP3 RV	CAGAAAGGCACAGTGGTGAGT
ULBP4 FW	AGCACTTGGGGAGAATTGAC
ULBP4 RV	CTTGCAGAGTGGAAGGATCAC
GAPDH FW	AGC CACATCGCTCAGACAA
GAPDH RV	GCCCAATACGACCAAATCC
PBGD FW	AGTGTGGTGGGAACCAGC
PBGD RV	CAGGATGATGGCACTGAACTC
PBGD2 FW	CGCATCTGGAGTTCAGGAGTA
PBGD2 RV	CCAGGATGATGGCACTGA
sgRNA Production primer	
Name	Sequence (5'→3')
MLL(9)-AF4_sgRNA	taatacgactcactataGGCCATGGCTTTTGGGTAGGgttttagagctagaaATAGC
MLL(11)-AF4_sgRNA	aatacgactcactataGGTGCCTTCTCAGTCAGTTGgttttagagctagaaATAGC
MLL(9)-AF9_sgRNA	taatacgactcactataGGTTTGATGCTAGCAGAGGTgttttagagctagaaATAGC
MLL(11)-AF9_sgRNA	taatacgactcactataGGATATGGAGAAAGTTGTAGgttttagagctagaaATAGC
Universal_RV	AGCACCGACTCGGTGCCACT
Analysis primer for MLL translocations	
Name	Sequence (5'→3')
MLL(11)-AF4_FW	ATTCCCTGTTTAAACCAGCTAAAGAA

PCR Primer MLL(11)-AF4_RV	GACATTTTCATCTCAAATCCGTCTTC
MLL(11)-AF9_FW	TCTTGACTTCTGTTCCTATAACACCC
MLL(11)-AF9_RV	CAAGTTGTGAATGCAAAGGAAAAGTT

Plasmids

Table 14 Plasmids

Commercial plasmids for lentivirus production		
Name	Description	Source
pMD2.G	VSV-G envelope expressing plasmid	addgene
psPAX2	Envelope (pol & gag) expressing plasmid	addgene
Commercial plasmids CRISPR-Cas9 based gene editing plasmids		
Name	Description	Source
pKLV2-U6gRNA5(BbsI)-PGKpuro2ABFP-W	CRISPR gRNA expression vector with an improved scaffold and puro/BFP markers	addgene
pKLV2-EF1a-Cas9Bsd-W	Lentiviral vector expressing Cas9 fused with the Blasticidin resistant gene	addgene
pKLV2-U6gRNA5(gGFP)-PGKBFP2AGFP-W	Cas9 activity reporter with BFP and GFP	addgene
New guide plasmids for CRISPR-Cas9 based gene editing plasmids Sequences according to Toronto library [142]		
Name	Description	Source
pKLV2_MICA.1_KO	MICA Knockout	This thesis
pKLV2_MICA.2_KO		This thesis
pKLV2_MICA.3_KO		This thesis
pKLV2_MICB.1_KO	MICB Knockout	This thesis
pKLV2_MICB.2_KO		This thesis
pKLV2_MICB.3_KO		This thesis
pKLV2_MICB.4_KO		This thesis
pKLV2_ULBP1.1_KO	ULBP1 Knockout	This thesis
pKLV2_ULBP1.2_KO		This thesis
pKLV2_ULBP1.3_KO		This thesis
pKLV2_ULBP1.4_KO		This thesis

Software

Table 15 Software

Name	Description	Source/reference
DeepL	Open source: machine translation and text optimization service	https://www.deepl.com/write/write-mobile [143]
Fiji	Open source image processing package based on the ImageJ2 distribution of ImageJ	[144]
FlowJo	Software package for analysing flow cytometry data	Bd bioscinces (New Jersey, United States)
Graphpad Prism	2D graphing and statistics software	GraphPad Software (San Diego, USA)
IDEAS	Imagestream Analysis software	Cytek Biosciences (California, USA) [145]
Leica Application Suite (LAS) X	Leica microscopy user interface	Leica Microsystems GmbH (Wetzlar, Germany)
Microsoft Office	Family of services developed by Microsoft for office applications	Microsoft (Washington, United States)
Snapgene	Molecular biology software used to do in-silico cloning of vectors and inspection and alignment of Sanger-sequencing results	Snapgene (Chicago, USA)
Snapgene Viewer	Free version of Snapgene molecular biology software used to visualize and annotate plasmids and DNA sequences	Snapgene (Chicago, USA)
Zen Blue	Zeiss microscopy user interface and image processing software	Carl Zeiss AG (Oberkochen, Germany)

Methods

Nucleotide based methods

Cloning strategy NKG2DL knock out

During this project, I observed that NKG2DL were present in all cells intracellularly, meaning that we were lacking a negative control to guarantee reagent specificity. To provide a negative control, I choose the CRISPR-Cas9 system to knock out the most frequent human NKG2DL: MICA, MICB, ULBP1 [73].

To perform this knockout, I decided to use the Clustered Regularly Interspaced Short Palindromic Repeats-CRISPR-Associated 9 (CRISPR-Cas9) gene editing system to modify endogenous genome sequences via lentiviral transduction. The CRISPR-Cas9 system was originally discovered in E.coli as a defense mechanism against bacteriophages and can be used to precisely modify genomic DNA in various organisms including human cells *in vitro* [146].The system uses specific guide RNAs to precisely target complementary DNA sequences via the Cas9 endonuclease. To enable the knockout, I used two lentiviral vectors for:

1: Cas-9 expression
2: gRNA expression

First, I stably integrated Cas9 into SKM-1 cells, which were chosen due to their high NKG2DL expression for all NKG2DL, and performed an antibiotic mediated selection using blasticidin and the stable integration of MICA, MICB, ULBP1 targeting gRNAs based on the Toronto library [142].

The Cas9 overexpression vector is based on the vector pKLV2-EF1a, which was first described in [147] and is commercially available. This plasmid carries the expression cassettes for Cas9 driven by the promotor EF1a and an expression cassette for blasticidin resistance driven by the CMV promotor.

Isolation of DNA

DNA was isolated from bacteria using the QIAGEN Plasmid Plus Maxi Kit (25) or the QIAprep Spin MiniprepKit and human cells according to the manufacturer's instructions.

Isolation of RNA

RNA from human cells was isolated using the Rneasy Mini Kit according to the manufacturer's instructions.

Polymerase chain reaction

DNA fragments were amplified by PCR using Phusion® High-Fidelity DNA Polymerase or Q5 Hifi Polymerase according to the manufacturer's instructions without DMSO. When DNA fragments were to be isolated post-PCR, 50 µl reactions were used. When PCR was performed for integration control or to profile

bacterial colonies during cloning, the reaction was performed in a final volume of 25 µl. In general, 1 µl of template DNA containing less than 1000 ng of DNA was used. Primers were designed using SnapGene software with melting temperatures between 54-60°C. Primers were ordered from Microsynth as a 100µM solution. Stock solutions were stored at -20°C and diluted 1:10 for a final working solution of 10 µM. The reactions were mixed by vortexing and briefly pelleted by centrifugation before amplification using the cycling conditions listed below.

Table 16 PCR program

Process Step	Temperature [°C]	Time[s]	Cycles
Initial Denaturation	95	180	1
Denaturation	95	15	30
Primer Annealing	54-60	15	
Elongation	72	20	
Final Elongation	72	120	1

cDNA synthesis

For RNA analysis, complementary DNA (cDNA) was synthesized using the High-Capacity cDNA Reverse Transcription Kit in combination with Protector Rnase-Inhibitor according to manufacturer's instructions. 0.5-2µg were used as template RNA and cDNA was stored at -20°C.

Restriction digestion

Enzymatic restriction digestion of DNA was performed using 1-3 commercial enzymes per reaction. For preliminary digestion and characterization of plasmids and colonies during cloning, 1 µg of DNA was used in a final volume of 50 µl. Digestion was performed using high-fidelity (HF) enzymes, which are fully active over a wide range of conditions while minimizing off-target product, even at longer reaction times [148]. Incubation was performed at 37°C for 30min-1h. If necessary, 1 µl of Quick CIP (NEB) was added for the last 10 min of digestion to dephosphorylate DNA ends, e.g., when linearizing vectors during cloning.

Agarose gel electrophoresis

For size separation of DNA fragments, agarose gel electrophoresis was performed using 1% w/v agarose gels in TAE buffer. DNA was mixed with 6x loading dye supplemented with Midori green and run for 30 minutes at 120 V next to either 4 µl GeneRuler 1 kb DNA Ladder or GeneRuler Low Range DNA Ladder. Visualization of DNA fragments was performed using a UV transilluminator. If necessary, gel pieces containing specific DNA fragments were excised with a scalpel for subsequent purification.

DNA purification from agarose gels

DNA fragments from agarose gels after electrophoresis by excision of the target bands from the gel were recovered and purified using the QIAquick PCR & Gel Cleanup Kit according to the manufacturer's instructions. Elution was performed with 35 µl ddH2O. The purified DNA was used directly for cloning purposes and was not stored.

Oligo annealing

DNA oligonucleotides (gRNA oligos) were annealed and phosphorylated prior to insertion into linearized vectors. The oligos were mixed and annealed using a thermocycler with the reaction parameters listed below.

Table 17 Oligo annealing reaction mixture

Component	Volume
ddH_2O	6 µl
100 µM oligo 1 (10µM)	1 µl
100 µM oligo 2 (10µM)	1 µl
10x T4 PNK buffer	1 µl
T4 PNK	1 µl

Table 18 Oligo annealing reaction program

Step	**Temp**	**Time**
Phosphorylation	37°C	30 min
Denaturation	95°C	5 min
Annealing	95° → 25°C	Cooling time with machine shutdown

DNA ligation

To ligate gRNA oligo-DNA fragments with compatible sticky ends to a linearized vector, DNA ligation was performed using T4 ligase. For annealing, 1 µl of previously annealed and phosphorylated oligos were mixed with 100 ng of linearized vector in a 20 µl reaction volume and incubated overnight at 16°C before transformation into competent bacteria. The ligation components are listed below.

Table 19 Ligation reaction mixture

Component	Volume
ddH_2O	to 20 µl
Linearized vector (100 ng)	variable
Annealed oligos	1 µl
10x T4 DNA ligase buffer	2 µl
T4 DNA ligase	1 µl

Transformation

Plasmid DNA was introduced into commercially available chemically competent NEB Stable Competent E. coli by heat shock. 1 µg of plasmid DNA was added to 50 µl of E. coli cell suspension without pipetting up and down. The transformation mixture was incubated for 30 minutes on ice before a 42°C heat shock was applied for 30 seconds. Bacteria were returned to ice for 5 minutes before 300 µl of SOC outgrowth medium was added and pre-cultured at 37°C for 1 hour.

Plasmid amplification and purification

After transformation of ligation mixtures, 200 µl of the mixture were inoculated onto LB agar plates containing 100 µg/ml ampicillin using an inoculation loop and incubated at 37°C for 7-18 hours until a clear bacterial colony was visible. Single colonies or a fraction of a bacterial stock for retransformation were picked and amplified in 4(Miniprep)/250(Maxiprep) ml LB broth containing 100 µg/ml ampicillin by incubation overnight at 37°C and 250 rpm in a plasmid bacterial shaker.

For long-term storage, 500 µl of the bacterial solution was mixed with 500 µl 50% glycerol in ddH2O, transferred to a cryotube and stored at -80°C.

DNA was isolated using QIAprep Spin MiniprepKit or QIAGEN Plasmid Plus Maxi Kit according to the manufacturer's instructions. Elution was performed with 50(Miniprep)/1000(Maxiprep) µl ddH2O. Plasmid DNA was stored at -20°C.

DNA sequencing

DNA was sequenced by a third-party service provider, Microsynth, using the Single-Tube Sanger Sequencing service. DNA samples were prepared according to the sample submission guidelines provided online, while primers were provided by Microsynth. Samples were sent for sequencing in standard 1.5ml tubes at room temperature and results were available online within 1-2 business days. Sequences received were aligned to *in silico* generated reference constructs using SnapGene software. Sequences were checked for quality by inspecting base calling files for duplicate peaks, signal-to-noise ratio, and sequence length before base calling peaks degraded.

DNA transfection

DNA transfection was performed using a total of 3.2 µg per 1 kb plasmid size (e.g., 32 µg for a 10 kb plasmid) of purified plasmid DNA per reaction. Multiple plasmids were transfected at the same time using the same copy number of plasmid DNA per reaction. 5x10^6 HEK293TLX cells were seeded into each of 4 10cm Ø dishes and incubated overnight to adhere to the plate. Plasmid DNA was added to a total of 2mL Opti-Mem and mixed thoroughly by vortexing. In a separate tube, 80µl Lipofectamine 2000 was added to 2mL Opti-MEM and vortexed thoroughly. The 2 Opti-MEM solutions were combined, vortexed thoroughly and incubated for 20

minutes at room temperature. 1ml of the combined solution was added dropwise to each of 4 10cm Ø dishes and incubated for 6 hours or overnight at 37°C and the medium was replaced with fresh high glucose DMEM medium containing 10% FBS and 200µM sodium pyruvate.

Lentivirus production and purification

Lentivirus production was initiated by transfecting HEK293TLX cells according to the protocol above, and cells were transfected using the plasmid DNA listed in the table below:

Table 20 Plasmids for lentiviral production

Name	Size [bp]	Mass [µg]
pMD2.G	5822	18,65
psPAX2	10717	34,29
Plasmid of interest	Variable	Variable

Lentiviruses are produced in HEK293TLX cells and released upon cell lysis, resulting in lentiviral accumulation in the supernatant. The supernatant was collected 48- and 72-hours post-transfection and fresh medium was added at the 48-hour time point. The viral solution was combined and centrifuged at 500g for 10 minutes, and the supernatant was additionally filtered through a 0.45µm filter. The viral solution was added to a Vivaspin 20 column and centrifuged for 1 hour at 3000g or until the total volume was < 500µl. Concentrated virus was aliquoted and stored at -80°C in screw-capped cryovials.

Transduction using lentiviruses using spinfection

Lentiviral transduction of suspension cell lines was performed by spinfection. 250,000 cells in 1ml medium containing 10µg/mL polybrene were added to a 24-well plate and 50µl of concentrated virus solution was added to the cell suspension and mixed by pipetting. The plate was sealed with parafilm and centrifuged at 37°C for 90 minutes at 500g. 100µl of fresh medium was added to the cell suspension and the cells were incubated overnight at 37°C 5% CO2. The next day, the cells were washed once in PBS and fresh medium was added to the cells.

Cells were cultured at 37°C 5% CO2 for 48 hours before selection with either puromycin (5µg/mL) or blasticidin (10µg/mL) until control cells were completely dead.

Transduction using lentiviruses using retronectin

Lentiviral transduction of primary or primary like cells (MLLr) was performed using Retronectin. Retronectin is a recombinant human fibronectin fragment containing

a cell-binding and a heparin-binding domain that binds viral particles [149]. A 24-well plate was coated by adding 200 µl of PBS containing 100 µg/mL Retronectin to each well and incubated for 2 hours at RT. Retronectin was collected and frozen for future use. The coated wells were washed once with PBS and PBS containing 1% w/v BSA was added and incubated for 2 hours at RT. The BSA solution was discarded and 450µl PBS and 50µl concentrated virus solution were added per well and centrifuged at 1000g for 2h at 37°C. The supernatant was discarded and 500,000 cells in 500µl were added to each well, centrifuged for 10min at 300g and incubated overnight at 37°C 5% CO2. The next day, the cells were washed once in PBS and fresh medium was added to the cells.

Cells were cultured at 37°C 5% CO2 for 48h before selection with either puromycin (5µg/mL) or blasticidin (10µg/mL) until control cells were completely dead.

Quantitative reverse transcriptase polymerase reaction (RT-qPCR)

RT-qPCR was used to detect and quantify RNA of genes of interest. cDNA synthesized as described above was used according to the tables below.

Table 21 RT-qPCR reaction mixture

Component	Volume [µl]
Maxima SYBR Green Master Mix	10
Forward primer (100nM)	1
Reverse primer (100nM)	1
cDNA (10-40ng/µl)	5
ddH_2O	4

Samples were measured in triplicate and the two housekeeping genes TBP and PBGD were always measured as reference.

Protein based molecular biology methods

Protein extraction and concentration determination

To isolate proteins from human cells, 1-5x10^6 cells were frozen as cell pellets at -80°C and resuspended in 60-200µl of lysis buffer, vigorously vortexed every 10 minutes for 60 minutes, centrifuged and the supernatant was transferred to a new tube.

Protein concentration was determined using the DC protein assay kit according to manufacturer's instructions and a standard curve ranging from 125- 2000 ng/ µl

SDS Page

Samples were incubated at 95°C for 5-10 minutes, residual cell debris was pelleted by centrifugation at 21,000g for 20 minutes at 4°C, and the supernatant was collected prior to gel electrophoresis. Samples were loaded onto a home-

made 10% acrylamide gel with a maximum of 40 µl wells. The gel components are listed in the table below. For reference, 5 µl of stained protein ruler (PageRuler™ Plus Prestained Protein Ladder) was loaded in one to two lanes. Electrophoresis was performed at 130 V for approximately 60 min in 1X SDS Running Buffer freshly diluted from a 10X stock.

Table 22 SDS-gel mixture

Component	Separation gel	Collection gel
30% Acrylamide	1,7 mL	330 µL
1,5 M Tris/HCL, pH 8,8	1,3 mL	-
0,5 Tris/HCL, pH 6,8	-	500µL
10% SDS	50 µL	20 µL
ddH_2O	2 mL	1,15 mL
TEMED	2 µL	2 µL
10% APS	50 µL	20 µL

Western Blot

After gel electrophoresis, the gels were transferred to a nitrocellulose membrane using Trans-Blot Turbo Mini 0.2 µm Nitrocellulose Transfer Packs according to the manufacturer's instructions and blotted using Trans-Blot Turbo according to the manufacturer's instructions. Total protein staining was performed using the Revert™ 700 Total Protein Stain and Wash Solution Kit according to the manufacturer's instructions to determine the amount of protein transferred. Nonspecific binding was blocked by incubating the membrane in TBST buffer containing 5% w/v milk powder for 1 hour at RT. Primary antibodies were diluted in blocking buffer and incubated over night at 4°C on a shaker. On the next day, the blot was washed for 3x10minutes in TBST. Secondary antibodies were diluted in blocking buffer and the membrane was incubated for 1h at RT on a shaker, washed for 3x10minutes in TBST and developed at the Vilber FUSION FX.

Isolation of primary cells

Isolation of PBMCs

Human cells were isolated directly from blood samples anticoagulated using EDTA. Blood samples from AML patients or healthy donors were collected following informed consent (in accordance with the declaration of Helsinki) approval by the Ethics Review and anonymized before use. PBMCs were isolated using density gradient centrifuged via SepMates according to the manufacturer's instructions and cells were frozen in RPMI1640 medium supplemented with 20% FCS and 10% DMSO.

Isolation of HSPC

HSPC were isolated from PBMC isolated from human cord blood using the direct and indirect CD34 microbead kit according to the manufacturer's instructions.

Cell biology methods

Cultivation of cell lines

AML cell lines (EOL-1, HL-60, HNT-34, Kasumi-1, Kasumi-3, Molm-13, SKM-1, SKNO-1) were cultivated according to the providers protocol with the additive of 1% P/S.

HEK293T Lenti X cells were cultivated according to the provider's protocol with the additive of 1% P/S. High glucose DMEM was used as a cultivation medium during virus production.

Cultivation of MLLr cells

MLLr cells were cultivated in human StemMACS™ HSC Expansion Media XF supplemented with 50 ng/µm FLT-3-L; SCF, G-CSF; IL-3; IL-6, TPO and 0,375 µM SR-1, UM729. Cells were split 3 times a week and cell concentration adjusted to 1x10^6 cells/ mL

Colony Forming Unit (CFU) Assay

To measure the clonogenic activity cells were cultivated in of semi-solid methylcellulose- based MethoCult medium according to the table below:

Table 23 Cell numbers for CFU Assay

Cell type	Cell number [n]
Cell lines	1000
MLLr cells	5000

Cells were counted, centrifuged at 300g for 10 minutes and resuspended to the desired cell number in 100 µL. The cell suspension was added to 4 mL MethoCult, vortexed vigorously and incubated for 5 minutes at RT. The MethoCult cell suspension was aspirated using a needle and syringe and triplicates of 1 ml of the solution were transferred to 35 x 10 mm cell culture dishes. The cell culture dishes were transferred to a 145 x 20 mm cell culture dish containing an open 35 x 10 mm dish of PBS and cultured for 14 days at 37°C and 5% CO2.

At the end of the incubation period, the colonies formed were counted under a light microscope.

For secondary CFU assays, the MethoCult cell suspension was liquefied with 30 ml of 37°C warm PBS, washed again with 20 ml warm PBS, counted and the CFU assay was performed again as above.

Fluorescence-activated cell sorting (FACS)

FACS was performed using antibodies stated in "Table 7 Antibodies and nanobodies" according to [150], and analyses on a BD LSR II Fortessa.

FACS sorting

Cells were sorted by the Flow Cytometry Core Facility – Berg according to the gating strategy described in Figure 10:

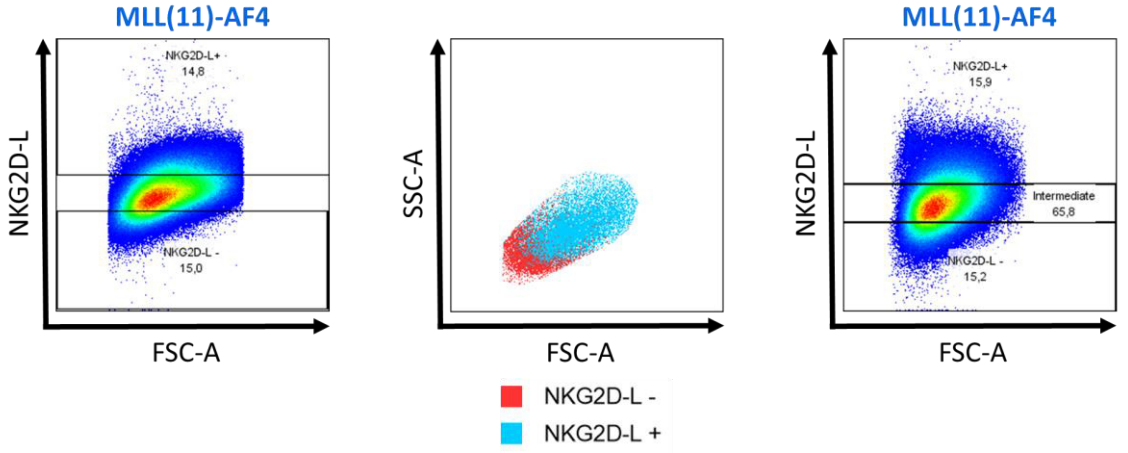

Figure 10 Illustration of FACS sorting strategy

Resazurin assay

Resazurin was used to measure metabolic activity via a redox reaction carried out by the dehydrogenase enzymes to reduce resazurin to resorufin. The absorbance peaks for resazurin and resorufin were found to be 610 and 575 nm, respectively.

10% of the total volume of resazurin was added to cell suspensions or the corresponding control cell culture medium and the cells were incubated for 4 hours before measuring the absorbance at 575 nm using a spectrophotometer. Background values were subtracted and absolute values were expressed relative to control samples.

Treatments

Cells were counted, centrifuged at 300g for 10 minutes and resuspended in a concentration of 1x10^6/ml and 200 µl were used per well of a 96 well plate. The cell suspension was spiked with commercially available drugs, see table 4 Chemicals and reagents, as stated in specific experiments for 48h at 37°C 5% CO2.

Methods performed and written by Collaboration partners (Estelle Erkner)

Induction of MLL-AF4 (Intron 9 and 11) and MLL-AF9 (Intron 9 and 11) using CRISPR/Cas9

Genome editing with ribonucleoproteins (RNPs) was performed using the P3 Primary Cell 4D Nucleofector Kit. Before starting the work, all work surfaces were cleaned with RNase Zap. To induce a MLL-AF4 (Intron 9 and 11) and MLL-AF9 (Intron 9 and 11) chromosomal translocation, 1 µg of Cas9 protein and 1 µg of the

corresponding in vitro transcribed sgRNA were incubated for 15-30 min at RT. Per nucleofection approach, 3 x 105 HSPC were centrifuged (300 g, 5 min, RT) and resuspended in 17 µl P3 solution. After carefully mixing the cells with the Cas9-sgRNA-RNP complex, the cells were electroporated with the 4D-NucleofectorTM X Unit (program: EO-100) and incubated for 3 min at RT. The reaction was stopped by the addition of SCM. As a control, cells were incubated without RNP complex or with pmaxGFP plasmid. Cells were transferred equally into two 96-wells each (U-bottom) and cultured in SCM at 37 °C and 5% CO2. After 48 hours, 20 µM of the caspase inhibitor z-Vad-FMK was added, and the cell population was transferred to a 24-well plate for long-term cultivation after reaching a cell density of at least 1 x 106 cells/ml.

The translocation was detected by PCR and specifically designed primers. A pure CRISPR/Cas9 MLLr cell population was defined by the presence of at least 90% translocated cells detected by fluorescence in situ hybridization (see below). Design and production of sgRNA

Fluorescence in situ hybridization (FISH)

To determine the percentage of translocated cells in the culture, fluorescence in situ hybridization (FISH) was performed with a MLL1-specific two-color Breakapart probe in collaboration with the Institute of Pathology and Neuropathology at the University Hospital Tübingen.

For this, 1.5 x 10^6 cells per sample were taken from the culture, centrifuged (300 g, 5 min, RT) and washed in 1 ml PBS. After the cells were fixed in 250 µl formaldehyde (4%) on ice for 30 min, 10 µl of the cell suspension was applied to a silanized SuperFrost Plus slide. After drying, the slide was incubated in sodium citrate buffer for 40 min at 95 °C. The samples were then demineralized in water and 0.25 mg/ml pepsin working solution was applied dropwise to the slide and incubated for 4 min at 37 °C. The slides were rehydrated in an ascending ethanol series (70% and 100%) before being dried again. Both the slide and the KMT2A-Breakapart probe were heated to 37 °C for 5 min, and 4 µl of the probe was applied to the slide. Samples were covered with coverslips, sealed with Fixogum, and denatured in the HYBrite hybridization system at 75 °C for 10 min. Incubation was performed overnight at 37 °C. The next day, coverslips and Fixogum were carefully removed and samples were treated with the ZytoLight FISH-Cytology Implementation Kit according to the manufacturer's instructions. After washing three times with pre-warmed Cytology Stringency Wash Buffer SSC for 30 min, 1 min, and 5 min, respectively, the samples were dehydrated in ascending ethanol series (70%, 85%, and 100%) for 1 min each. Finally, 3.2 µl of DAPI/DuraTect solution was applied to the slide and sealed with a coverslip.

The slides were analyzed using an Axio Imager M2 and 100 cells per sample were counted to determine the percentage of KMT2Ar cells in the culture.

Statistical analysis

Data are shown as mean ± SD. Comparisons were performed using (un)paired Student t tests or one-way ANOVA. All analyses were performed with GraphPad Prism v9.4.1 and statistical significance is defined as a P value < 0.05.

Results:

As previously discussed, NKG2DL molecules are immunogens. They display the second highest polymorphisms of human protein groups, and various structurally diverse NKG2DL variants have been reported. The coexisting presence of multiple NKG2DL variants is known to be advantageous to the host in counteracting malignant immune evasion strategies. NKG2DL is not present on the surface of healthy cells, but it can be induced by cellular stress, including malignant transformation. When cells present NKG2DL, they become vulnerable to immune surveillance by cytotoxic (CD8) T cells and NK cells that express the NKG2DR. The literature describes the expression of NKG2DL in malignant cells at the mRNA level, as well as in the context of surface presentation and shedding into the supernatant as a soluble ligand form through metalloprotease shedding [115].

In cancers, such as AML, NKG2DL may be downregulated or removed from the cell surface through the shedding process, leading to cancer cell escape from immune-mediated recognition and killing. As shown by our research group, the chemotherapy-resistance leukemia initiating LSC compartment also preferentially downregulates NKG2DL surface expression leading to selective immune evasion of LSC.

However, there is limited understanding of the intracellular expression and function of NKG2DL in healthy cells, as well as the mechanisms that lead to surface expression during malignant transformation.

The aim of this thesis is to investigate NKG2DL expression in healthy hematopoietic cells at steady state and in hematopoietic cells that have undergone malignant transformation, in order to characterize a potential system for studying changes in NKG2DL expression profiles.

To achieve this goal, I systematically characterized NKG2DL expression levels from mRNA to release as sNKG2DL using RT-qPCR, western blotting, ELISA and immunofluorescence assays in healthy hematopoietic cells, including HSPC under steady-state conditions. Additionally, I evaluated the safety and potential impact of current (azacytidine, cytarabine and venetoclax) and potential future AML therapies (PARP1 and GATA2 inhibition) in relation to NKG2DL expression. The impact of malignant transformation resulting from the introduction of breakpoints in the MLL1 gene on NKG2DL expression was characterized similarly to healthy hematopoietic cells. The latter may serve as a novel system to investigate NKG2DL biology in LSC. Crucially, an improved understanding of NKG2DL presentation and retention in these malignant cells could lead to novel strategies for targeting therapy resistant cancer cells such as AML LSC.

Main Results:

Phenotyping of healthy PBMCs and HSPC

According to current literature [151], NKG2DL are not present on the cell surface of healthy cells. To characterize the NKG2DL landscape across different cellular populations, I first aimed to confirm this phenotype. To achieve this, I conducted flow cytometry experiments and analyses using NKG2D-Fc, a commercially available fusion protein binding to all known (and unknown) NKG2DL, to detect NKG2DL surface expression in various adult healthy PBMC compartments. Secondary only control (Streptavidin-PE) was used to determine NKG2DL positivity. I analyzed freshly thawed NK (CD3-/CD56+) cells, T cells (helper (CD3+/CD4+) and cytotoxic (CD3+/CD8+)), B cells (CD19+), monocytes (CD14+) (n=6), as well as HSPC (CD34+/n=15) for their surface expression of indicated lineage markers (Figure 11, for gating strategy see Figure 21, supplementary data). HSPC were isolated from cord blood, containing small amounts (approximately 1 %) of HSPC, via magnetic activated cell sorting (MACS) using CD34 beads. I observed the absence (<5 %) of surface NKG2DL in NK cells (mean 3.8 %, standard deviation (SD) 3.3 %), both CD4 (mean 1.4 % SD 1.3 %) and CD8 T cells (mean 0.8 %, SD 0.9 %), freshly isolated monocytes (data not shown) and CB HSPC (0%). Conversely, I noted a NKG2DL surface signal for 2.6 to 46.6 % of B cells and 85 to 97 % for viable frozen and thawed monocytes, which may have been induced for surface presentation during the freeze-thaw process. The absence of surface NKG2DL that I observed was consistent with current literature findings in all analyzed cell types, except for the positive signal observed in thawed monocytes (Figure 11). This might reflect the fact that this cell subpopulation is particularly prone to react with NKG2DL surface upregulation to cellular stress (e.g., as occurring during the freeze-thaw process).

Next, I investigated NKG2DR surface expression on PBMC subsets. Current literature suggests that NKG2DR is present on NK cells and CD8 cytotoxic T cells, but is absent from CD4 helper T cells, B cells and monocytes which I could confirm. In this experiment, I examined the PBMC compartments (NK, T-CD4/8, B cells and monocytes) of six individuals by flow cytometry. I was able to detect NKG2DR expression in NK and cytotoxic T cells, but not in T helper cells, B cells and monocytes, and the results are consistent with the current literature (Figure 16).

HSPC are typically absent or present at a very low frequency in adult human blood [153], making it an ineffective source for HSPC isolation. Therefore, cord blood samples, which contain approximately 1% HSPC, were used for isolation [154]. Due to the rarity and small volume of cord blood samples (only up to 20-100 ml), only 200,000-1,000,000 cells could be isolated per sample. However, this amount is not enough to analyze the same donor with various molecular analysis methods, such as Western blot and image flow cytometry. Therefore, I expanded

HSPC *in vitro* for five days in StemMACS™ HSC Expansion Media XF medium containing cytokines (for details refer to table 5). I used flow cytometry to analyze samples (n=5) for stemness (CD34, absence of CD38, CD117), myeloid (CD33), and lymphoid (CD3 and CD19) lineage markers at both day 0 (start of culture) and day 5 (Figure 11).

On day 0, the average CD34 expression in isolated HSPC was 93.7%. Over the next 5 days, this expression decreased to an average of 77.9% (Figure 11 D). Additionally, there was a 46.5% decrease in CD117 expression and a 96.9% increase in CD33 expression over the same period. However, culture for 5 days did not affect the expression of CD3, CD19, CD38, and NKG2DL (Figure 11 E). Together, these data suggest that while *in vitro* cultures lead to progressive loss of stemness they do retain cellular populations with progenitor potential over longer periods of time.

After confirming the absence of NKG2DL on the cell surface, I investigated whether the lack of surface expression was due to healthy cells not expressing NKG2DL or due to cells shedding them through metalloprotease-mediated cleavage, similar to cancer cells. To examine the potential shedding of NKG2DL, I harvested the supernatant from HSPC cultured for 5 days and performed ELISAs designed to detect the three most commonly occurring human NKG2DLs: MICA, MICB, and ULBP1, to measure sNKG2DLs (Figure 12 A). Surprisingly, measurable levels of sMICA and sMICB were observed, but not sULBP1, similar to findings in AML cell lines (SKM-1, Kasumi-1) (Figure 25, supplementary data).

After demonstrating that HSPC shed NKG2DL, I collected HSPC (n=5) and PBMCs (n=7) to analyze the mRNA and protein expression of MICA, MICB, and ULBP1 in freshly isolated healthy cells. I conducted RT-qPCR (n=5) and Western blot (n=7 and 5, respectively). Detectable mRNA and protein levels were observed in all analyzed samples. To gain a better understanding of ligand localization, I used imaging flow cytometry (Imagestream) and analyzed the images using IDAS software. I observed that all ligands showed intracellular localization (Figure 12) (n=5 samples with n=10000 cells, 2 representative pictures shown)) and Figure 23 for the full data set).

A

Cell Type	Markers
B-cells	CD19+
NK-cells	CD3-; CD56+
CD4 T-cells	CD3+; CD4+
CD8 T-cells	CD3+; CD8+
Monocytes	CD14+
HSPCs	CD34+

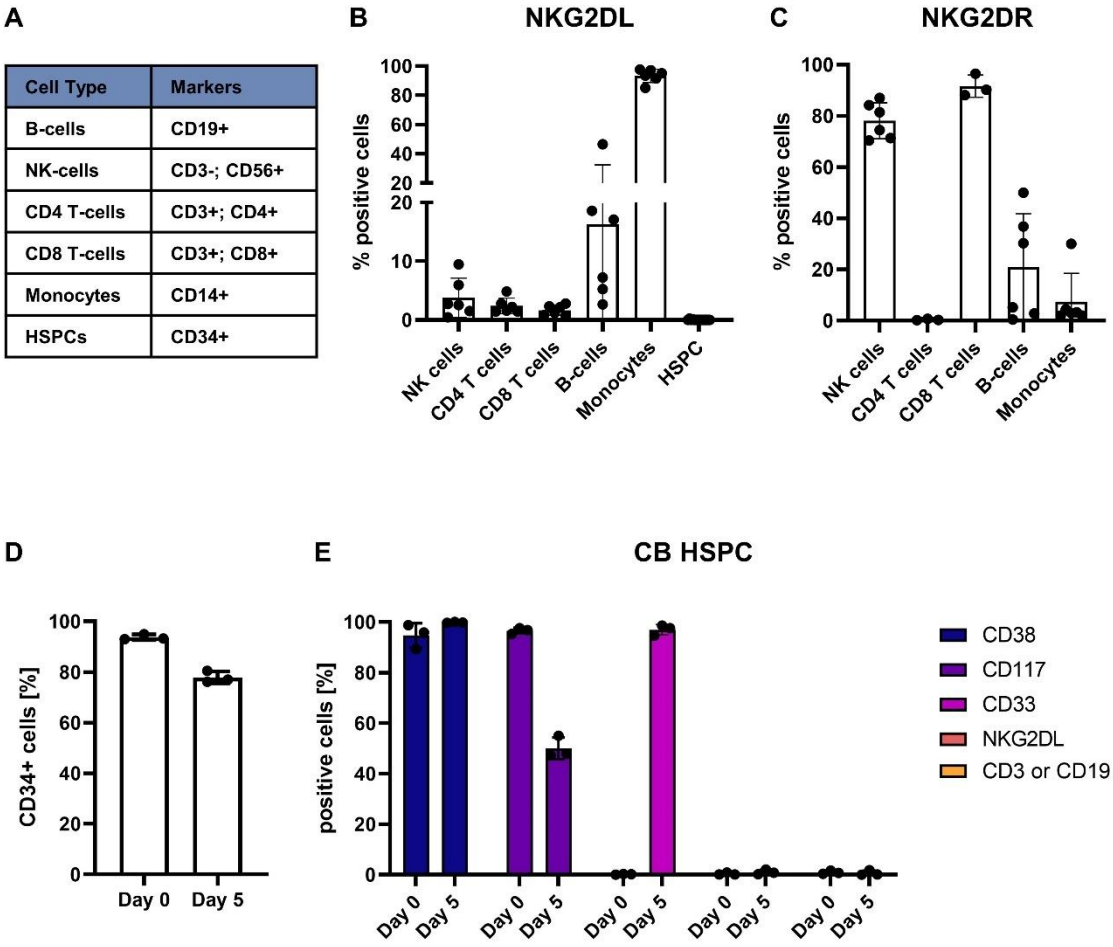

Figure 11 Phenotyping of NKG2DL and NKG2DR in PBMCs and HSPC
(A) Tabular overview of markers used to identify PBMC subtypes (B) Flow cytometry analysis using NKG2D-Fc to determine percentages of NKG2DL surface expression of PBMC subtypes (C) Flow cytometry analysis to determine percentages of NKG2DR surface expression of PBMC subtypes (D) Flow cytometry analysis to determine CD34 expression of CB HSPC at day 0 and day 5 after isolation (E) Flow cytometry analysis to determine CD38, CD117, CD33, NKG2DL, CD3 and CD19 expression of CB HSPC at day 0 and day 5 after isolation

Intriguingly, the mRNA levels of NKG2DL were even higher in healthy cells than in AML cell lines (Figure 24, supplementary data). Specifically, MICA mRNA levels were 4-fold higher in HPSCs and 8-fold higher in PBMCs, while MICB mRNA levels were 2 and 6-fold higher, respectively, and ULBP1 mRNA levels were 20 and 5-fold higher, respectively (Figure 12 B). The size of the MICA/ULBP1 protein varied greatly in the HSPC (n= 4) and PBMC (n=8) samples likely representing different isoforms, but the protein signals remained consistent within cell types. Protein signals ranging from 35 to 130 kDa were observed. Strong bands were present at 50 kDa for MICA and 35 and 130 kDa for ULBP1 in PBMCs, and at 35 kDa for MICA and 35 and 70 kDa for ULBP1 in HSPC. Representative images are shown in Figure 12 C/D (Figure 23 for extended data). Imagestream was performed on unMACSed CBMCs, and CD34 was used as a cell surface marker

for HSPC, providing membrane staining. A clear intracellular signal was observed for both MICA and ULBP1 in all analyzed cells (n=5,10000 cells per n) (Representative images are shown in Figure 12 E/F and extended data in Figure 23, supplementary data).

In summary, I observed that - while absent on the cell surface - NKG2DLs are very robustly expressed intracellularly in healthy hematopoietic cells, indicating that NKG2DL proteins are either retained in the cytoplasm and/or transported to the cytoplasmic membrane where they are immediately shed from the cell surface. While a combination of both mechanisms cannot be excluded, I could confirm shedding of NKG2DL into culture supernatants. These findings suggest a possible function of intracellular NKG2DL in the immediate response of healthy cells to stress stimuli as they would be readily available for cell surface presentation.

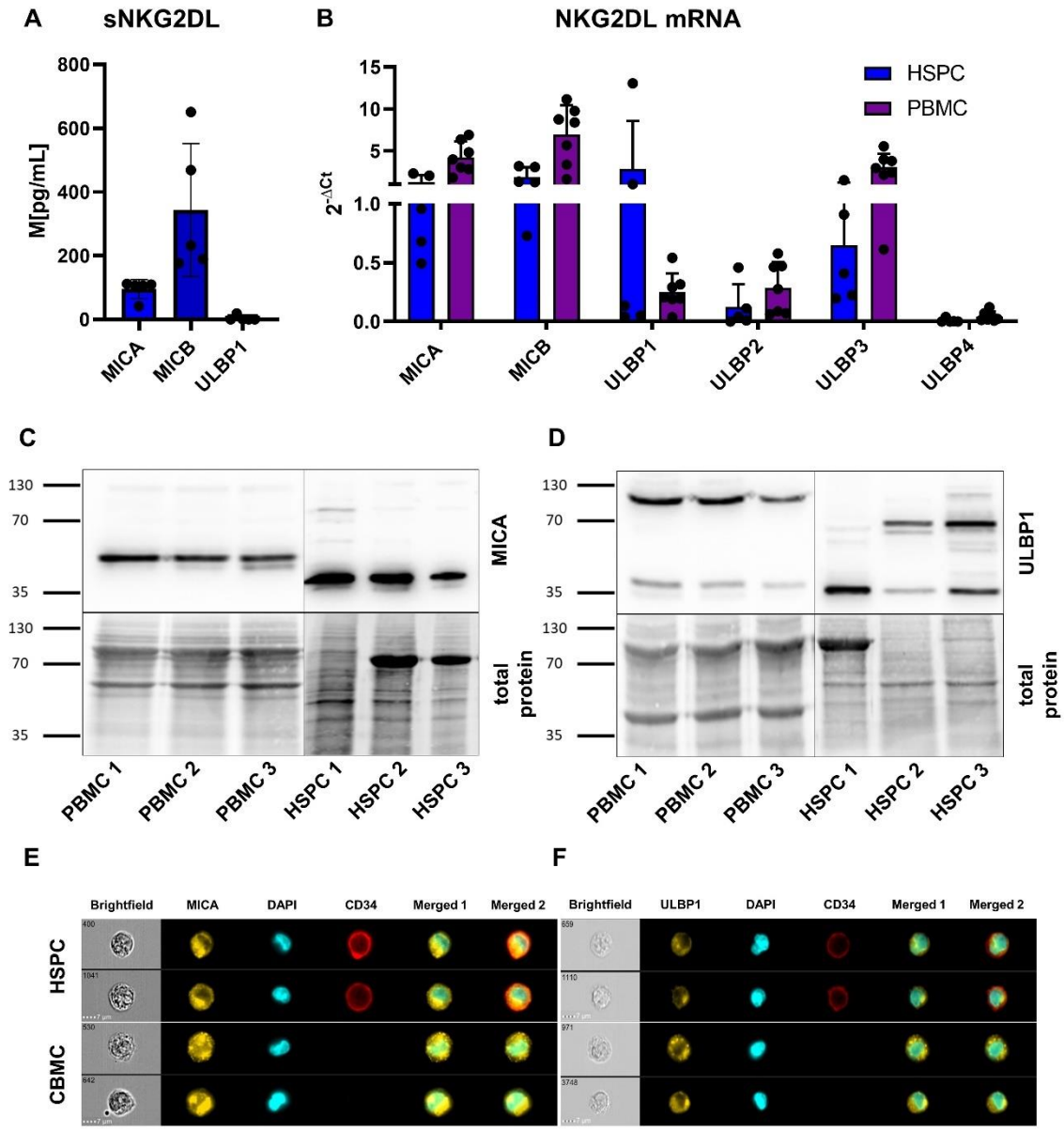

Figure 12 *NKG2DL are absent on the cell surface of healthy hematopoietic cells but are intracellularly expressed*
(A) ELISA analysis of sNKG2DLs (MICA, MICB, ULBP1) in HSPC culture medium (n=5) (B) Flow cytometry analysis using NKG2D-Fc to determine percentages of NKG2DL surface expression in healthy PBMC (n=6) and HSPC (n=15) (C) Comparison of NKG2DL mRNA level of PBMCs (n=7) and HSPC (n=5) (D/E) Western Blot Analysis of MICA and ULBP1 in PBMCs and HSPC (n=3 representative) (F) Image flow cytometry analysis using antibodies for MICA/ULBP1. Representative images of HSPC and CBMCs (Brightfield (upper left, cell number), DAPI (cyan), NKG2DL (yellow), CD34 (red), Composite) (n=2 representatives). Scale bar, 7 µm

Screening AML cell lines for negative control

As positive signal and expression were observed at all stages in all test samples, the lack of a negative control raises concerns about assay, primer, and antibody specificity. To identify a potential negative control that does not express NKG2DLs proteins at any level, I first screened the AML cell lines SKM-1, Kasumi-1, HNT-34, EOL-1, SKNO-1, HL-60, Molm-13 and Kasumi-3 for NKG2DL surface expression by flow cytometry. All studied cell lines express NKG2DL, with varying levels of surface expression. The Kasumi-1 cell line showed the least expression, while SKM-1 showed the highest (Figure 13).

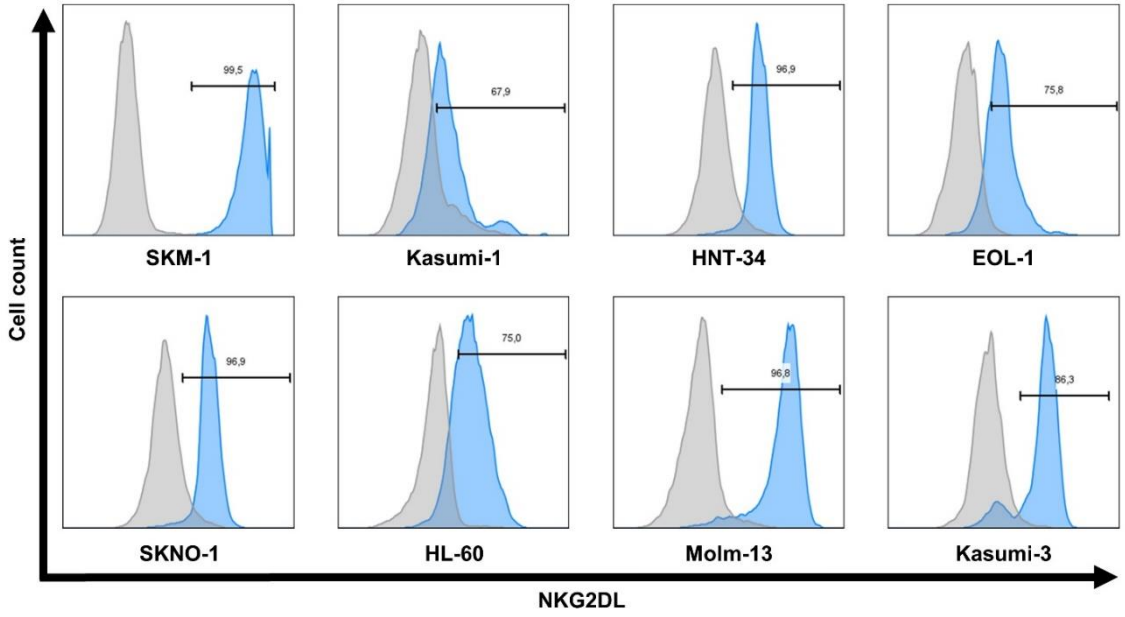

Figure 13 AML cell lines show surface expression of NKG2DL
Flow cytometry analysis using NKG2D– Fc to determine NKG2DL surface expression in AML cell lines SKM-1, Kasumi-1, HNT-34, EOL-1, SKNO-1, HL-60, Molm-13, Kasumi-3. Secondary AB only control (grey) stained (blue)

Generation of MICA, MICB, ULBP1 knockout cell lines as assay controls

To generate a negative control, I aimed to create NKG2DL knockout cell lines in SKM-1 cells, which showed the highest frequency of NKG2DL positive cells as well as the highest mean fluorescence intensity (MFI) among all cell lines.

I used a dual lentiviral transduction system and CRISPR-Cas9 technology to achieve specific knockouts for the three major NKG2DLs: MICA, MICB, and ULBP1. CRISPR-Cas9 is a gene-editing technology that enables the removal, addition, or modification of DNA sequences. It consists of two key molecules: (I) the Cas9 enzyme, which cleaves DNA strands at specific sites, and (II) a designed gRNA sequence, which forms a complex with and guides Cas9 to the complementary DNA sequence where it introduces a DNA double strand break

(DSB). A knockout of the target gene occurs due to defects introduced by DSB repair and subsequent nonsense-mediated decay of the mRNA.

In a first step, the cells were lentiviral transduced to stably express Cas-9 and a blasticidin resistance, which was used for antibiotic-mediated selection of Cas9+ cells (see section cloning strategy NKG2DL knock out). In a second step, Cas9+ cells were lentiviral transduced with a plasmid carrying the gRNAs sequence and puromycin resistance gene, which was again used for antibiotic-mediated selection. Single knockouts were performed using all available gRNAs from the Toronto library, including three gRNAs for MICA and four gRNAs for MICB and ULBP1, respectively [142]. Eleven stable SKM-1-KO cell lines were created (Figure 14).

Flow cytometry was used to confirm successful knockouts by detecting surface expression of MICA, MICB, and ULBP1 in all eleven knockout cell lines using antibodies specific for each protein. Successful knockout of MICA was observed with gRNA No. 3 and ULBP1 with gRNA No. 2, as evidenced by the absence of protein signal. However, none of the gRNAs tested for MICB resulted in protein absence on the surface (Figure 14 B).

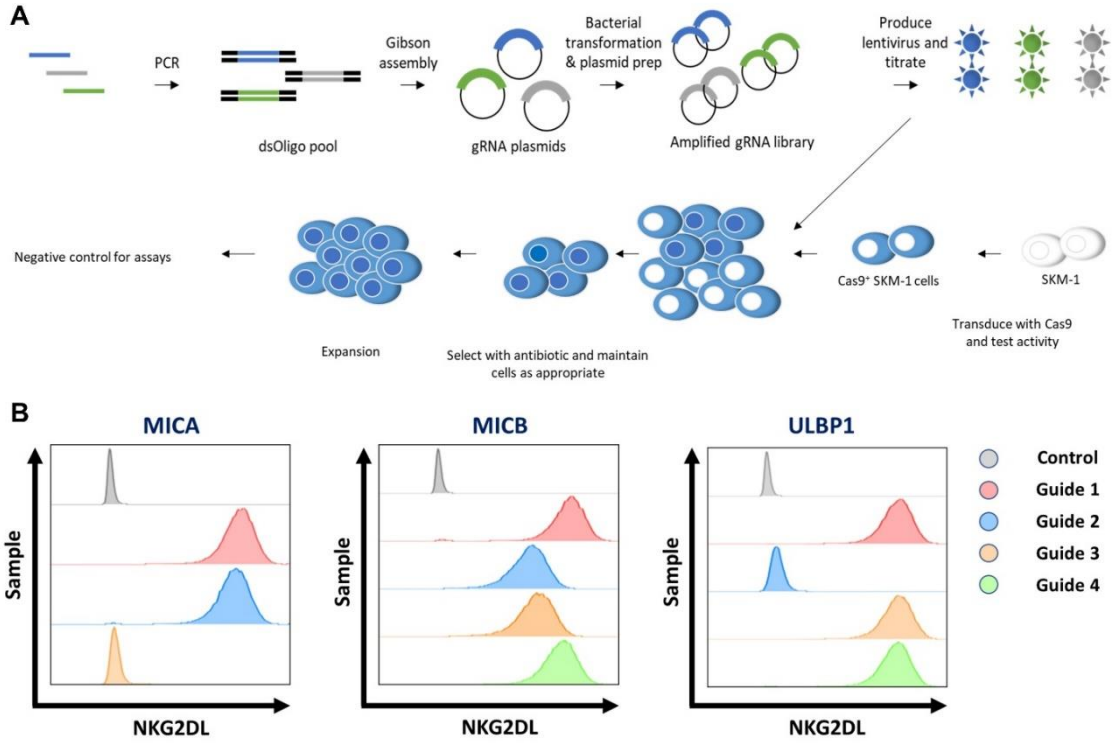

Figure 14 Creation of SKM-1-MICA/ULBP1-KO cell lines
(A) Schematic of the creation of SKM-1-KO cell lines using a dual lentiviral system (I) introduces Cas9 (II) introduces gRNA targeted against specific NKG2DL (MICA, MICB, ULBP1) (B) Flow cytometry analysis for NKG2DL (MICA, MICB, ULBP1) to screen for NKG2DL KO.

The specificity of antibodies and primers for RT-qPCR, Western blot and image flow cytometry assays was tested using the SKM-1-MICA-KO and SKM-ULBP1-KO cell lines in addition to unmanipulated AML cell lines. The mRNA analysis was performed using RT-qPCR, and no measurable mRNA levels for MICA and ULBP1 were detected in the respective KO cell lines. However, the mRNA levels of NKG2DLs that were not affected by CRISPR-Cas9 knockout (MICA, MICB, ULBP1-4) remained unaffected. SKM-1-Cas9 Cells transduced using a safe guide RNA (SKM-1-SG) were used as control (Figure 15 A). Western blot analysis revealed clear protein signals for both MICA and ULBP1 in all AML cell lines, while the corresponding SKM-1 KO cell lines showed an absence of NKG2DL protein signal (Figure 15 B/C). Using image flow cytometry, no signal for MICA and ULBP1 was detected in their respective knockout cell lines, confirming successful knockout of MICA and ULBP1 without affecting the signal of the other NKG2DL.

Although the negative controls characterized here are only specific for MICA and ULBP1, these results confirm the robustness and specificity of the assays and tools used to characterize NKG2DL expression profiles in healthy cells. Absence of specific signals in KO cell lines indicates that the previously described detection of NKG2DL at different levels in healthy cells is indeed specific.

Current therapies for AML do not affect the surface expression of NKG2DL in HSPC.

In the field of AML, the absence of NKG2DL can serve as a marker for detecting chemotherapy resistant LSC. Studies have shown that PARP1 suppresses the surface presentation of NKG2DL, but inhibiting PARP1 genetically or pharmacologically can induce NKG2DLs on the surface of LSC. However, this effect is not observed in cord blood HSPC [73]. In previous experiments, HSPC isolated from cord blood were used. However, as AML therapies are predominantly administered to adult patients (with a mean age of 68 [155]) HSPC isolated from adult healthy probands (allogenic blood donations) or patients (autologous blood donation) will be used for future experiments. As a similar phenotype was observed in HSPC (absence of surface NKG2DL, but intracellular presence) as in LSC (Figure 11/12), the effects of current clinical treatments of AML, inhibition of PARP1 on NKG2DL surface expression in adult PBMCs and HSPC, which are directly co-treated alongside AML cells, were investigated (Figure 16). In addition, we explored the effects of GATA2 inhibition on NKG2DL expression in our system. GATA2 was identified in a CRISPR-Cas9 screening project in our lab as a potential other regulator of NKG2DL expression in AML (Rudat *et al*, unpublished).

Adult PBMCs containing HSPC were obtained from healthy individuals (allogenic stem cell donations, n=12) or patients with non-hematopoietic cancers (autologous stem cell donations, n=6) administered G-CSF to mobilize HSPC from the bone marrow to the peripheral blood during routine clinical procedures.

Residual frozen material (not used in clinical procedures) was analyzed in accordance to ethical approval according to the methods outlined in section isolation of PBMCs, Figure 16 A. Isolated PBMCs of these samples were treated for 48h with azacytidine (5 µM), cytarabine (1 µM, determined in Figure 28, supplementary data), and venetoclax (1 µM), as well as the PARP1 inhibitor AG-14361 (10 or 20 µM) or respectively the GATA2 inhibitor K-7174 (20 µM), along with LPS (100 nM) to induce an inflammatory response. After treatment, I analyzed NKG2DL cell surface expression of PBMCs (CD34-) and HSPC (CD34+).

Samples were analyzed for viability, singularity and surface expression of CD34 and NKG2DL using flow cytometry (Figure 16 B). The viability of the untreated control cells showed significant variability, ranging from 11.4 % to 90.9 % for autologous samples and 22.8 % to 94 % for allogenic samples. Treatment with either currently used clinical therapies or the GATA2 inhibitor did not affect viability. Treatment with the PARP1 inhibitor AG-14361 at both 10 and 20 µM decreased sample viability from mean 52.2 % to 40.5 % and 26 %, respectively (Figure 16 C). Surface expression percentages of NKG2DL could be observed in both autologous and allogenic stem cell transplantation samples. In autologous samples I detected surface expression of NKG2DL both in CD34-expressing and CD34 non-expressing cells, reaching up to 4 % and 80 % respectively, whereas samples from allogenic stem cell transplantation showed minor surface expression (<1%) of NKG2DL in CD34-expressing and 1 to 90 % NKG2DL surface expression in CD34 non-expressing cells. Treatment with compounds however, did not significantly change NKG2DL surface expression percentage or frequency in either autologous or allogenic stem cell transplantation samples (Figure 16 C and Figure 29, supplementary data).

In summary, both autologous and allogenic samples show a low viability with high variability and minor expression of NKG2DL on the cell surface of HSPC (CD34+) (<2 % mean). Interestingly, I observed varying levels (mean <35 % for autologous and <25 % for allogenic) of NKG2DL surface expression in PBMCs (CD34-), but NKG2DL surface expression was not modulated by current AML chemotherapies or treatment with PARP1 or GATA2 inhibitors.

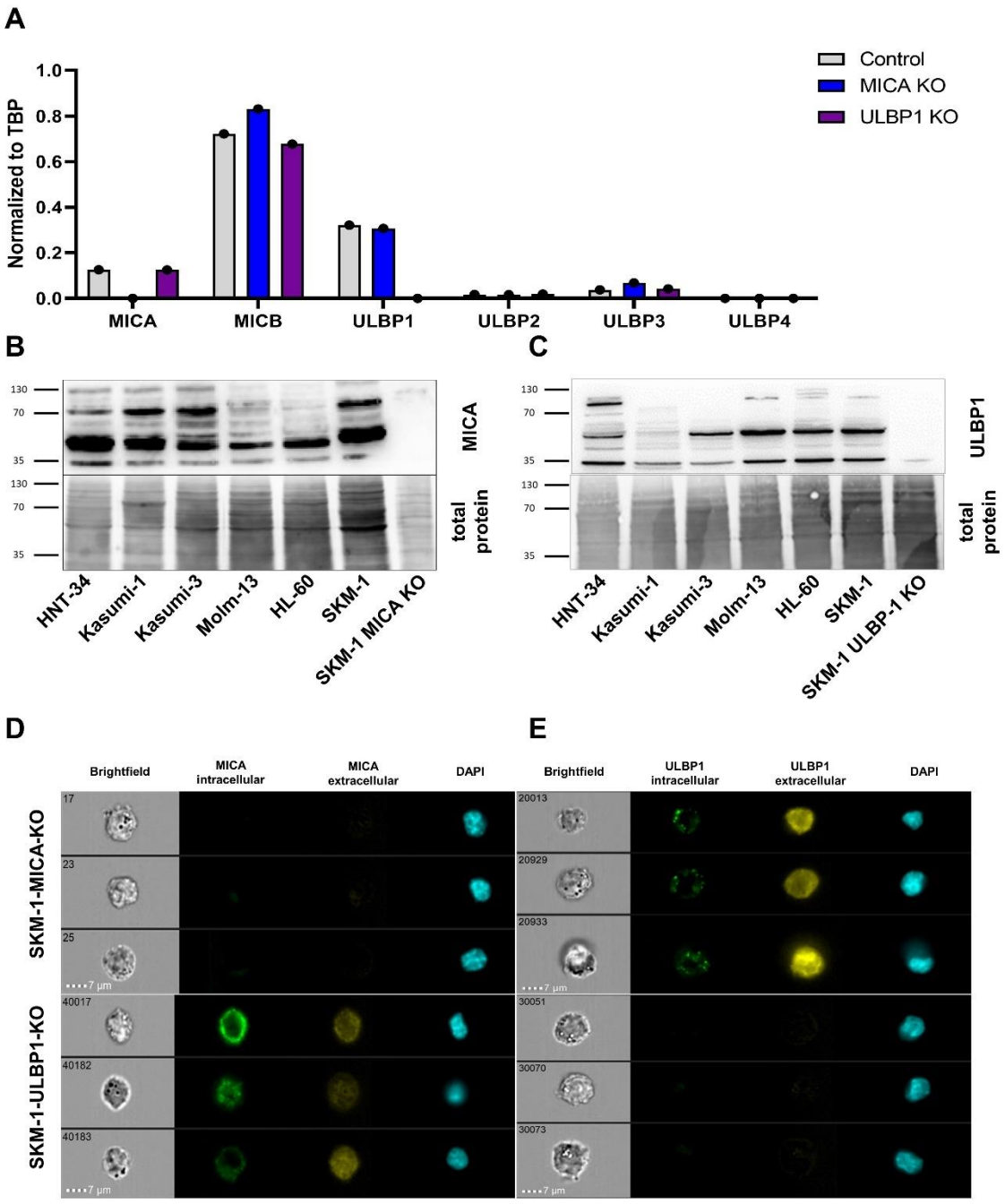

Figure 15 Knockout of MICA and ULBP1 confirms antibody and assay specificity
(A) RT-qPCR (SKM-1-SG were used as control) (D) Western blot (E) image flow cytometry in SKM-1-MICA-KO and SKM-1-ULBP1-KO cell lines to determine assay specificity (Brightfield (upper left corner, cell number), NKG2DL (intracellular, green; extracellular, yellow). Scale bar, 7 µm.

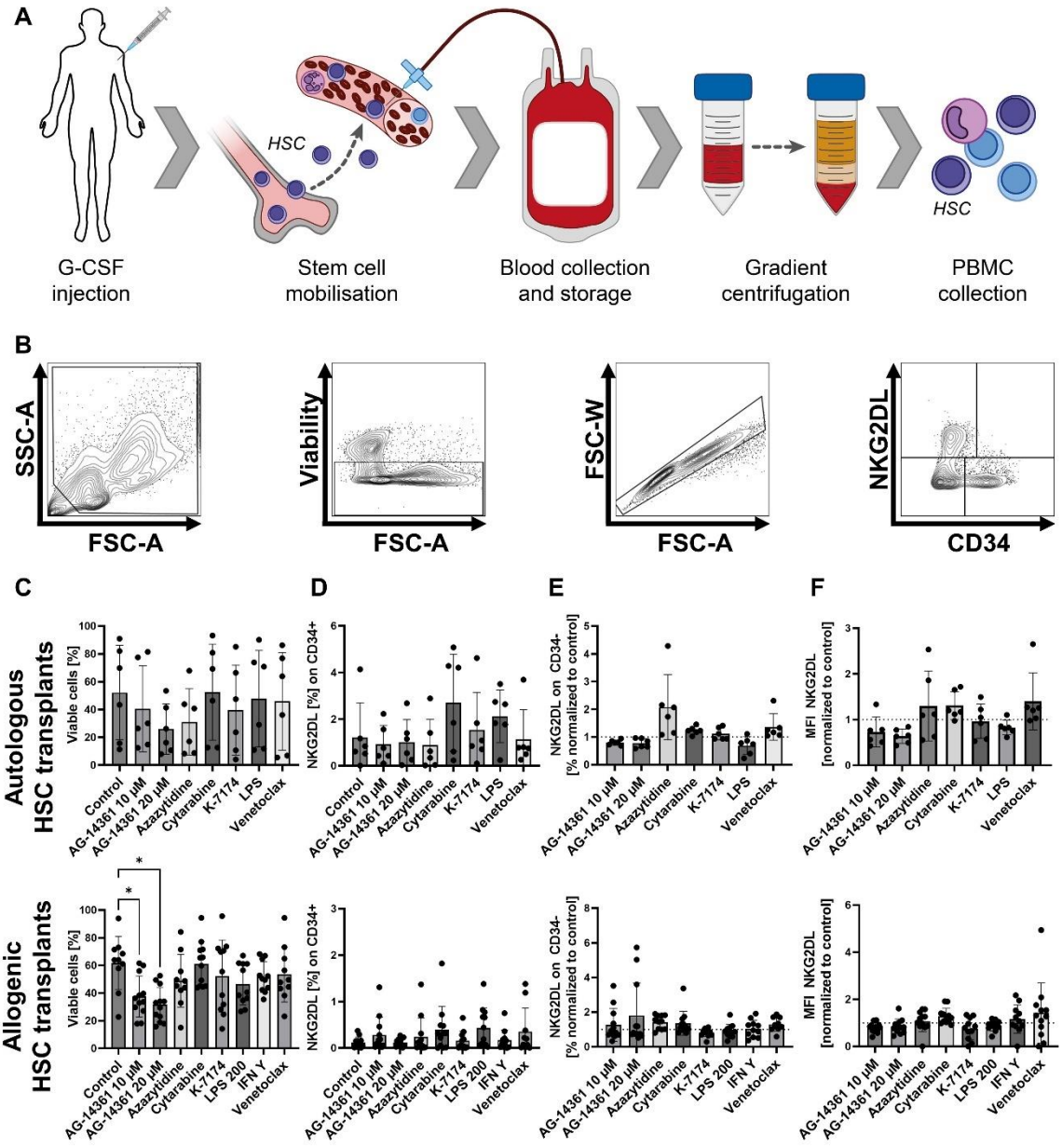

Figure 16 Current therapy does not affect NKG2DL surface expression of healthy HSPC
(A) Visual representation of methodology: Patients/probands are treated with GCSF to mobilize HSPC from the bone marrow to the peripheral blood. Blood is taken and frozen for an extended period. PBMCs are isolated using SepMates and cultured/treated for 48h and analyzed using FACS (B) Gating strategy to obtain percentages of CD34+-/NKG2DL+- populations. Cells are selected based on their viability, singularity, and size. NKG2DL/CD34 gating is determined using FMO controls. Flow cytometry analysis of viability (C/G), percentage of CD34+/NKG2DL + (D/H), percentage of CD34-/NKG2DL+ normalized to control (untreated cells) (E/I), MFI normalized to control (untreated cells) (F/J) treated as indicated.

MLL rearranged (MLLr) cells show distinct NKG2DL expression patterns.

I was able to show that healthy hematopoietic cells exhibit intracellular presence of NKG2DL as well as shedding of sNKG2DL into the extracellular fluids without significant levels of NKG2DL on the cell surface. In addition, I show that NKG2DL surface expression is not induced in healthy cells by current clinical AML therapy approaches in an *in vitro* cell based setting. This phenotype is reminiscent of chemotherapy resistant LSC in AML.

To explore potential differences between healthy HSPCs and LSC, the underlying mechanism of NKG2DL surface retention and presentation was further investigated. As primary human AML cells are notoriously difficult to culture *in vitro* due to their reliance on complex interactions with the microenvironment, MLLr cells were used as a surrogate system [72]. MLL is an aggressive type of leukemia characterized by the expression of fusion genes created through a breakpoint at the BCR in the MLL1 gene, which can be associated with a phenotype resembling either AML or ALL. Literature regarding the role of human NKG2DL in MLL is scarce, but distinct phenotypes regarding NKG2DL surface expression have been reported in murine MLL [73].

Using CRISPR-Cas9 technology, my collaboration partners (Rahel Fitzel and Estelle Erkner from Corina Schneidawind´s research group) genetically modified healthy HSPC derived from CB to introduce a designed MLL breakpoint at either intron 9 or 11 and in combination with fusion partner AF4 or AF9. MLLr cells, compared to HSPC, have a proliferation and survival advantage *in vitro* [137] and were cultivated over time until a pure MLL cell suspension was created. With this system, they induced three distinct MLL rearrangements: AF4 (Intron 11), AF9 (Intron 9), and AF9 (Intron 11) that I used for my experiments.

Using flow cytometry, I phenotyped MLLr cells for the lineage markers CD3 (T cells), CD19 (B cells), CD33 (myeloid cells), and CD34 (stem cells) and NKG2DL (Figure 26, supplementary data). All MLLr cells displayed a clear lineage phenotype associated with AML blasts (CD3/CD19/CD34- and CD33+). Additionally, I observed unique NKG2DL surface expression profiles for each translocation (Figure 17 and Figure 27, supplementary data).

Specifically, MLL-AF4 (Intron 11) samples between 34.2 to 72.1 % (mean 53.6 %, SD 16.6 %) of cells showed surface NKG2DL expression (n=6), whereas nearly all MLL-AF9 (Intron 9) cells showed a NKG2DL surface expression (mean=96.2 %), SD 3 % n=5). In contrast, nearly no surface NKG2DL was detected in MLL-AF9 intron 11) cells (mean= 4.52 %, SD 3.7 %, n=7) (Figure 17 B). To analyze the shedding of NKG2DL in MLLr cells, they were cultured for 5 days, and the culture medium analyzed using ELISA. I used AML cell lines (SKM-1, Kasumi-1 and HNT-34 (Figure 17 C-E, Figure 25, supplementary data) as positive controls to quantify sMICA, sMICB, and sULBP1. In comparison to HSPC or AML cell lines, I observed a significantly lower amount of sMICA in the supernatant, which, however, was still above the detection limit level for MLL-AF4 (Intron 11) (3.0-fold) and MLL-AF9 (Intron 9) (5.9-fold), while no sMICA could be detected for MLL-AF9 (Intron 11) (Figure 17C). For sMICB, I obtained similar results as for sMICA, except for MLL-AF4 (Intron 11), which showed similar mean levels of sMICB as HSPC (Figure 17 D). Interestingly, similar to HSPC, no sULBP1 was detected in any of the samples analyzed, except for 2 out of 9 MLL-AF9 (Intron 11) samples measured (Figure 17 E).

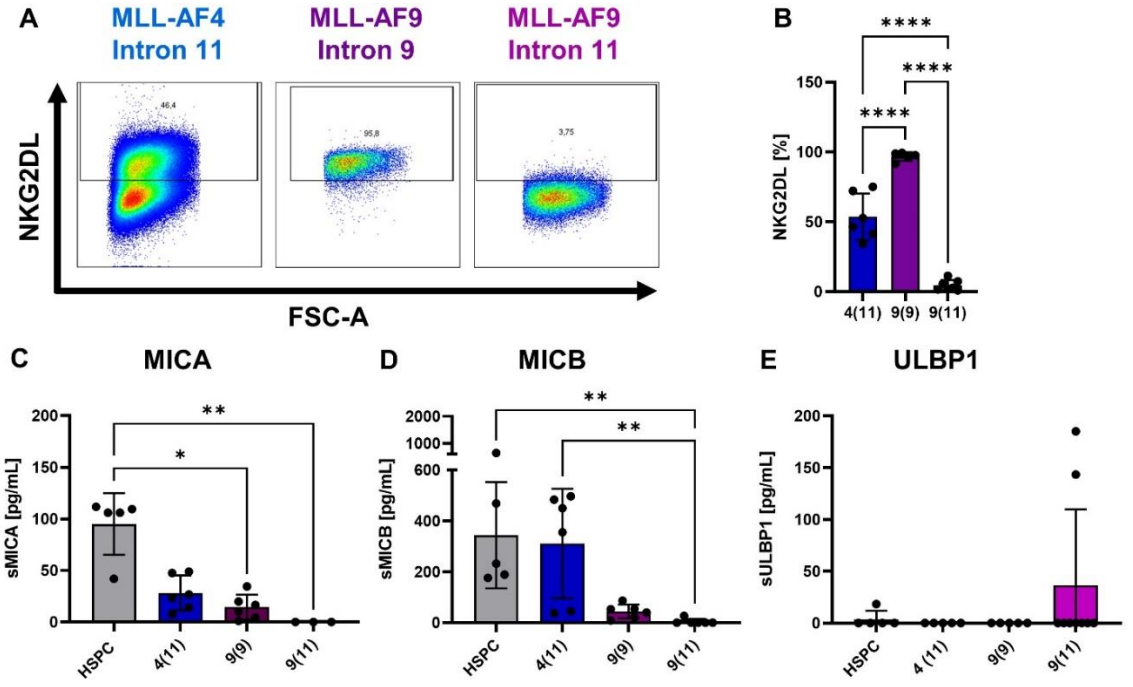

Figure 17: MLL Fusions show distinct NKG2DL surface expression patterns
(A) Exemplary dot plots showing NKG2DL surface expression on MLLr cells from one donor as determined by flow cytometry using the NKG2D-Fc to stain cells. (B) Shown are additional MLLr cell lines generated from a total of n=6 donors and analyzed as described for panel A. (C-E) ELISA analysis of sNKG2DL (MICA, MICB, ULBP1) of cultivated (5 days) HSPC (control, n=5) and MLLr cells (n=5).

Using RT-qPCR to examine NKG2DL mRNA levels in MLLr cells, similar levels of NKG2DL mRNA were observed in MLL rearrangements (n=5 per rearrangement) compared to HSPC (n=5) for all NKG2DLs analyzed except MICA. MICA mRNA levels in MLL-AF4/9 (Intron 11) were significantly lower (3.5- and 5.2-fold respectively) compared to MLL-AF9 (Intron 9) MICA mRNA level (Figure 18 A). Using Western blot, I visualized total MICA and ULBP1 protein levels and observed that protein size/variants varied widely between MLL translocations, similar to PBMCs/HSPC. Protein signals were observed in all donors of each MLL translocation analyzed, although their intensity varied. In MLL-AF4 (11), MICA and ULBP1 were observed with stronger bands at 50/70/130 kDa and 35/70 kDa, respectively. In MLL-AF9, both MICA and ULBP1 had higher signals at 35/70 kDa for both intron 9 and 11 (Figure 18 B/C, 3 representative samples are shown). In parallel, imaging flow cytometry presented a clear intracellular signal for both MICA and ULBP1 in all samples analyzed (10000 cells per sample) (Figure 18 D/F).

In summary, I observed that CB HSPC transformed into MLLr cells, carrying a specific translocation, presented a distinct NKG2DL surface expression pattern. In addition, I observed that all translocations, regardless of their NKG2DL surface expression, had measurable levels of NKG2DL mRNA and protein, which could also be visualized in the cell to confirm intracellular expression.

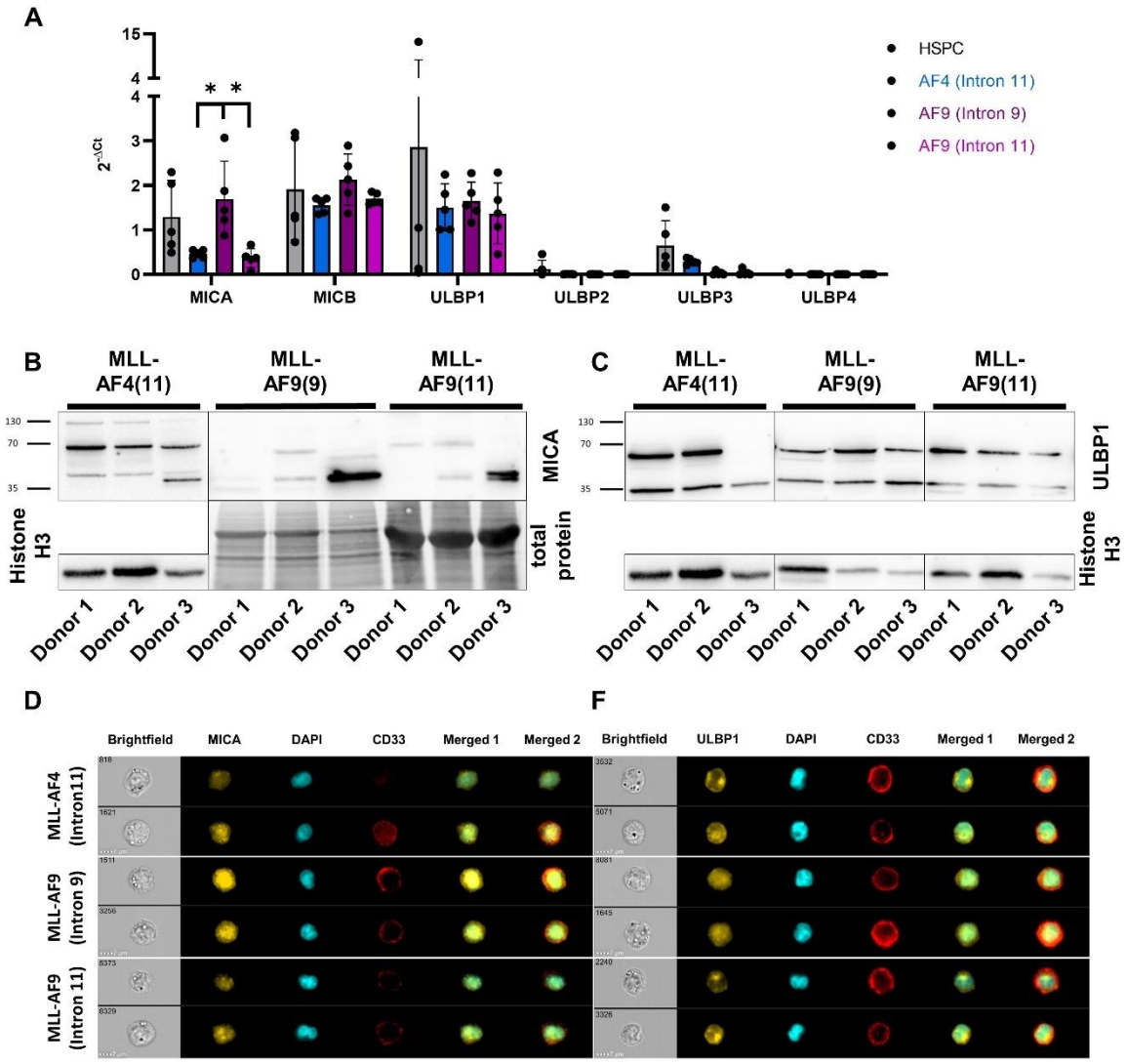

Figure 18 MLLr cells show distinct NKG2DL expression patterns
(A) Comparison of NKG2DL mRNA level of HSPC (n=5) and MLLr cells (n=5). (B/C) Western Blot analysis of MICA and ULBP1 in MLLr cells (D/F) Image flow cytometry analysis using antibodies for MICA/ULBP1. Representative images of MLLr cells (Brightfield (upper left corner, cell number), DAPI (cyan), NKG2DL (yellow), CD34 (red), Merged 1(NKG2DL + DAPI)/2 (NKG2DL + DAPI + CD33)) (n=2 representative). Scale bar, 7 µm

MLL-AF4 (Intron11) NKG2DL surface negative cells have higher clonogenic potential than their counterpart

As absence of NKG2DL on the cell surface is a marker for LSC in human primary AML samples, I investigated whether NKG2DL can also function as a stem cell marker for MLLr cells. For this application, I used MLL-AF4 (Intron 11) samples, as they display the same NKG2DL surface phenotype as primary AML (where only few patients display either 0% or 100% of NKG2DL-negative cells) and present with a mixed population of NKG2DL+ and NKG2DL- cells (partial NKG2DL surface expression).

To investigate stemness in relation to NKG2DL surface expression cells were sorted into three different populations: top, bottom 15% and intermediate. I then seeded the cells in methylcellulose to quantify the number of colonies 14 days later. This assay, called colony forming unit (CFU) assay, is a milestone in determining stemness in healthy and malignant hematopoiesis. I observed that non-NKG2DL-expressing cells, similar to what has been observed in AML, were significantly smaller than NKG2DL-presenting cells (Figure 4A/B). Interestingly, both NKG2DL-presenting and non-presenting cell populations were able to form colonies. However, non-presenting cells showed a significantly higher clonogenic activity in all samples investigated (n=9). I additionally performed CFU assay and replating assays for all MLL translocations (Section Colony Forming Unit (CFU) Assay, Figure 27, supplementary data)

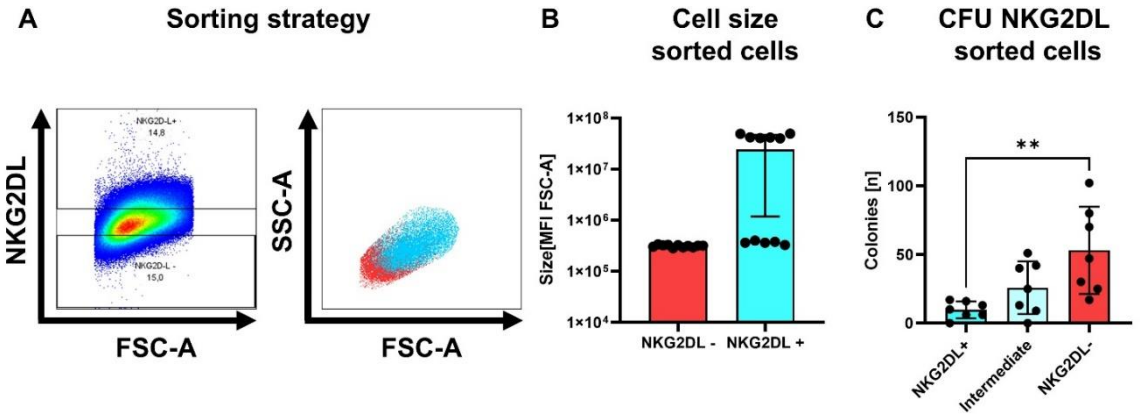

Figure 19 MLL-AF4 (Intron11) non-NKG2DL surface have higher clonogenic potential than their counterpart (A) Visual representation of flow cytometry sorting strategy. Top/bottom 15% of NKG2DL surface expressing cells were sorted and (B) analyzed for their size and granularity. (C) CFU assays of MLL-AF4 (Intron 11) samples were performed (5000 cells per well, n=7).

One of the key challenges in treating AML is the persistence of chemotherapy resistant LSC, which can cause relapse and ultimately lead to patient death. In this study, I utilized the MLL-AF4 (Intron11) samples as a surrogate system for primary AML to induce NKG2DL expression on the cell surface through drug administration previously used in this thesis. Viability of MLL-AF4 (Intron11)

donors showed minimal variation, ranging from 69.6 to 80.8 % (74.5 % mean). Treatment with PARP1 inhibitor AG-14361 (10 or 20 µM), GATA2 inhibitor K-7147 (20 µM), IFN γ (200 U/mL) and LPS (100 nM) did not significantly affect viability. However, treatment with azacytidine (5 µM), cytarabine (1 µM) or venetoclax (1 µM) significantly reduced viability to 8 %, 47.8 and 31.2 %, respectively (Figure 4D). The percentage of cells expressing NKG2DL varied widely among MLL-AF4 (Intron11) donors, ranging from 16,1 to 87,0 percent (mean 60.5 %), but the overall phenotype of partial NKG2DL surface expression was conserved. Treatments did not significantly affect NKG2DL, except for azacytidine (down to 8 % on average) (Figure 20 A). The MFI of NKG2DL surface signal was normalized to untreated (control) cells, and treatments did not significantly affect MFI, except for IFN γ, which increased MFI 3,4-fold.

Here, I established the effect of current AML treatment on MLL-AF4 (11) and healthy samples and observed the reduction of viability with the commonly known therapeutic drugs, but no effect through inhibition of potential NKG2DL regulators (PARP1 or GATA2) on viability or NKG2DL surface expression. Interestingly treatment with IFN γ did not affect cell viability, but increased NKG2DL surface percentage and MFI on MLL-AF4 (Intron 11) cells only, whereas LPS did not affect NKG2DL on either cell type. As Paczulla *et al*. previously showed, that inhibition of PARP1 resulted in upregulation of NKG2DL in the LSC compartment of AML, I performed co-treatments of the therapeutics previously administered to MLL cells with PARP1 inhibitor AG-14361 at either 10 or 20 µM in MLL-AF4 (11) and the previously treated autologous and allogenic samples.

Co-treatment with PARP1 inhibitor AG-14361 at either 10 or 20 µM did not result in a significant synergistic effect with any of the other co-administered conditions, but significant effects in viability (azacytidine and venetoclax) (Figure 20 B) and NKG2DL MFI (IFN γ) among samples were observed. Additionally, a slight, but not significant reduction in viability (5 % on average) was observed (Figure 20 B). Furthermore, the surface presentation of NKG2DL (Figure 20 E/F) and its MFI (Figure 20 H/I) were not affected by any potential synergistic effects.

In summary, MLL viability was significantly affected by all established AML treatments, but not with potential new therapies (PARP1 and GATA2 inhibition) or infection/inflammation stimuli (LPS, IFN γ). Interestingly, IFN γ, while not affecting percentage of NKG2DL surface positive cells, increased the amount of NKG2DL molecules (MFI) on the surface. Co-treatment of PARP1 inhibitor AG-14361 did not result in significant synergistic effects with other treatments administered to the cells.

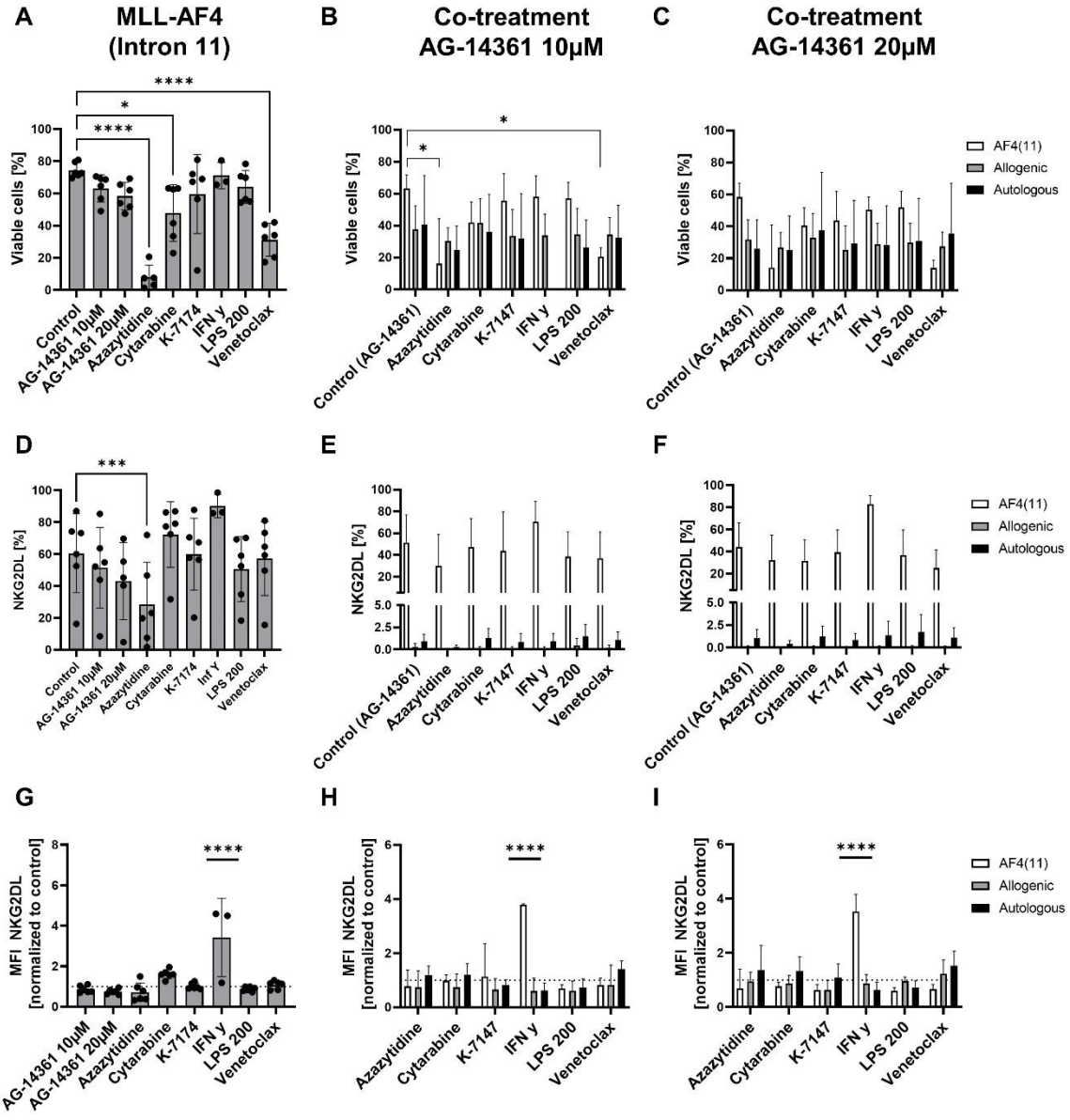

Figure 20 Co-treatment of PARP1 inhibitor AG-14361 has no synergistic effect with other AML therapeutics in HSPC and MLL-AF4 (Intron 11) samples
(A,D,G) MLL-AF4 (Intron 11) cells were treated as shown for 48h and analyzed for viability, NKG2DL expression and NKG2DL MFI via flow cytometry (for gating strategy see Figure16) (B, E, H) MLL-AF4 (Intron 11), allogenic and autologous HSPC samples were co-treated with PARP inhibitor AG-14361 at 10 µM and indicated substances (azacytidine 5 µM; cytarabine 1 µM; venetoclax 1 µM; GATA2i K-7147 20 µM, IFN γ 200 U/mL; LPS 100 nM) (C,F,I) MLL-AF4 (Intron 11), allogenic and autologous HSPC sample were co-treated with PARP inhibitor AG-14361 at 20 µM and indicated substance substances (azacytidine 5 µM; cytarabine 1 µM; venetoclax 1 µM; GATA2i K-7147 20 µM, IFN γ 200 U/mL; LPS 100 nM)

Supplementary results

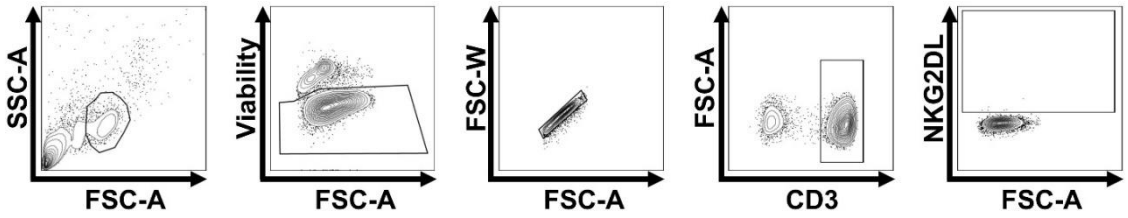

Figure 21 Exemplary gating strategy used in Figure 1
Example gating strategy to obtain percentages of NKG2DL populations in T cells. Cells are selected based on their viability, singularity, and size. NKG2DL/CD34 gating is determined using FMO controls. Flow cytometry analysis of viability

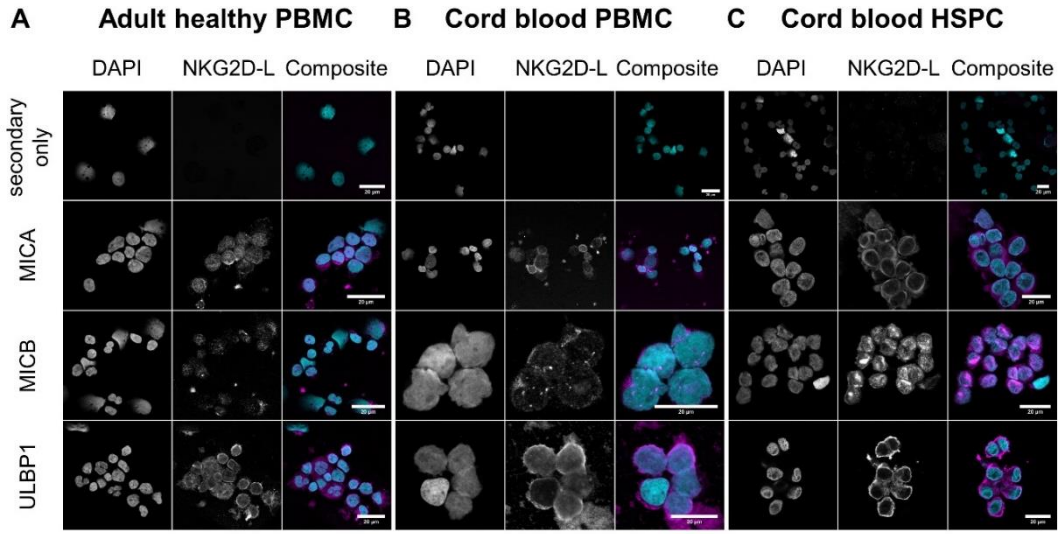

Figure 22 Phenotyping of intracellular NKG2DL
Confocal microscopy using antibodies for MICA/MICB/ULBP1. Representative images of adult PBMCs, CBMCs, CB HSPC (DAPI (cyan), NKG2DL (magenta), Composite) (n=3 representatives)

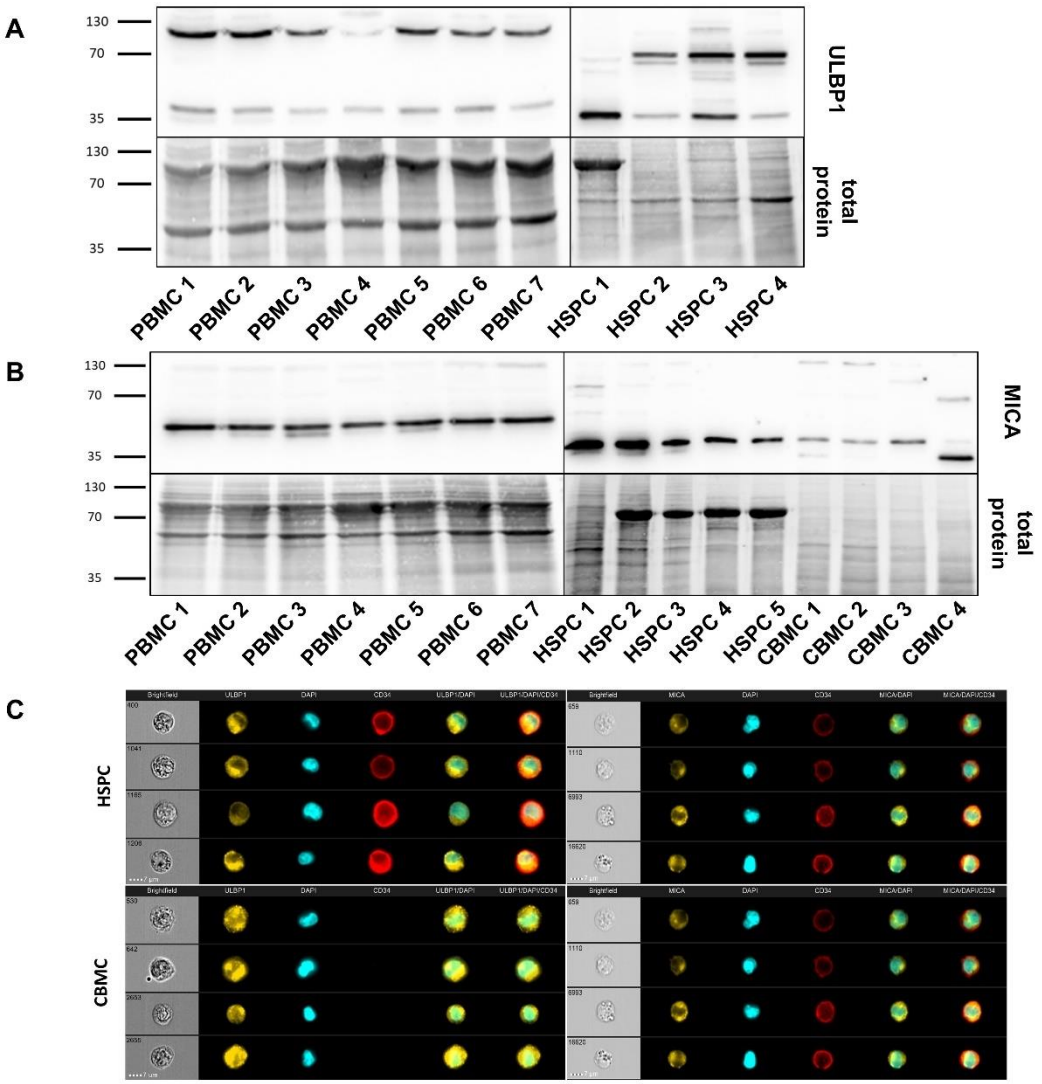

Figure 23 Extended data of Figure 12
(A) Western Blot Analysis of ULBP1 in PBMCs (n=7) and HSPC (n=4) (B) Western Blot Analysis of ULBP1 in PBMCs (n=7) and HSPC (n=5) and CBMCs (n=4) Image flow cytometry analysis using antibodies for MICA/ULBP1. Representative images of HSPC and CBMC (Brightfield (left upper corner, cell number), DAPI (cyan), NKG2DL (yellow), CD34 (red), Composite) (n=4 representatives). Scale bar, 7 µm

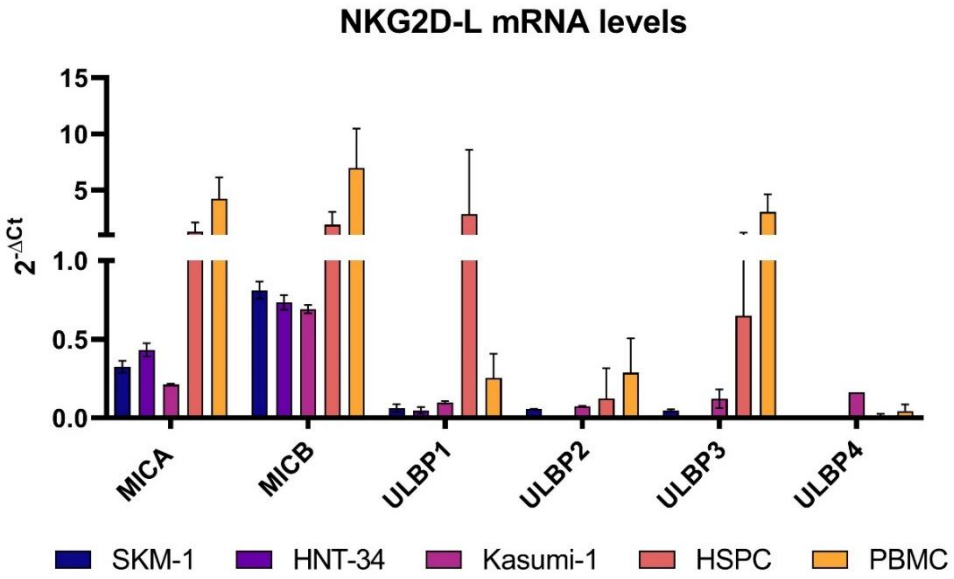

Figure 24 NKG2DL mRNA in AML cell lines, HSPC and PBMCs

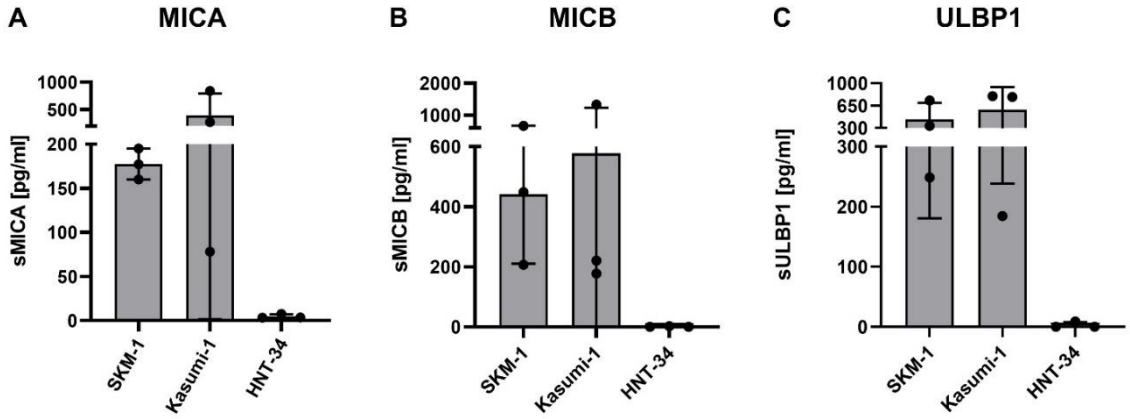

Figure 25 Determination of sNKG2DL in AML cell lines

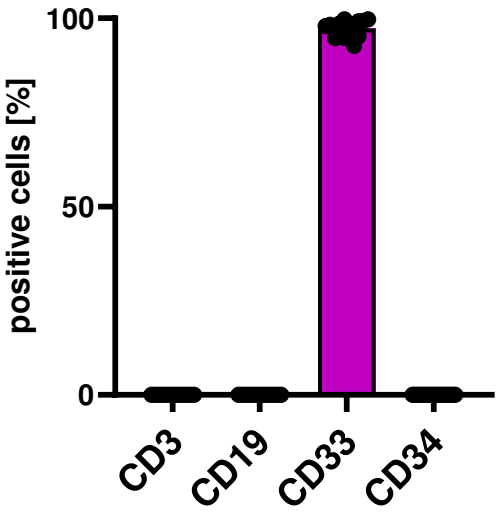

Figure 26 MLLr phenotype
Flow cytometry analysis to determine CD3, CD19, CD33, and CD34 expression of MLLr cells (n=12-20)

CFU show clonogenic activity for MLLr cells

Figure 17 shows that MLL rearrangements present distinct NKG2DL surface expression phenotypes. In addition, I phenotyped MLL-AF4 (Intron9) (created by collaboration partners from Corina Schneidawind´s research group) and observed that the cells were also fully NKG2DL positive (Figure 27 A). Previously I also observed that the low/high expression of NKG2DL within MLL-AF4 (Intron11) samples coincided with their clonogenic activity. Here, I further investigated whether NKG2DL phenotypes also coincide with clonogenicity in connection with additional MLL rearrangements and performed CFU assays in 5 donors per MLL translocation.

Interestingly, clonogenicity did not correlate with NKG2DL expression. Cells that were fully positive for NKG2DL showed the highest average number of colonies per sample (96 and 200 for MLL-AF4 (Intron 9)/AF9 (Intron 9), respectively), whereas non- or partially positive NKG2DL cells gave rise to fewer or no colonies (22 and 13 for MLL-AF4 (Intron 11)/AF9 (Intron 11), respectively) (Figure 27 B). This might reflect the fact that CFU assays indeed identify both LSC and progenitor cells, and that NKG2DL- LSCs might have a proliferation defect impairing them from forming colonies in this system.

In addition, I collected all colony-forming samples (Figure 17) and replated them up to two times. Only two samples were able to give rise to secondary colonies, and the original expression of NKG2DL did not coincide with clonogenic activity during replating (Figure 27 C/D). This confirms the notion that the initially clonogenic population of NKG2DL positive cells was composed of progenitors

with limited self-renewal potential, instead of containing true LSC. Further *in vivo* investigations in xenograft models are needed to answer these questions.

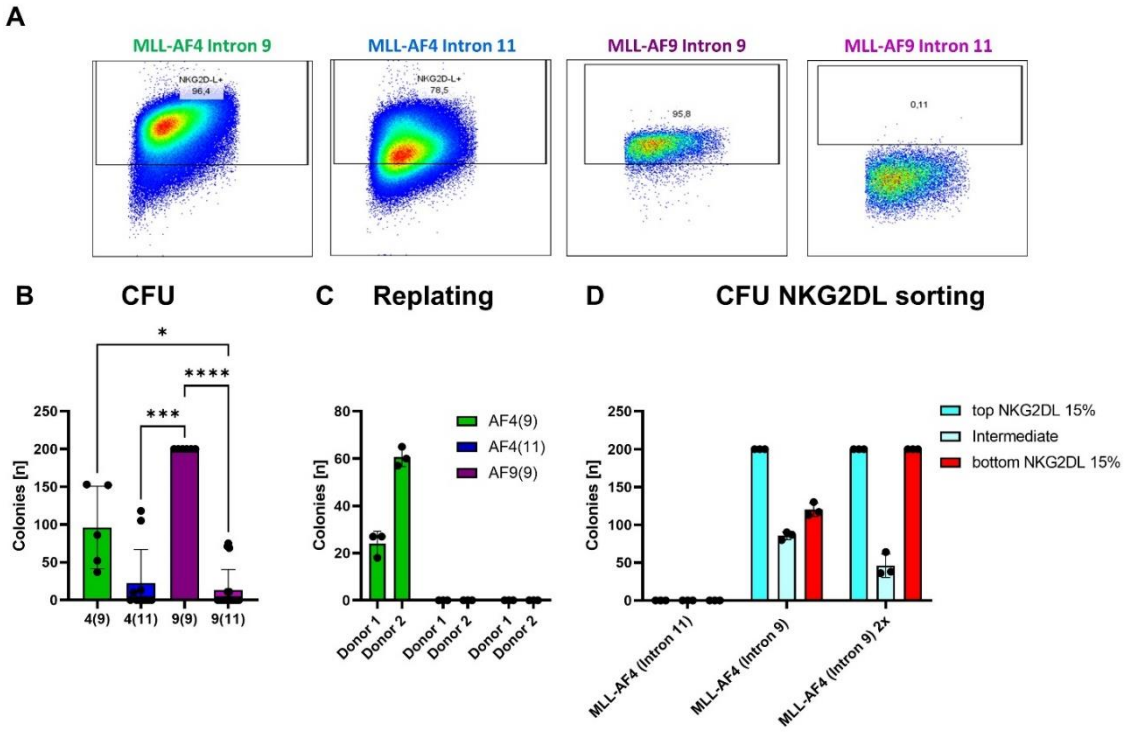

Figure 27 MLL Fusions show distinct NKG2DL surface expression patterns
(A) Flow cytometry analysis using NKG2D-Fc to determine percentages of NKG2DL surface expression in MLLr cells (B) CFU assay on MLLr cells (5000 cells per samples, n=5) (C) Replating of CFU samples of (B) (C) Replating of CFU assay in Figure 17. Experiment performed in collaboration with Rahel Fitzel (Schneidawind research group)

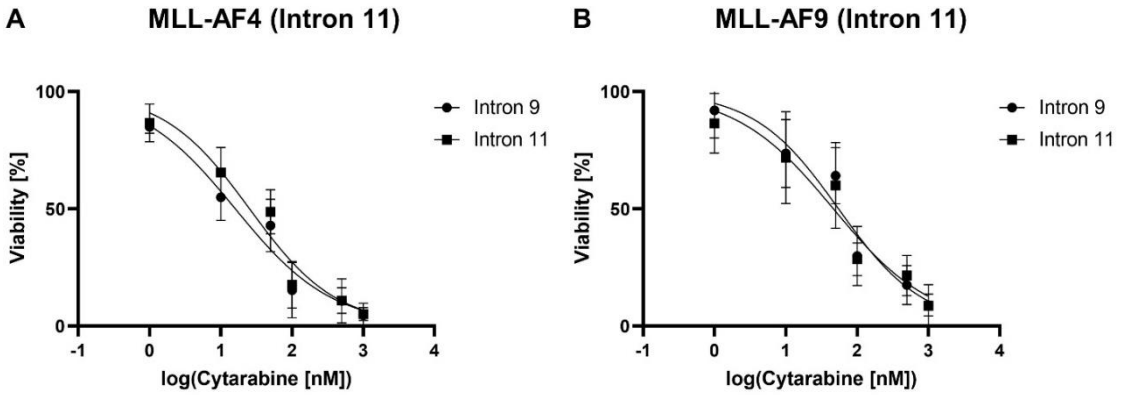

Figure 28 Dose-Response curve of cytarabine in MLLr cells
(A) Flow cytometry analysis of MLL-AF4 (Intron 11) cells for viability at different cytarabine concentrations (B) Flow cytometry analysis of MLL-AF9 (Intron 11) cells for viability at different cytarabine concentrations that gave rise to colonies (5000 cells per sample) Experiment performed by Rahel Fitzel (Schneidawind research group)

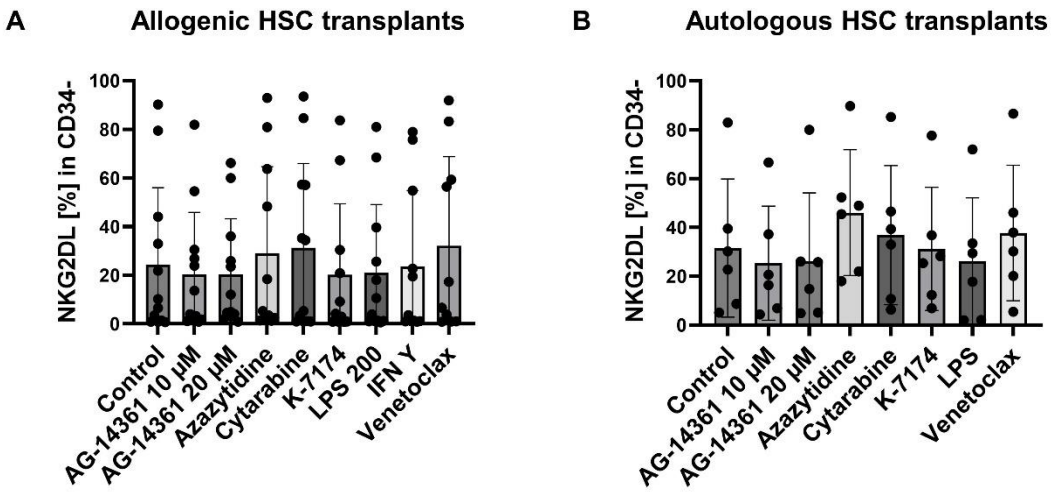

Figure 29 Extended Figure 20
Flow cytometry analysis to determine NKG2DL percentages in (A) Allogenic HSC transplants and (B) Autologous HSC transplants

Discussion and outlook

Despite considerable efforts and remarkable progress, AML remains a deadly cancer with a 5-year overall survival rate of only 19% in patients older than 60 years. [156]. Despite often achieving remissions, patients with AML often experience relapse (up to 40%) due to the persistence of therapy resistant LSC. Additionally, AML is a highly heterogeneous disease, making the identification and eradication of LSC particularly challenging. Notably, our laboratory has recently identified an additional functional marker for LSC: the absence of NKG2DL [72] .

NKG2DL are immunogenic molecules believed to be absent in healthy cells. Surface presentation of NKG2DL is induced following cellular stress or malignant transformation, rendering cells vulnerable to immune surveillance by NK and cytotoxic T-cells, which express the activating receptor NKG2DR [79].

The aim of this study was to systematically characterize the expression of NKG2DL in both malignant and healthy hematopoietic cells under steady-state conditions. My results demonstrate that NKG2DL are localized intracellularly at both mRNA and protein levels in healthy PBMCs (including HSPC), AML cell lines, and MLLr cells. Additionally, sNKG2DL are released into extracellular fluids during the *in vitro* culture of HSPC, AML cell lines and MLLr cells. I further demonstrated that current and potential new treatments for AML, such as PARP1 or GATA2 inhibitors, or co-treatment with the PARP1 inhibitor and standard therapeutic agents, do not impact the surface expression of NKG2DL in healthy HSPC.

Different patterns of NKG2DL surface expression were observed in MLL rearrangements. MLL-AF9 (Intron 9) and MLL-AF4 (Intron 9) cells both presented NKG2DL on the cell surface of the entire population. In contrast, MLL-AF4 (Intron 11) showed a similar expression pattern to primary AML samples, with only partial expression of NKG2DL at the surface, and MLL-AF9 (Intron 11) retained NKG2DL intracellularly, similar to LSC. The absence of NKG2DL at the cell surface coincided with an increased clonogenic potential in MLL-AF4 (Intron 11) samples, consistent with previous observations in primary AML and demonstrating an enrichment of LSC in the NKG2DL negative cell population. Based on current literature, this work presents the first systematic approach characterizing the presence of NKG2DL in a variety of healthy hematopoietic cells, including the stem cell compartment at the steady state.

NKG2DL presentation guards against malignant transformation

While the presence of NKG2DL at the cell surface is primarily associated with malignant cells, surface presentation of NKG2DL has also been reported in a variety of healthy hematopoietic cells that are experiencing cellular stress [79]. For instance, NKG2DL surface presentation has been observed in hyperproliferating cells during embryogenesis or wound healing, as well as in

activated T-cells [90, 92]. This mechanism is believed to ensure continuous immune surveillance of hyperproliferating cells that are more likely to undergo malignant transformation and thus may need to be cleared rapidly [90]. As a similar mechanism, HSPC have been shown to constitutively present MHC class II antigens, which enables interaction with antigen specific CD4 T cells to effectively detect and eliminate transformed HSPC and prevent leukemogenesis [157].

NKG2DL are intracellularly detectable in healthy hematopoietic cells

In a singular study, intracellular NKG2DL expression has been reported in various healthy solid tissues, including breast, colon, pancreas, and liver [158]. However, our understanding of the presence of NKG2DL in healthy hematopoietic cells, particularly in the stem cell department at the steady state is limited. Therefore, I aimed to investigate the presence of NKG2DL in healthy hematopoietic cells.

I performed a broad range of assays to measure NKG2DL expression in HSPC, from mRNA to protein to their release into the extracellular fluids (Figure 11/12). Despite being negative for NKG2DL at the cell surface, as determined by flow cytometry, I could show that NKG2DL mRNA and protein, specifically MICA and ULBP1, were present in healthy HSPC. Specifically, I could show that NKG2DL mRNA was readily detectable in qRT-PCR experiments. Subsequently, I determined that NKG2DL mRNA was also translated as the respective proteins could be detected in the cytoplasm by intracellular staining. These findings show the intracellular presence of NKG2DL in healthy HSPC for the first time.

The presence of intracellular NKG2DL could either point to a potential intracellular function of NKG2DL in the steady state or suggest that maintenance of an intracellular pool of NKG2DL protein is otherwise beneficial for healthy cells. However, there is currently no known role of intracellular NKG2DL. Therefore, to assess if NKG2DL have potential intracellular functions, simultaneous knockout of all known NKG2DL should be performed in healthy cells, where NKG2DL has no known function. By analyzing the viability of such cell lines, potential secondary functions of NKG2DL could be revealed.

In the absence of a specific intracellular function, maintaining a pool of intracellular NKG2DL could also offer other benefits to the cell. The absence of NKG2DL on the cell surface of healthy cells – while being expressed intracellularly at significant levels – would allow for rapid surface presentation upon the occurrence of stress stimuli, such as viral infection or malignant transformation. This, in turn, could lead to immediate immune detection and clearance when inhibitory signaling in immune cells is lost or activation signals are engaged. Such a mechanism could prove essential for HSCs or HSPC, given the importance of HSC function and integrity, to prevent e.g., leukemogenesis.

sNKG2DL are released from healthy hematopoietic stem cells

Absence of NKG2DL on the cell surface through downregulation of protein expression or upregulation of NKG2DL shedding – the process of cleaving NKG2DL from the cell surface – is often associated with immune evasion mechanisms of cancers such as AML or lymphoma [73, 122]. Cancer cells often adapt mechanisms from healthy cells, raising the question if downregulation of overall NKG2DL levels or shedding of NKG2DL also plays a role in maintaining low surface presentation of NKG2DL in healthy cells, or if absence of surface NKG2DL is due to another mechanisms, such as intracellular retention [159, 160].

Therefore, I interrogated the discrepancy between intracellular presence and extracellular absence of NKG2DL proteins. I expanded CB HSPC *in vitro*, analyzed NKG2DL surface presentation and measured sNKG2DL in the cell culture supernatant (Figure 12). Here, I observed similar or higher levels of intracellular NKG2DL in healthy compared to malignant cells, absence of surface NKG2DL in healthy compared to malignant cells, and lower levels of soluble NKG2DL in the supernatant of healthy cells compared to malignant cells. The maintenance of intracellular NKG2DL protein pools comparable to those found in malignant cells, coupled with absence of NKG2DL at the cell surface, suggest that in healthy cells, NKG2DL is either not trafficked to the cell surface, or immediately removed upon arrival at the surface, either by cleavage [115], secretion [161] or internalization [162]. As only low levels of sNKG2DL could be found in the supernatant of healthy cells compared to malignant cells, there is no evidence of significant shedding or other secretion, e.g., via exosomes, of NKG2DL in healthy compared to malignant cells. This indicates that while NKG2DL is produced in similar levels in healthy hematopoietic cells compared to malignant cells, it may be retained intracellularly, or surface presentation may be exceedingly transient.

Few is known about the intracellular posttranslational regulation of NKG2DL. While many cells regulate the levels of surface NKG2DL by shedding and/or release of NKG2DL into the supernatant, other mechanisms have been proposed that may determine the cellular localization of NKG2DL, including alternative splicing and posttranslational modification [79]. For example, ubiquitination of MICA has been shown to cause rapid internalization and subsequent degradation, reducing surface NKG2DL levels during Kaposi's sarcoma-associated herpesvirus infection [163]. Interestingly, a similar mechanism has been observed in murine cells, where the mNKG2DL MULT1 is ubiquitinylated and degraded in healthy cells and only retained at the cell surface after exposure to cellular damage [99]. Other mechanisms, such as sequestration in the ER, as has been observed for immature forms of MICA in melanoma cancer cells, may also play a role in shifting the localization balance of NKG2DL to an intracellular state [114]. To further investigate these posttranslational modifications, pulldown of NKG2DL in healthy and malignant cells (both intracellularly and on the cell surface) and

subsequent mass spectrometry could be performed to identify key posttranslational regulators and protein motifs for further investigation.

HSC are crucial for blood generation throughout an organism's lifespan and accidental clearance of HSC would have drastic effects. Studies have shown that HSC possess immune privilege and are protected by the microenvironment of the HSC niche. For example, they colocalize with regulatory T cells that secrete IL-10 to inhibit immune response. Furthermore, HSC have the ability to suppress the immune response by presenting immune inhibitory molecules on their surface, such as CD47 (for macrophages [164]) and CD247 (for T-cells [165]). These molecules are upregulated 10-fold in HSPC cultured in STFIA medium, indicating an activation of immunosuppressing pathways [166].

Such immunosuppressing pathways could also result in the release of sNKG2DL into the extracellular matrix, which enables immune evasion. Similar phenomena have been observed in cancer cells, such as breast cancer [167] and multiple myeloma [168], where shedding of sNKG2DL is associated with poor clinical outcome [128, 169]. This could be further investigated by exposing HSPC to cellular stress stimuli, such as transduction using lentiviruses, and measuring sNKG2DL levels in the culture supernatant.

Although levels of sNKG2DL were lower in the supernatant of healthy HSC compared malignant cells, sNKG2DL could nevertheless be detected (Figure 12/25). It is however unclear if the levels of sNKG2DL detected here represent levels as would be present in the human body or if they are a byproduct of cellular stress caused by culturing conditions. For example, cultured HSC may experience increased cell proliferation due to administered cytokines, which also caused a 48 % decrease in CD117 and an 95 % increase in CD33 expression, indicating a commitment to the myeloid lineage. This, in turn, could induce shedding or excretion of NKG2DL.

Therefore, further experiments regarding the release of sNKG2DL into the extracellular fluids must be performed, as it remains unclear whether the sNKG2DL is released by shedding from the cell surface [115] or through secretion within exosomes [170]. To investigate this question, one could inhibit metalloproteases-mediated shedding by using inhibitors such as tissue inhibitors of metalloproteinases (TIMPs) [171] or isolate exosomes from supernatants using sucrose gradient mediated ultracentrifugation and subsequently use ELISA to determine if NKG2DL are present in the exosomes [161].

Nevertheless, the lack of surface expression, in parallel with intracellular presence of NKG2DL in healthy cells is intriguing, as it could enhance our understanding of NKG2DL biology and potentially lead to the identification of new therapeutic options, such as inhibition of specific posttranslational modifications of NKG2DLs to increase surface presentation of NKG2DL.

NKG2DL in leukemia

Paczulla *et al.* reported that NKG2DL surface expression is reduced in LSC and identified the PARP1, which can be targeted through inhibition, as a NKG2DL suppressing molecule [73].

LSC are believed to form through the accumulation of leukemogenic events, such as genetic alterations [172] and epigenetic or environmental factors like chromatin remodeling and ionizing radiation, in either healthy HSC or progenitor cells [173, 174]. These healthy cells do not present NGK2DL on the cell surface under steady-state conditions [76], and malignant transformation should in theory induce NKG2DL surface presentation and subsequent killing via the immune response. However, in the rare case of leukemogenesis, surface presentation of NKG2DL is inhibited by e.g., upregulation of NKG2DL repressors such as PARP1. This phenotype of absence of NKG2DL at the surface is also seen in other cancers, such as human melanomas, which retain NKG2DL intracellularly [175].

Although there have been notable improvements in culturing primary AML samples in recent years, such as the expansion of primary AML *ex vivo* or co-cultivation with mesenchymal stem cells, primary AML samples remain notoriously difficult to culture *in vitro* [176]. This is especially problematic in the context of NKG2DL expression, as these ligands are directly upregulated by cellular stress induced by suboptimal culture conditions present *in vitro* compared to *in vivo*. Therefore, a surrogate system was necessary to study the intracellular retention or induction of NKG2DL, since all tested AML cell lines exhibited complete NKG2DL surface positivity.

MLL rearrangements result in distinct NKG2DL surface expression patterns

Murine MLLr cells had a distinct NKG2DL expression pattern. Murine MLL-ENL and MLL-PTD translocations had a partial presentation of murine NKG2DL, while murine MLL-AF9 (Intron 11) did not exhibit NKG2DL on the cell surface [62]. As murine MLL translocations presented with a unique NKG2DL surface expression patterns and because there is a lack of information on NKG2DL expression in MLLr human cells, I further investigated cord blood derived human MLLr cells as a potential surrogate system for NKG2DL surface expression.

To investigate this hypothesis, our collaboration partners from Corina Schneidawind´s research group generated MLL-AF4 (Intron 9 or 11) and MLL-AF9 (Intron 9 or 11) samples using CRISPR-Cas9 technology in cord blood HSPC. These cells have been well-characterized and can be directed towards a stem cell and AML phenotype by adding the respective cytokines to the culture medium. MLLr cells can be cultivated indefinitely while remaining in a state between primary material and cell line [177]. However, during prolonged cultivation, we observed slight alterations in the expression patterns of ITGA7,

among other factors (data not shown), indicating their progression towards a more cell-line like state.

Cord blood MLLr cells also exhibit a unique surface NKG2DL phenotype *in vitro*, depending on the specific translocation they carry. Specifically, while MLL rearrangements at intron 9 allowed for NKG2DL cell surface presentation in the whole cell population, MLL cells with rearrangements at intron 11 partially or fully retained NKG2DL intracellularly. This phenotype is associated with primary AML (partial NKG2DL expression) and LSC (no surface NKG2DL expression), respectively (Figure 17). Intriguingly, in clinical cases of MLL, breakpoint at intron 11 is linked to a more severe disease progression, which may be linked to absence of NKG2DL on the cell surface, resulting in evasion of the immune response [122]. Using the MLLr cells carrying different breakpoints generated here, the linkage between breakpoint, NKG2DL surface presentation phenotype and immune evasion could be tested by co-culturing/ performing killing assays of different MLLr cells with NK and CD8 T cells.

MLL-AF4 (Intron 11) samples exhibit the same NKG2DL phenotype as primary AML, where NKG2DL negative cells (LSC) are associated with increased clonogenic potential compared to their positive counterpart in *in vitro* CFU assays. I then investigated if this held true for the NKG2DL negative MLL-AF4 (Intron 11) cells and observed, that MLL-AF4 (Intron 11) cells that did not express NKG2DL on the cell surface exhibited greater clonogenic activity than the NKG2DL surface expressing counterpart in the first plating of a colony forming unit (CFU) assay. However, this trend was not observed during secondary or tertiary plating, as the number of colonies in both populations was similar or samples did not form colonies in sequential CFU assays (Figure 19). This suggests that the samples did not exhibit long-term stemness characteristics and the ability to give rise to subsequent colonies, or that impurities in the flow cytometry-based sorting process led to the formation of colonies in the NKG2DL presenting population, which may occur despite confirmation of sort purity. Alternatively, the few NKG2DL surface expressing cells, that gave colonies, possessed higher clonogenic activity and were enriched through CFU assay, as the cell number for replating stayed consistent within the experiment. While this initial finding suggests biological similarity of MLL-AF4 (Intron 11) cells and primary AML and that the MLL-AF4 (Intron 11) system could potentially serve as a viable surrogate for primary AML due to its potential for unlimited growth, it is important to note that these findings are based solely on *in vitro* work and requires further validation *in vivo,* e.g., by injecting sorted MLL-AF4 (Intron 11) samples into immunocompromised mice and observing potential leukemogenesis.

While all MLL translocations have the potential to grow unlimited *in vitro*, MLL-AF9 (Intron 9) showed the highest proliferation rate, followed by MLL-AF4 (Intron 9), then MLL-AF4 (Intron 11) and last MLL-AF9 (Intron 11) (Data provided by

collaboration partners from the Schneidawind research group, manuscript in preparation and data not shown). Proliferation, specifically through E2F transcription factors, has been reported as a direct regulator of NKG2DL through transcriptional upregulation. Here, I observed direct correlation of NKG2DL surface presentation with proliferation speed of specific MLL fusion genes, indicating a regulatory role of the MLL fusion gene for proliferation and thereby potentially NKG2DL surface expression.

When comparing the clonogenic activity of different MLL translocations of the same donor origin, I observed - contrary to expectations - that those with NKG2DL presented on the cell surface exhibited significantly higher clonogenic activity compared to those without or with only partial presentation of NKG2DL (Figure 27). This could be an artefact of the different proliferation rates of MLLr cells harboring distinct rearrangements as the presence of colonies - especially after the first plating - could also result from a higher proliferation rate. Subsequent replatings of CFUs would have been necessary to be able to make an informed statement on long-term self-renewal capacity but yielded contrary results. Of note, it is important to carefully examine clonogenicity in MLLr samples as these cells are in a state between primary material and cell line. With prolonged culture time and increased total proliferation steps, they acquire mutations and slowly transition to a more cell line like state. It is worth noting that cell lines, even without stemness, sometimes produce more colonies compared to primary material, which may explain the observed clonogenicity. However, further analysis and characterization of these cells is essential, such as next generation sequencing and RNAseq to understand MLLr biology and LSC signatures (which is an ongoing project in collaboration with the Schneidawind group).

Additionally, MLL cells carrying translocations at intron 11 have been shown to be more susceptible to imperfect culture conditions *in vitro*, such as e.g., cell density, than the intron 9 counterparts (data provided by the Schneidawind group, manuscript in preparation and data not shown). Therefore, they may be more sensitive to changes in cultivation conditions, such as transitioning from *in vitro* cultivation for over 80 days to methylcellulose with different cytokines and growth factors, potentially resulting in increased cell death and fewer colonies. Alternatively, the Intron 9 samples may have acquired more mutations due to their higher proliferation and mutation speed. This could have caused them to behave more like a cell line *in vitro*, resulting in higher colony numbers despite their lack of stemness characteristics.

Although lack of surface NKG2DL was a marker for increased clonogenicity in MLL-AF4 (11) samples (Figure 19), it may not be a suitable marker for stemness *in vitro*, as it is also upregulated under cellular stress occurring in cell culture such as oxidative or mechanical stress and nutrient deprivation. Additionally, these cells were cultured solely *in vitro* without the presence of immune cells, and therefore

did not experience evolutionary pressure to adapt to immunosurveillance. Cancer cells adapt to their surrounding tissue environments through a process called adaptive oncology or EcoOncogenesis [178] where the evolutionary pressure of the microenvironment dictates the phenotype of the cells within that environment. Without the interactions with immune cells, there would be a lack of evolutionary pressure and adaptation to limit NKG2DL surface expression. To investigate this, co-cultivation of MLLr cells with immune cells, such as NK and T cells over a prolonged time period, and continuous phenotyping of surface NKG2DL could be performed.

Further *in vivo* experiments and characterization of stemness markers and gene expression signatures of MLLr samples are necessary to address questions regarding NKG2DL as a stemness marker *in vitro*, the stem-like state of MLLr cells, and their potential to function as a surrogate system for primary AML *in vitro*. In collaboration with other members of the Lengerke laboratory, I have already started *in vivo* experiments to further investigate the leukemogenic potential of MLLr cells in correlation with their NKG2DL surface phenotypes.

In the first set of experiments, I aim to evaluate the ability of MLL-AF4 (Intron 11) cells to initiate leukemia in immunocompromised NSG mice. Additionally, I am interested to see, if their ability to induce leukemia in mice is defined by their NKG2DL surface expression similar to the phenotype of primary AML, where only the NKG2DL-negative population was able to engraft in NSG mice and elicit leukemia. Therefore, I separated the top and bottom 15% of NKG2DL expressing cells of three MLL-AF4 (11) samples via fluorescence activated cell sorting. These two populations were then injected into three mice each, which will give insight about the leukemogenic potential dependent on NKG2DL surface expression.

Additionally, to investigate the leukemic potential of MLLr cells dependent on their NKG2DL phenotype, we transplanted unsorted MLLr samples of each MLL translocation, originating from the same CB donors, into immunocompromised NSG mice to assess the ability of each MLL translocation to induce leukemia.

However, as MLLr cells require a significant amount of time to repopulate *in vivo*, it was not possible to analyze the results of these experiments within the framework of this thesis. It is important to note that these MLL samples were previously cultured under myeloid conditions for 80-100 days prior to injection into mice, possibly resulting in continuous acquisition of mutations and pressure towards myeloid differentiation. NSG mice have previously been shown to favor lymphoid differentiation, which could pose a challenge for repopulation *in vivo* [179]. Therefore, MLLr may need to adapt to these new conditions, which could be particularly problematic for MLL-AF9 samples due to their more AML-like phenotype in humans.

NKG2DL presentation in MLLr cells is not susceptible to PARP1 or GATA2 inhibition

Previously, I observed an LSC-like phenotype in MLL-AF9 (Intron 11) samples (NKG2DL-negative) and a primary AML phenotype in MLL-AF4 (Intron 11) samples (mixed population of NKG2DL positive and negative cells) (Figure 17). Therefore, I aimed to investigate how current AML therapies affect the viability and NKG2DL surface presentation of these MLLr cells to evaluate their similarity to primary AML. However, experiments using the MLL-AF9 (Intron 11) cells, which would be more suitable for investigating the induction of NKG2DL due to their general absence at the cell surface, proved to be unfeasible due cells being very fragile and having a slow proliferation speed *in vitro.* Therefore, they were excluded from therapy-related experiments and all subsequent experiments were carried out in MLL-AF4 (Intron 11) samples.

Paczulla *et al.* demonstrated that the absence of NKG2DL can define LSC and that PARP1 suppresses NKG2DL surface presentation in LSC. This suppression can be reversed through pharmaceutical or genetic inhibition. PARP1 is a chromatin-associated enzyme responsible for poly(ADP)ribosylation of various nuclear proteins [180]. It plays a crucial role in DNA damage repair, chromatin remodeling, and stabilization of DNA replication forks [181]. PARP1 is particularly important in repairing nucleotide excision, single-strand, and double-strand DNA breaks [182]. Its clinical relevance is demonstrated in the treatment of breast cancers that display the BRCA mutation. Cells with BRCA mutations are unable to repair DNA damage through homologous recombination, making them dependent on PARP1 for DNA damage repair. However, inhibiting PARP1 results in synthetic lethality, a genetic interaction where cells remain viable with the loss of individual gene function, but not with the loss of both gene functions [183, 184].

Treatment with all tested, clinically available AML therapies (azacytidine, cytarabine, venetoclax) resulted in a significant decrease in cell viability when treating MLL-AF4 (Intron 11) cells, while healthy control cells remained unaffected.

GATA2 is a transcription factor involved in several biological processes, including hematopoiesis and regulation of the immune system. Mutations in GATA2 have been associated with immunodeficiency, bone marrow failure, and predisposition to myelodysplastic syndrome and AML. Our laboratory recently identified GATA2 as a potential regulator of NKG2DL expression in AML in a CRISPR-Cas9 screening project. Here, the sgRNA library was designed to target a total of 569 genes, including (I) the top differentially regulated genes as determined by our previous RNA-seq analyses of NKG2DL- vs. NKG2DL+ cells from five AML patients [73], (II) genes involved in cell cycle regulation, as reduced cell proliferation has been linked to suppressed NKG2DL expression [90], and (III) control sgRNAs. The NKG2DL expressing cell population was FACS sorted and

subjected to next generation sequencing and bioinformatic analysis to identify enriched or depleted sgRNAs in the sorted populations compared to the unsorted bulk, which allowed us to determine a list of 36 genes (not shown), including GATA2, whose knockouts are associated with particularly high or low NKG2DL expression (Rudat *et al*, unpublished).

However, inhibition of the potential NKG2DL regulators PARP1 and GATA2 or LPS and IFN γ treatment used to mimic *in vivo* inflammatory or infectious conditions did not result in a decrease in cell viability (Figure 16/20).

Neither PARP1 nor GATA2 inhibition affected the percentages or levels of NKG2DL surface expression, which was unexpected given that PARP1 inhibition has been shown to upregulate NKG2DL on the LSC compartment of AML. Additionally, co-treatment of PARP1 with other current therapies did not have an effect on NKG2DL surface presentation. This suggests that the upregulation of NKG2DL is only true for a subset of very heterogeneous AML. Paczulla *et al*. also demonstrated that the induction of NKG2DL expression by PARP1 inhibition was ineffective in subsets of AML such as CD34 negative AML, which is often associated with NPM1 mutations.

Although GATA2 has been identified as a potential master regulator of NKG2DL presentation (unpublished data from our group), inhibiting GATA2 using K-7147 did not result in the presentation of NKG2DL on the cell surface in both HPSCs and MLL-AF4 (11) cells. Of note, K-7147 not only inhibits GATA2 but also affects the proteasome possibly resulting in off-target effects [185]. Previous studies have shown that HBV infection in human hepatoma cells upregulates GATA2 (and GATA3), which in turn suppresses NKG2DL expression. However, inhibiting GATA2 may not be a viable option in a clinical setting, as it is also essential for healthy tissues [186].

NKG2DL surface levels are significantly upregulated by IFN γ *in vitro*

Interferon γ (IFN γ) is a cytokine released by activated T and NK cells. It plays an important role in the activation of cellular immunity, such as the activation of macrophages, is involved in regulation of specific immune pathways such as JAK-STAT pathway [187, 188] and enhances the expression and presentation of MHC molecules [189]. Here, we used IFN γ to mimic conditions patients may face during hospitalization, such as infection.

Treatment with IFN γ did not increase the percentage of NKG2DL-presenting cells, however, it significantly increased the number of NKG2DL molecules presented (MFI) on the cells (Figure 20). This is in contrast to previous reports, where treatment with IFN γ not only reduced NKG2DL presentation on the cell surface of melanoma and glioblastoma cell lines, but also reduced NKG2DR expression on NK and CD8 T cells [80]. Additionally, IFN γ has been shown to play a crucial role in transitioning from the innate to the adaptive immunity, as

exemplified by T cells, which are downregulated by reduced expression of NKG2DR upon exposure to IFN γ. This reduction is thought to protect healthy cells from being killed during infection [190]. The same study did not delve into the mechanistic details of the downregulation of NKG2DL and NKG2DR. However, it suggests that the downregulation of NKG2DL is synergistic with the downregulation of NKG2DR as an immune evasion tactic during systemic stress. In contrast to these reports, the upregulation of NKG2DL in MLLr cells after treatment with a proinflammatory cytokine such as IFN γ as seen here seems intuitive, as IFN γ induces cell stress, which is directly related to the presentation of NKG2DL. However, this only appeared to impact cells that already displayed NKG2DL on their cell surface. Although the level of expression (MFI) increased, the overall percentage of NKG2DL-presenting cells remained unchanged.

This discovery warrants further investigation. Interestingly, IFN γ has been shown to upregulate proliferation of HSCs in vitro and may similarly increase proliferation and therefore NKG2DL surface expression of MLL-AF4 (Intron 11) cells [191]. IFN γ treatment should be conducted in other MLL translocation cases with both presenting and non-presenting phenotypes. Additionally, populations of MLL-AF4 (Intron 11) should be sorted into groups based on their presentation of NKG2DL and exposed to IFN γ treatment to determine if the upregulation of NKG2DL levels indeed only affects the NKG2DL positive population or if it is able to induce NKG2DL in the NKG2DL negative compartment.

To find more compounds which affect NKG2DL surface presentation, additional treatments should be performed since only azacitidine affected the percentage of NKG2DL presenting cells in MLL-AF4 (Intron 11) cells. This is most likely due to killing off the NKG2DL surface expressing population, as shown by similar findings in primary AML [73] and should be further investigated by treating MLLr translocation, which are fully NKG2DL surface positive.

In order to investigate additional regulators of NKG2DL surface expression, the recently 21 differentially regulated genes in NKG2DL non-presenting compared to NKG2DL presenting cells (including GPR56 and PARP1) should be investigated as potential regulators of NKG2DL surface presentation in AML. For example, one of the differentially expressed genes, MRC2 has recently been identified as a potential new marker for LSC. Its function involves interaction with the extracellular matrix through components such as collagen [192]. MRC2 was upregulated through the SMAD pathway, which is activated by transforming growth factors b (TGF-b, project in our group), a known regulator of NKG2DL that has been shown to be upregulated during malignant progression, which resulted in transcriptional inhibition of MICA, ULBP2 and ULBP4 mRNA [193].

Technical optimization of assays

Due to the small size of AML cells and their large nucleus (which occupies approximately 80% of the cell), AML may not be a suitable cancer model for studying the intracellular mechanism of NKG2DL processing. Previous attempts to perform colocalization assays with other cell organelles, such as the Golgi apparatus or endoplasmic reticulum, have encountered technical difficulties due to the small volume of the cytoplasm. Although NKG2DL glycolysis or retention of NKG2DL in the ER through accumulation of endoH-sensitive forms of MICA has been previously demonstrated, further insight into the mechanism of NKG2DL absence on the cell surface coupled with intracellular presence is required [114]. In addition to LSC, and healthy hematopoietic cells, intracellular retention of NKG2DL has been reported in solid healthy tissues, such as the heart, lung, or liver. If induction of NKG2DL surface expression using drugs or infection is possible in these tissues, it would be a more technically feasible model to follow NKG2DL as they are synthesized and transported to the cell surface. To identify possible candidates for this application, other cancer cell lines and primary material should be phenotyped for NKG2DL surface and intracellular expression at the steady state, and subsequently feasible induction stimuli such as e.g., lentiviral infection, should be established.

During the phenotyping of NKG2DL in healthy PBMCs, I observed absence of surface NKG2DL expression in all investigated PBMC compartments except for viably frozen and thawed monocytes, which displayed a high surface expression of NKG2DL (mean 93%) (Figure 11) compared to freshly isolated monocytes, which displayed no surface expression of NKG2DL (data not shown). This suggests that surface NKG2DL expression may have been induced by cellular stress during the freeze-thaw process. Therefore, the use of samples that were freshly isolated might be more appropriate.

Both allogenic and autologous stem cell samples containing mobilized HSPC are very rare samples. In addition, the samples that were received had low viability (with some not viable at all) due to their storage for at least 10 years. CD34+ cells that were successfully isolated from allogenic donations appeared to have lower (<1 %) levels of NKG2DL on the cell surface, compared to CD34+ cells from autologous donors (< 5%) (Figure 16). This phenotype could possibly be caused by cellular stress due cancer therapy preceding autologous stem cell donation or artifacts from prolonged storage. The use of fresh cells e.g., adult BM HSPCs, or at least cells with a high level of viability, should be a prerequisite for a more accurate assessment of the effects of current or new therapies.

Potential experiments to investigate NKG2DL regulation.

The identification of MLL-AF4 (Intron 11) cells as an *in vitro* system mimicking AML provides many opportunities to study the intracellular retention of NKG2DL,

as it contains both NKG2DL presenting and non-presenting cells within the same cell population. Similar mechanisms of intracellular retention are also observed with other proteins, such as the melanocortin 4 receptor (MC4R), a key regulator of energy homeostasis, which is often retained intracellularly due to being trapped in the secondary pathway or the DNAM1 activating receptor PVR, that is retained intracellularly by SUMOylation in multiple myeloma [194]. Additionally, there are proteins such as Bip/Grp78 or calreticulin that contain specific sequences in order to be retained at specific cell organelles, such as the endoplasmic reticulum, due to sequences like KDEL or KKXX [195].

To identify potential regulators of NKG2DL, mass spectrometry could be performed on intracellular and extracellular NKG2DL from presenting and non-presenting cells, and differences in protein modifications, such as methylation [196] or glycosylation [98], as well as protein structure, could be further investigated. RNA sequencing or a CRISPR screen of potential regulators, such as PLA2G4A, which hydrolyzes membrane phospholipids, has been shown to repress NKG2DL in leukemia cell lines (THP1, HL60) *in vitro*, could also be used to identify mechanisms involved in NKG2DL processing and presentation [197]. In addition, if additional cell system with larger cytoplasm can be developed, NKG2DL biogenesis and transport could be visualized by tagging specific species of NKG2DL and following their path through the cell via (life-cell) microscopy.

NKG2DL regulation is a complex network most likely relying on multiple proteins. Therefore, a systematic approach, similar to that used to identify the Yamanaka or OSKM factors, could be used to identify key regulators. Here, experiments were initiated with a subset of 24 candidate genes which were administered in different combinations to mouse fibroblast cells. Subsequently, a process of elimination was used to characterize genes essential for reprogramming, ending with the identification of the four key genes Oct3/4, Sox2, Klf4, and c-Myc (which has recently been shown not to be essential [198]), which were sufficient to reprogram somatic cells back to pluripotency [199]. Interestingly, both c-Myc as well Klf-4 have been associated with upregulation of ULBP1,2,3 and MICA respectively in AML [200, 201]. Additionally, other potential regulators of NKG2DL have been identified in recent years. Similarly, the ATM-Chk2 mediate checkpoint pathway has shown to upregulate NKG2DL in multiple colon cancer cell lines [202].

Knocking out a single NKG2DL most likely provokes redundancy caused by the presence of other NKG2DL on the cell surface, which has been shown to be sufficient for immunological detection and subsequent immune clearance [151]. Therefore, knock-out of multiple, or all NKG2DL would be necessary to exclude a potential compensation mechanism. The same experiments could also shed light on the question, if expression of any NKG2DL intracellularly is essential for cell survival, due to potential novel secondary intracellular functions of members of the NKG2DL protein family. Additionally, use of antibodies against specific

NKG2DL instead of the NKG2D-Fc should be established, as knockouts of single members of the NKG2DL family as performed here did not affect expression of other NKG2DL, implying that regulation of NKG2DL might be specific for each protein independently.

Conclusion

In this dissertation, I report that NKG2DL is present in healthy cells but is retained intracellularly and released into the extracellular fluids in low levels. This suggests that NKG2DL is stored intracellularly until external stress stimuli occur, allowing for more rapid presentation on cells. This, in turn, facilitates rapid and effective clearance of cells undergoing malignant transformation by the immune system. Treatment of HSPC with current AML therapies, as well as co-treatment with an inhibitor of the known regulator of NKG2DL, PARP1, did not result in upregulation of NKG2DL at the cell surface, indicating that PARP1 inhibitor treatment may represent a safe and well-tolerable therapeutic avenue for AML patients.

I observed that the introduction of MLL translocations causing malignant transformation of CB HSPC resulted in distinct NKG2DL surface phenotypes that were dependent on the specific MLL translocation introduced. Specifically, the MLL-AF4 translocation at intron 11 showed partial cell surface NKG2DL presentation with clonogenicity corresponding to NKG2DL surface levels, similar to primary AML. This new system allows for the study of molecular and functional differences between NKG2DL presenting and non-presenting cells in the future. MLL-AF4 (Intron 11) samples may serve as an *in vitro* surrogate system for studying AML biology due to their similarity in biological properties, particularly in relation to their NKG2DL surface presentation. *In vivo* experiments in immunosuppressed mice have been initiated to further investigate this property, but results are not yet available due to time limitations.

To validate the similarity of MLL-AF4 (Intron11) cells to primary AML, I treated samples with current AML therapies and observed a decrease in cell viability caused by treatment with all established drugs used for AML therapy but could not see a decrease in cell viability during treatment with novel compounds such as PARP1 and GATA2 inhibitors. Interestingly, IFN γ treatment did not affect the percentage of NKG2DL presenting cells, but significantly increased the NKG2DL surface levels (MFI).

This dissertation presents results that provide additional information on NKG2DL biology in hematopoietic cells and suggest a mechanism of intracellular retention in healthy and malignant stem-like cells, albeit the exact underlying mechanisms still warrant further investigation. Using MLL rearranged cells, I characterized a potential surrogate system for primary AML and established assays to characterize NKG2DL expression at all expression stages, laying the groundwork for investigating novel aspects of NKG2DL biology such as the mechanisms governing intracellular NKG2DL retention. This could lead to the determination of key regulators of NKG2DL, which could improve not only AML therapy but have broader implications for the treatment of other cancer types.

References

1. Maximow, A., *Der Lymphozyt als gemeinsame Stammzelle der verschiedenen Blutelemente in der embryonalen Entwicklung und im postfetalen Leben der Säugetiere*.
2. Lorenz, E., et al., *Modification of irradiation injury in mice and guinea pigs by bone marrow injections.* J Natl Cancer Inst, 1951. **12**(1): p. 197-201.
3. Till, J.E. and C.E. Mc, *A direct measurement of the radiation sensitivity of normal mouse bone marrow cells.* Radiat Res, 1961. **14**: p. 213-22.
4. Becker, A.J., C.E. Mc, and J.E. Till, *Cytological demonstration of the clonal nature of spleen colonies derived from transplanted mouse marrow cells.* Nature, 1963. **197**: p. 452-4.
5. Doulatov, S., et al., *Hematopoiesis: a human perspective.* Cell Stem Cell, 2012. **10**(2): p. 120-36.
6. Bosma, G.C., R.P. Custer, and M.J. Bosma, *A severe combined immunodeficiency mutation in the mouse.* Nature, 1983. **301**(5900): p. 527-30.
7. Fulop, G.M. and R.A. Phillips, *The scid mutation in mice causes a general defect in DNA repair.* Nature, 1990. **347**(6292): p. 479-82.
8. Orkin, S.H. and L.I. Zon, *Hematopoiesis: an evolving paradigm for stem cell biology.* Cell, 2008. **132**(4): p. 631-44.
9. Bonnet, D., et al., *Direct and reversible inhibitory effect of the tetrapeptide acetyl-N-Ser-Asp-Lys-Pro (Seraspenide) on the growth of human CD34+ subpopulations in response to growth factors.* Blood, 1993. **82**(11): p. 3307-14.
10. Notta, F., et al., *Isolation of single human hematopoietic stem cells capable of long-term multilineage engraftment.* Science, 2011. **333**(6039): p. 218-21.
11. Somuncular, E., et al., *Combination of CD49b and CD229 Reveals a Subset of Multipotent Progenitors With Short-Term Activity Within the Hematopoietic Stem Cell Compartment.* Stem Cells Transl Med, 2023. **12**(11): p. 720-726.
12. Baum, C.M., et al., *Isolation of a candidate human hematopoietic stem-cell population.* Proc Natl Acad Sci U S A, 1992. **89**(7): p. 2804-8.
13. Weksberg, D.C., et al., *CD150- side population cells represent a functionally distinct population of long-term hematopoietic stem cells.* Blood, 2008. **111**(4): p. 2444-51.
14. Bhatia, M., et al., *Purification of primitive human hematopoietic cells capable of repopulating immune-deficient mice.* Proc Natl Acad Sci U S A, 1997. **94**(10): p. 5320-5.
15. Benveniste, P., et al., *Intermediate-term hematopoietic stem cells with extended but time-limited reconstitution potential.* Cell Stem Cell, 2010. **6**(1): p. 48-58.
16. Reya, T., et al., *Stem cells, cancer, and cancer stem cells.* Nature, 2001. **414**(6859): p. 105-11.

17. Akashi, K., et al., *A clonogenic common myeloid progenitor that gives rise to all myeloid lineages.* Nature, 2000. **404**(6774): p. 193-7.
18. Hao, Q.L., et al., *Extended long-term culture reveals a highly quiescent and primitive human hematopoietic progenitor population.* Blood, 1996. **88**(9): p. 3306-13.
19. Wang, K., G. Wei, and D. Liu, *CD19: a biomarker for B cell development, lymphoma diagnosis and therapy.* Exp Hematol Oncol, 2012. **1**(1): p. 36.
20. Ruuls, S.R., et al., *Novel human antibody therapeutics: the age of the Umabs.* Biotechnol J, 2008. **3**(9-10): p. 1157-71.
21. Janeway, C.A., Jr. and R. Medzhitov, *Innate immune recognition.* Annu Rev Immunol, 2002. **20**: p. 197-216.
22. Greenberg, A.H., *The origins of the NK cell, or a Canadian in King Ivan's court.* Clin Invest Med, 1994. **17**(6): p. 626-31.
23. Kaufmann, K.B., et al., *A latent subset of human hematopoietic stem cells resists regenerative stress to preserve stemness.* Nat Immunol, 2021. **22**(6): p. 723-734.
24. Simon, A.K., G.A. Hollander, and A. McMichael, *Evolution of the immune system in humans from infancy to old age.* Proc Biol Sci, 2015. **282**(1821): p. 20143085.
25. Palis, J. and M.C. Yoder, *Yolk-sac hematopoiesis: the first blood cells of mouse and man.* Exp Hematol, 2001. **29**(8): p. 927-36.
26. Cumano, A. and I. Godin, *Ontogeny of the hematopoietic system.* Annu Rev Immunol, 2007. **25**: p. 745-85.
27. Neo, W.H., et al., *Contributions of Embryonic HSC-Independent Hematopoiesis to Organogenesis and the Adult Hematopoietic System.* Front Cell Dev Biol, 2021. **9**: p. 631699.
28. Walker, J.M. and M.K. Slifka, *Longevity of T-cell memory following acute viral infection.* Adv Exp Med Biol, 2010. **684**: p. 96-107.
29. Matamoros, S., et al., *Development of intestinal microbiota in infants and its impact on health.* Trends Microbiol, 2013. **21**(4): p. 167-73.
30. Müller, N., et al., *The immune system and schizophrenia. An integrative view.* Ann N Y Acad Sci, 2000. **917**: p. 456-67.
31. Janeway, C.A., Jr., *Presidential Address to The American Association of Immunologists. The road less traveled by: the role of innate immunity in the adaptive immune response.* J Immunol, 1998. **161**(2): p. 539-44.
32. Lacy, P. and J.L. Stow, *Cytokine release from innate immune cells: association with diverse membrane trafficking pathways.* Blood, 2011. **118**(1): p. 9-18.
33. Bonilla, F.A. and H.C. Oettgen, *Adaptive immunity.* J Allergy Clin Immunol, 2010. **125**(2 Suppl 2): p. S33-40.
34. Lowell, A., *immunology overview how-does our immune system protect us.* 2024.
35. Societ, A.C., *Cancer Stat Facts: Leukemia*. 2024, https://seer.cancer.gov/statfacts/html/leuks.html.
36. Juliusson, G. and R. Hough, *Leukemia.* Prog Tumor Res, 2016. **43**: p. 87-100.

37. Dong, Y., et al., *Leukemia incidence trends at the global, regional, and national level between 1990 and 2017.* Exp Hematol Oncol, 2020. **9**: p. 14.
38. Ci, T., et al., *Delivery strategies in treatments of leukemia.* Chem Soc Rev, 2022. **51**(6): p. 2121-2144.
39. Behrmann, L., J. Wellbrock, and W. Fiedler, *Acute Myeloid Leukemia and the Bone Marrow Niche-Take a Closer Look.* Front Oncol, 2018. **8**: p. 444.
40. Rosnet, O., et al., *Expression and signal transduction of the FLT3 tyrosine kinase receptor.* Acta Haematol, 1996. **95**(3-4): p. 218-23.
41. Chou, W.C., et al., *Distinct clinical and biological features of de novo acute myeloid leukemia with additional sex comb-like 1 (ASXL1) mutations.* Blood, 2010. **116**(20): p. 4086-94.
42. Abelson, S., et al., *Prediction of acute myeloid leukaemia risk in healthy individuals.* Nature, 2018. **559**(7714): p. 400-404.
43. Tartaglia, M., et al., *Somatic mutations in PTPN11 in juvenile myelomonocytic leukemia, myelodysplastic syndromes and acute myeloid leukemia.* Nat Genet, 2003. **34**(2): p. 148-50.
44. Lübbert, M., et al., *Prevalence of N-ras mutations in children with myelodysplastic syndromes and acute myeloid leukemia.* Oncogene, 1992. **7**(2): p. 263-8.
45. Bowen, D.T., et al., *RAS mutation in acute myeloid leukemia is associated with distinct cytogenetic subgroups but does not influence outcome in patients younger than 60 years.* Blood, 2005. **106**(6): p. 2113-9.
46. Metzeler, K.H. and C.D. Bloomfield, *Clinical Relevance of RUNX1 and CBFB Alterations in Acute Myeloid Leukemia and Other Hematological Disorders.* Adv Exp Med Biol, 2017. **962**: p. 175-199.
47. Su, L., et al., *Mutational spectrum of acute myeloid leukemia patients with double CEBPA mutations based on next-generation sequencing and its prognostic significance.* Oncotarget, 2018. **9**(38): p. 24970-24979.
48. Luesink, M., et al., *High GATA2 expression is a poor prognostic marker in pediatric acute myeloid leukemia.* Blood, 2012. **120**(10): p. 2064-75.
49. Shaikh, A.R.K., et al., *TET2 mutations in acute myeloid leukemia: a comprehensive study in patients of Sindh, Pakistan.* PeerJ, 2021. **9**: p. e10678.
50. Ley, T.J., et al., *DNMT3A mutations in acute myeloid leukemia.* N Engl J Med, 2010. **363**(25): p. 2424-33.
51. Finn, L., A. Dalovisio, and J. Foran, *Older Patients With Acute Myeloid Leukemia: Treatment Challenges and Future Directions.* Ochsner J, 2017. **17**(4): p. 398-404.
52. Sánchez-Corrales, Y.E., et al., *Taming Cell-to-Cell Heterogeneity in Acute Myeloid Leukaemia With Machine Learning.* Front Oncol, 2021. **11**: p. 666829.
53. Bouligny, I.M., K.R. Maher, and S. Grant, *Secondary-Type Mutations in Acute Myeloid Leukemia: Updates from ELN 2022.* Cancers (Basel), 2023. **15**(13).
54. Huber, S., et al., *AML classification in the year 2023: How to avoid a Babylonian confusion of languages.* Leukemia, 2023. **37**(7): p. 1413-1420.

55. Turkalj, S., F.A. Radtke, and P. Vyas, *An Overview of Targeted Therapies in Acute Myeloid Leukemia.* Hemasphere, 2023. **7**(6): p. e914.
56. Reitman, Z.J. and H. Yan, *Isocitrate dehydrogenase 1 and 2 mutations in cancer: alterations at a crossroads of cellular metabolism.* J Natl Cancer Inst, 2010. **102**(13): p. 932-41.
57. Chou, F.J., et al., *D-2-Hydroxyglutarate in Glioma Biology.* Cells, 2021. **10**(9).
58. Gilliland, D.G. and J.D. Griffin, *The roles of FLT3 in hematopoiesis and leukemia.* Blood, 2002. **100**(5): p. 1532-42.
59. Naqvi, K., M. Konopleva, and F. Ravandi, *Targeted therapies in Acute Myeloid Leukemia: a focus on FLT-3 inhibitors and ABT199.* Expert Rev Hematol, 2017. **10**(10): p. 863-874.
60. Ong, F., K. Kim, and M.Y. Konopleva, *Venetoclax resistance: mechanistic insights and future strategies.* Cancer Drug Resist, 2022. **5**(2): p. 380-400.
61. Wilde, L., S. Ramanathan, and M. Kasner, *B-cell lymphoma-2 inhibition and resistance in acute myeloid leukemia.* World J Clin Oncol, 2020. **11**(8): p. 528-540.
62. Hardwick, J.M. and L. Soane, *Multiple functions of BCL-2 family proteins.* Cold Spring Harb Perspect Biol, 2013. **5**(2).
63. Kordella, C., E. Lamprianidou, and I. Kotsianidis, *Mechanisms of Action of Hypomethylating Agents: Endogenous Retroelements at the Epicenter.* Front Oncol, 2021. **11**: p. 650473.
64. Blair, H.A., *Daunorubicin/Cytarabine Liposome: A Review in Acute Myeloid Leukaemia.* Drugs, 2018. **78**(18): p. 1903-1910.
65. Mayer, L.D., P. Tardi, and A.C. Louie, *CPX-351: a nanoscale liposomal co-formulation of daunorubicin and cytarabine with unique biodistribution and tumor cell uptake properties.* Int J Nanomedicine, 2019. **14**: p. 3819-3830.
66. Institute, N.C., *Acute Myeloid Leukemia Treatment (PDQ®)–Health Professional Version*. 2024: https://www.cancer.gov/types/leukemia/hp/adult-aml-treatment-pdq.
67. Koschade, S.E., et al., *Relapse surveillance of acute myeloid leukemia patients in first remission after consolidation chemotherapy: diagnostic value of regular bone marrow aspirations.* Ann Hematol, 2022. **101**(8): p. 1703-1710.
68. Yilmaz, M., et al., *Late relapse in acute myeloid leukemia (AML): clonal evolution or therapy-related leukemia?* Blood Cancer J, 2019. **9**(2): p. 7.
69. Hanahan, D. and R.A. Weinberg, *Hallmarks of cancer: the next generation.* Cell, 2011. **144**(5): p. 646-74.
70. Hanahan, D., *Hallmarks of Cancer: New Dimensions.* Cancer Discov, 2022. **12**(1): p. 31-46.
71. Bonnet, D. and J.E. Dick, *Human acute myeloid leukemia is organized as a hierarchy that originates from a primitive hematopoietic cell.* Nat Med, 1997. **3**(7): p. 730-7.
72. Stelmach, P. and A. Trumpp, *Leukemic stem cells and therapy resistance in acute myeloid leukemia.* Haematologica, 2023. **108**(2): p. 353-366.

73. Paczulla, A.M., et al., *Absence of NKG2D ligands defines leukaemia stem cells and mediates their immune evasion.* Nature, 2019. **572**(7768): p. 254-259.
74. Chopra, M. and S.K. Bohlander, *The cell of origin and the leukemia stem cell in acute myeloid leukemia.* Genes Chromosomes Cancer, 2019. **58**(12): p. 850-858.
75. Arnone, M., et al., *Acute Myeloid Leukemia Stem Cells: The Challenges of Phenotypic Heterogeneity.* Cancers (Basel), 2020. **12**(12).
76. Huntly, B.J. and D.G. Gilliland, *Leukaemia stem cells and the evolution of cancer-stem-cell research*, in *Nat Rev Cancer*. 2005: England. p. 311-21.
77. Raulet, D.H., *Roles of the NKG2D immunoreceptor and its ligands.* Nat Rev Immunol, 2003. **3**(10): p. 781-90.
78. Houchins, J.P., et al., *DNA sequence analysis of NKG2, a family of related cDNA clones encoding type II integral membrane proteins on human natural killer cells.* J Exp Med, 1991. **173**(4): p. 1017-20.
79. Stojanovic, A., M.P. Correia, and A. Cerwenka, *The NKG2D/NKG2DL Axis in the Crosstalk Between Lymphoid and Myeloid Cells in Health and Disease.* Front Immunol, 2018. **9**: p. 827.
80. Schwinn, N., et al., *Interferon-gamma down-regulates NKG2D ligand expression and impairs the NKG2D-mediated cytolysis of MHC class I-deficient melanoma by natural killer cells.* Int J Cancer, 2009. **124**(7): p. 1594-604.
81. Gasser, S., et al., *The DNA damage pathway regulates innate immune system ligands of the NKG2D receptor.* Nature, 2005. **436**(7054): p. 1186-90.
82. Cerboni, C., et al., *Antigen-activated human T lymphocytes express cell-surface NKG2D ligands via an ATM/ATR-dependent mechanism and become susceptible to autologous NK- cell lysis.* Blood, 2007. **110**(2): p. 606-15.
83. Tokuyama, M., et al., *Expression of the RAE-1 family of stimulatory NK-cell ligands requires activation of the PI3K pathway during viral infection and transformation.* PLoS Pathog, 2011. **7**(9): p. e1002265.
84. Ho, S.S. and S. Gasser, *NKG2D ligands link oncogenic RAS to innate immunity.* Oncoimmunology, 2013. **2**(1): p. e22244.
85. Zingoni, A., et al., *NKG2D and Its Ligands: "One for All, All for One".* Front Immunol, 2018. **9**: p. 476.
86. Samarakoon, A., H. Chu, and S. Malarkannan, *Murine NKG2D ligands: "double, double toil and trouble".* Mol Immunol, 2009. **46**(6): p. 1011-9.
87. Klussmeier, A., et al., *High-Throughput MICA/B Genotyping of Over Two Million Samples: Workflow and Allele Frequencies.* Front Immunol, 2020. **11**: p. 314.
88. Carapito, R. and S. Bahram, *Genetics, genomics, and evolutionary biology of NKG2D ligands.* Immunol Rev, 2015. **267**(1): p. 88-116.
89. Katsuyama, Y., et al., *Sequencing based typing for genetic polymorphisms in exons, 2, 3 and 4 of the MICA gene.* Tissue Antigens, 1999. **54**(2): p. 178-84.

90. Jung, H., et al., *RAE-1 ligands for the NKG2D receptor are regulated by E2F transcription factors, which control cell cycle entry.* J Exp Med, 2012. **209**(13): p. 2409-22.
91. Yang, D., et al., *NKG2D-CAR T cells eliminate senescent cells in aged mice and nonhuman primates.* Sci Transl Med, 2023. **15**(709): p. eadd1951.
92. Molinero, L.L., et al., *Activation-induced expression of MICA on T lymphocytes involves engagement of CD3 and CD28.* J Leukoc Biol, 2002. **71**(5): p. 791-7.
93. Colonna, M., et al., *A novel family of Ig-like receptors for HLA class I molecules that modulate function of lymphoid and myeloid cells.* J Leukoc Biol, 1999. **66**(3): p. 375-81.
94. Tan, G., K.M. Spillane, and J. Maher, *The Role and Regulation of the NKG2D/NKG2D Ligand System in Cancer.* Biology (Basel), 2023. **12**(8).
95. Schilling, D., et al., *NZ28-induced inhibition of HSF1, SP1 and NF-κB triggers the loss of the natural killer cell-activating ligands MICA/B on human tumor cells.* Cancer Immunol Immunother, 2015. **64**(5): p. 599-608.
96. Chalupny, N.J., et al., *Down-regulation of the NKG2D ligand MICA by the human cytomegalovirus glycoprotein UL142.* Biochem Biophys Res Commun, 2006. **346**(1): p. 175-81.
97. Bauman, Y. and O. Mandelboim, *MicroRNA based immunoevasion mechanism of human polyomaviruses.* RNA Biol, 2011. **8**(4): p. 591-4.
98. Andresen, L., et al., *2-deoxy D-glucose prevents cell surface expression of NKG2D ligands through inhibition of N-linked glycosylation.* J Immunol, 2012. **188**(4): p. 1847-55.
99. Nice, T.J., L. Coscoy, and D.H. Raulet, *Posttranslational regulation of the NKG2D ligand Mult1 in response to cell stress.* J Exp Med, 2009. **206**(2): p. 287-98.
100. Ray Chaudhuri, A. and A. Nussenzweig, *The multifaceted roles of PARP1 in DNA repair and chromatin remodelling.* Nat Rev Mol Cell Biol, 2017. **18**(10): p. 610-621.
101. Faraoni, I. and G. Graziani, *Role of BRCA Mutations in Cancer Treatment with Poly(ADP-ribose) Polymerase (PARP) Inhibitors.* Cancers (Basel), 2018. **10**(12).
102. Diefenbach, A., et al., *Selective associations with signaling proteins determine stimulatory versus costimulatory activity of NKG2D.* Nat Immunol, 2002. **3**(12): p. 1142-9.
103. Wensveen, F.M., V. Jelenčić, and B. Polić, *NKG2D: A Master Regulator of Immune Cell Responsiveness.* Front Immunol, 2018. **9**: p. 441.
104. Prager, I. and C. Watzl, *Mechanisms of natural killer cell-mediated cellular cytotoxicity.* J Leukoc Biol, 2019. **105**(6): p. 1319-1329.
105. Heibein, J.A., et al., *Granzyme B-mediated cytochrome c release is regulated by the Bcl-2 family members bid and Bax.* J Exp Med, 2000. **192**(10): p. 1391-402.

106. Pinkoski, M.J., et al., *Granzyme B-mediated apoptosis proceeds predominantly through a Bcl-2-inhibitable mitochondrial pathway.* J Biol Chem, 2001. **276**(15): p. 12060-7.
107. Trapani, J.A., *Granzymes: a family of lymphocyte granule serine proteases.* Genome Biol, 2001. **2**(12): p. Reviews3014.
108. Lieberman, J., *The ABCs of granule-mediated cytotoxicity: new weapons in the arsenal.* Nat Rev Immunol, 2003. **3**(5): p. 361-70.
109. Peter, M.E. and P.H. Krammer, *The CD95(APO-1/Fas) DISC and beyond.* Cell Death Differ, 2003. **10**(1): p. 26-35.
110. Wiley, S.R., et al., *Identification and characterization of a new member of the TNF family that induces apoptosis.* Immunity, 1995. **3**(6): p. 673-82.
111. Ramírez-Labrada, A., et al., *All About (NK Cell-Mediated) Death in Two Acts and an Unexpected Encore: Initiation, Execution and Activation of Adaptive Immunity.* Front Immunol, 2022. **13**: p. 896228.
112. Molfetta, R., et al., *Regulation of NKG2D-Dependent NK Cell Functions: The Yin and the Yang of Receptor Endocytosis.* Int J Mol Sci, 2017. **18**(8).
113. Hu, X.T., et al., *Histone deacetylase inhibitor apicidin increases expression of the α-secretase ADAM10 through transcription factor USF1-mediated mechanisms.* Faseb j, 2017. **31**(4): p. 1482-1493.
114. Fuertes, M.B., C.I. Domaica, and N.W. Zwirner, *Leveraging NKG2D Ligands in Immuno-Oncology.* Front Immunol, 2021. **12**: p. 713158.
115. Salih, H.R., H.G. Rammensee, and A. Steinle, *Cutting edge: down-regulation of MICA on human tumors by proteolytic shedding.* J Immunol, 2002. **169**(8): p. 4098-102.
116. Siemaszko, J., A. Marzec-Przyszlak, and K. Bogunia-Kubik, *NKG2D Natural Killer Cell Receptor-A Short Description and Potential Clinical Applications.* Cells, 2021. **10**(6).
117. Fernández-Messina, L., et al., *Differential mechanisms of shedding of the glycosylphosphatidylinositol (GPI)-anchored NKG2D ligands.* J Biol Chem, 2010. **285**(12): p. 8543-51.
118. Clayton, A., et al., *Human tumor-derived exosomes down-modulate NKG2D expression.* J Immunol, 2008. **180**(11): p. 7249-58.
119. Muntean, A.G. and J.L. Hess, *The pathogenesis of mixed-lineage leukemia.* Annu Rev Pathol, 2012. **7**: p. 283-301.
120. Tkachuk, D.C., S. Kohler, and M.L. Cleary, *Involvement of a homolog of Drosophila trithorax by 11q23 chromosomal translocations in acute leukemias.* Cell, 1992. **71**(4): p. 691-700.
121. Meyer, C., et al., *Human MLL/KMT2A gene exhibits a second breakpoint cluster region for recurrent MLL-USP2 fusions*, in *Leukemia*. 2019: England. p. 2306-2340.
122. Emerenciano, M., et al., *The distribution of MLL breakpoints correlates with outcome in infant acute leukaemia.* Br J Haematol, 2013. **161**(2): p. 224-36.
123. Winters, A.C. and K.M. Bernt, *MLL-Rearranged Leukemias-An Update on Science and Clinical Approaches.* Front Pediatr, 2017. **5**: p. 4.

124. Drynan, L.F., et al., *Mll fusions generated by Cre-loxP-mediated de novo translocations can induce lineage reassignment in tumorigenesis.* Embo j, 2005. **24**(17): p. 3136-46.
125. Meyer, C., et al., *The MLL recombinome of acute leukemias in 2013.* Leukemia, 2013. **27**(11): p. 2165-76.
126. Lin, C., et al., *AFF4, a component of the ELL/P-TEFb elongation complex and a shared subunit of MLL chimeras, can link transcription elongation to leukemia.* Mol Cell, 2010. **37**(3): p. 429-37.
127. Sun, X.F. and H. Zhang, *NFKB and NFKBI polymorphisms in relation to susceptibility of tumour and other diseases.* Histol Histopathol, 2007. **22**(12): p. 1387-98.
128. Li, Y., et al., *AF9 YEATS domain links histone acetylation to DOT1L-mediated H3K79 methylation.* Cell, 2014. **159**(3): p. 558-71.
129. Benedikt, A., et al., *The leukemogenic AF4-MLL fusion protein causes P-TEFb kinase activation and altered epigenetic signatures.* Leukemia, 2011. **25**(1): p. 135-44.
130. Mishra, B.P., et al., *The histone methyltransferase activity of MLL1 is dispensable for hematopoiesis and leukemogenesis.* Cell Rep, 2014. **7**(4): p. 1239-47.
131. Marschalek, R., *Systematic Classification of Mixed-Lineage Leukemia Fusion Partners Predicts Additional Cancer Pathways.* Ann Lab Med, 2016. **36**(2): p. 85-100.
132. Orlovsky, K., et al., *Down-regulation of homeobox genes MEIS1 and HOXA in MLL-rearranged acute leukemia impairs engraftment and reduces proliferation.* Proc Natl Acad Sci U S A, 2011. **108**(19): p. 7956-61.
133. Lavallée, V.P., et al., *The transcriptomic landscape and directed chemical interrogation of MLL-rearranged acute myeloid leukemias.* Nat Genet, 2015. **47**(9): p. 1030-7.
134. Lawrence, H.J., et al., *Loss of expression of the Hoxa-9 homeobox gene impairs the proliferation and repopulating ability of hematopoietic stem cells.* Blood, 2005. **106**(12): p. 3988-94.
135. Fitzel, R., et al., *Targeting MYC in combination with epigenetic regulators induces synergistic anti-leukemic effects in MLLr leukemia and simultaneously improves immunity.* Neoplasia, 2023. **41**: p. 100902.
136. Erkner, E., et al., *The RORɣ/SREBP2 pathway is a master regulator of cholesterol metabolism and serves as potential therapeutic target in t(4;11) leukemia.* Oncogene, 2023.
137. Secker, K.A., et al., *Inhibition of DOT1L and PRMT5 promote synergistic anti-tumor activity in a human MLL leukemia model induced by CRISPR/Cas9.* Oncogene, 2019. **38**(46): p. 7181-7195.
138. Albrecht, C., et al., *Comparison of Lentiviral Packaging Mixes and Producer Cell Lines for RNAi Applications.* Mol Biotechnol, 2015. **57**(6): p. 499-505.
139. Hamaguchi, H., et al., *Establishment of a novel human myeloid leukaemia cell line (HNT-34) with t(3;3)(q21;q26), t(9;22)(q34;q11) and the expression of EVI1 gene, P210 and P190 BCR/ABL chimaeric transcripts from a*

patient with AML after MDS with 3q21q26 syndrome. Br J Haematol, 1997. **98**(2): p. 399-407.
140. Asou, H., et al., *Establishment of a human acute myeloid leukemia cell line (Kasumi-1) with 8;21 chromosome translocation.* Blood, 1991. **77**(9): p. 2031-6.
141. Nakagawa, T., et al., *Loss of multiple point mutations of RAS genes associated with acquisition of chromosomal abnormalities during disease progression in myelodysplastic syndrome.* Br J Haematol, 1991. **77**(2): p. 250-2.
142. Hart, T., et al., *Evaluation and Design of Genome-Wide CRISPR/SpCas9 Knockout Screens.* G3 (Bethesda), 2017. **7**(8): p. 2719-2727.
143. DeepL, *DeepL write*. 2004: https://www.deepl.com/write/write-mobile.
144. Schindelin, J., et al., *Fiji: an open-source platform for biological-image analysis.* Nat Methods, 2012. **9**(7): p. 676-82.
145. Cytek, *Imagestream software*. 2024: https://cytekbio.com/pages/imagestream.
146. Jinek, M., et al., *A programmable dual-RNA-guided DNA endonuclease in adaptive bacterial immunity.* Science, 2012. **337**(6096): p. 816-21.
147. Tzelepis, K., et al., *A CRISPR Dropout Screen Identifies Genetic Vulnerabilities and Therapeutic Targets in Acute Myeloid Leukemia.* Cell Rep, 2016. **17**(4): p. 1193-1205.
148. Kamps-Hughes, N., et al., *Massively parallel characterization of restriction endonucleases.* Nucleic Acids Res, 2013. **41**(11): p. e119.
149. Bio, T., *Takara Bio submits Drug Master File to US FDA for RetroNectin GMP grade (liquid format)*. 2019: https://www.takarabio.com/about/announcements/takara-bio-submits-drug-master-file-to-us-fda-for-retronectin-gmp-grade.
150. Landerer, H., et al., *Two Flow Cytometric Approaches of NKG2D Ligand Surface Detection to Distinguish Stem Cells from Bulk Subpopulations in Acute Myeloid Leukemia.* J Vis Exp, 2021(168).
151. Wu, Z., et al., *Targeting the NKG2D/NKG2D-L axis in acute myeloid leukemia.* Biomed Pharmacother, 2021. **137**: p. 111299.
152. Andersen, M.N., et al., *Elimination of erroneous results in flow cytometry caused by antibody binding to Fc receptors on human monocytes and macrophages.* Cytometry A, 2016. **89**(11): p. 1001-1009.
153. Mende, N. and E. Laurenti, *Hematopoietic stem and progenitor cells outside the bone marrow: where, when, and why.* Exp Hematol, 2021. **104**: p. 9-16.
154. Nilsson, A.K., et al., *The proteome signature of cord blood plasma with high hematopoietic stem and progenitor cell count.* Stem Cell Res, 2022. **61**: p. 102752.
155. society, A.c., *Key Statistics for Acute Myeloid Leukemia (AML)*. 2024: https://www.cancer.org/cancer/types/acute-myeloid-leukemia/about/key-statistics.html.

156. Bazinet, A., et al., *Evolving trends and outcomes in older patients with acute myeloid leukemia including allogeneic stem cell transplantation.* Am J Hematol, 2023. **98**(9): p. 1383-1393.
157. Hernández-Malmierca, P., et al., *Antigen presentation safeguards the integrity of the hematopoietic stem cell pool.* Cell Stem Cell, 2022. **29**(5): p. 760-775.e10.
158. Ghadially, H., et al., *MHC class I chain-related protein A and B (MICA and MICB) are predominantly expressed intracellularly in tumour and normal tissue.* Br J Cancer, 2017. **116**(9): p. 1208-1217.
159. Gonzalez, H., C. Hagerling, and Z. Werb, *Roles of the immune system in cancer: from tumor initiation to metastatic progression.* Genes Dev, 2018. **32**(19-20): p. 1267-1284.
160. Venkataramani, V., et al., *Glioblastoma hijacks neuronal mechanisms for brain invasion.* Cell, 2022. **185**(16): p. 2899-2917.e31.
161. Hedlund, M., et al., *Thermal- and oxidative stress causes enhanced release of NKG2D ligand-bearing immunosuppressive exosomes in leukemia/lymphoma T and B cells.* PLoS One, 2011. **6**(2): p. e16899.
162. Fernández-Messina, L., H.T. Reyburn, and M. Valés-Gómez, *A short half-life of ULBP1 at the cell surface due to internalization and proteosomal degradation.* Immunol Cell Biol, 2016. **94**(5): p. 479-85.
163. Nachmani, D., et al., *Diverse herpesvirus microRNAs target the stress-induced immune ligand MICB to escape recognition by natural killer cells.* Cell Host Microbe, 2009. **5**(4): p. 376-85.
164. Jaiswal, S., et al., *Macrophages as mediators of tumor immunosurveillance.* Trends Immunol, 2010. **31**(6): p. 212-9.
165. Francisco, L.M., P.T. Sage, and A.H. Sharpe, *The PD-1 pathway in tolerance and autoimmunity.* Immunol Rev, 2010. **236**: p. 219-42.
166. Zheng, J., et al., *Ex vivo expanded hematopoietic stem cells overcome the MHC barrier in allogeneic transplantation.* Cell Stem Cell, 2011. **9**(2): p. 119-30.
167. Holdenrieder, S., et al., *Soluble MICA in malignant diseases.* Int J Cancer, 2006. **118**(3): p. 684-7.
168. Lee, Y.S., et al., *The combination of ionizing radiation and proteasomal inhibition by bortezomib enhances the expression of NKG2D ligands in multiple myeloma cells.* J Radiat Res, 2018. **59**(3): p. 245-252.
169. Tamaki, S., et al., *Association between soluble MICA levels and disease stage IV oral squamous cell carcinoma in Japanese patients.* Hum Immunol, 2008. **69**(2): p. 88-93.
170. Baragaño Raneros, A., B. Suarez-Álvarez, and C. López-Larrea, *Secretory pathways generating immunosuppressive NKG2D ligands: New targets for therapeutic intervention*, in *Oncoimmunology*. 2014: United States. p. e28497.
171. Winer, A., S. Adams, and P. Mignatti, *Matrix Metalloproteinase Inhibitors in Cancer Therapy: Turning Past Failures Into Future Successes.* Mol Cancer Ther, 2018. **17**(6): p. 1147-1155.

172. Willman, C.L. and M.H. Whittaker, *The molecular biology of acute myeloid leukemia. Proto-oncogene expression and function in normal and neoplastic myeloid cells.* Clin Lab Med, 1990. **10**(4): p. 769-96.
173. Goldman, S.L., et al., *Epigenetic Modifications in Acute Myeloid Leukemia: Prognosis, Treatment, and Heterogeneity.* Front Genet, 2019. **10**: p. 133.
174. Brandt, L., *Environmental factors and leukaemia.* Med Oncol Tumor Pharmacother, 1985. **2**(1): p. 7-10.
175. Fuertes, M.B., et al., *Intracellular retention of the NKG2D ligand MHC class I chain-related gene A in human melanomas confers immune privilege and prevents NK cell-mediated cytotoxicity.* J Immunol, 2008. **180**(7): p. 4606-14.
176. Pabst, C., et al., *Identification of small molecules that support human leukemia stem cell activity ex vivo.* Nat Methods, 2014. **11**(4): p. 436-42.
177. Secker, K.A., et al., *Only Hematopoietic Stem and Progenitor Cells from Cord Blood Are Susceptible to Malignant Transformation by MLL-AF4 Translocations.* Cancers (Basel), 2020. **12**(6).
178. *Adaptive Oncogenesis*. https://www.hup.harvard.edu/books/9780674545397.
179. Martinov, T., et al., *Building the Next Generation of Humanized Hemato-Lymphoid System Mice.* Front Immunol, 2021. **12**: p. 643852.
180. Zhu, T., et al., *Human PARP1 substrates and regulators of its catalytic activity: An updated overview.* Front Pharmacol, 2023. **14**: p. 1137151.
181. Kim, D.S., C.V. Camacho, and W.L. Kraus, *Alternate therapeutic pathways for PARP inhibitors and potential mechanisms of resistance.* Exp Mol Med, 2021. **53**(1): p. 42-51.
182. Pfeiffer, A., et al., *Poly(ADP-ribosyl)ation temporally confines SUMO-dependent ataxin-3 recruitment to control DNA double-strand break repair.* J Cell Sci, 2021. **134**(3).
183. Dias, M.P., et al., *Understanding and overcoming resistance to PARP inhibitors in cancer therapy.* Nat Rev Clin Oncol, 2021. **18**(12): p. 773-791.
184. Farmer, H., et al., *Targeting the DNA repair defect in BRCA mutant cells as a therapeutic strategy.* Nature, 2005. **434**(7035): p. 917-21.
185. Imagawa, S., et al., *A GATA-specific inhibitor (K-7174) rescues anemia induced by IL-1beta, TNF-alpha, or L-NMMA.* Faseb j, 2003. **17**(12): p. 1742-4.
186. Guan, Y., et al., *HBV suppresses expression of MICA/B on hepatoma cells through up-regulation of transcription factors GATA2 and GATA3 to escape from NK cell surveillance.* Oncotarget, 2016. **7**(35): p. 56107-56119.
187. Platanias, L.C., *Mechanisms of type-I- and type-II-interferon-mediated signalling.* Nat Rev Immunol, 2005. **5**(5): p. 375-86.
188. Castro, F., et al., *Interferon-Gamma at the Crossroads of Tumor Immune Surveillance or Evasion.* Front Immunol, 2018. **9**: p. 847.
189. Janeway, C., *Immunobiology 5 : the immune system in health and disease*. 5th ed. 2001, New York: Garland Pub. xviii, 732 p.
190. Duan, S., et al., *Natural killer group 2D receptor and its ligands in cancer immune escape.* Mol Cancer, 2019. **18**(1): p. 29.

191. Baldridge, M.T., et al., *Quiescent haematopoietic stem cells are activated by IFN-gamma in response to chronic infection.* Nature, 2010. **465**(7299): p. 793-7.
192. Arnone, M., *The Role of Mannose Receptor C-Type 2 (MRC2) in Leukemic Stem Cell Maintenance in AML*, Elsa Görsch , et al., Editors. 2022, *Blood* (2022) 140 (Supplement 1): 8706.: https://doi.org/10.1182/blood-2022-156799

https://ashpublications.org/blood/article/140/Supplement%201/8706/490748/The-Role-of-Mannose-Receptor-C-Type-2-MRC2-in.
193. Eisele, G., et al., *TGF-beta and metalloproteinases differentially suppress NKG2D ligand surface expression on malignant glioma cells.* Brain, 2006. **129**(Pt 9): p. 2416-25.
194. Zitti, B., et al., *Innate immune activating ligand SUMOylation affects tumor cell recognition by NK cells.* Sci Rep, 2017. **7**(1): p. 10445.
195. Stornaiuolo, M., et al., *KDEL and KKXX retrieval signals appended to the same reporter protein determine different trafficking between endoplasmic reticulum, intermediate compartment, and Golgi complex.* Mol Biol Cell, 2003. **14**(3): p. 889-902.
196. Baragaño Raneros, A., et al., *Methylation of NKG2D ligands contributes to immune system evasion in acute myeloid leukemia.* Genes Immun, 2015. **16**(1): p. 71-82.
197. Ye, Z., et al., *Fatty acid metabolism predicts prognosis and NK cell immunosurveillance of acute myeloid leukemia patients.* Front Oncol, 2022. **12**: p. 1018154.
198. Senís, E., et al., *AAVvector-mediated in vivo reprogramming into pluripotency.* Nat Commun, 2018. **9**(1): p. 2651.
199. Takahashi, K. and S. Yamanaka, *Induction of pluripotent stem cells from mouse embryonic and adult fibroblast cultures by defined factors.* Cell, 2006. **126**(4): p. 663-76.
200. Nanbakhsh, A., et al., *c-Myc regulates expression of NKG2D ligands ULBP1/2/3 in AML and modulates their susceptibility to NK-mediated lysis.* Blood, 2014. **123**(23): p. 3585-95.
201. Alkhayer, R., et al., *KLF4-mediated upregulation of the NKG2D ligand MICA in acute myeloid leukemia: a novel therapeutic target identified by enChIP.* Cell Commun Signal, 2023. **21**(1): p. 94.
202. Leung, W.H., et al., *Modulation of NKG2D ligand expression and metastasis in tumors by spironolactone via RXRγ activation.* J Exp Med, 2013. **210**(12): p. 2675-92.

Acknowledgements

I would like to thank everyone who supported me during my PhD. In particular, I would like to thank:

My supervisor Prof. Dr. Claudia Lengerke for giving me the opportunity to work on this project, funding it over the last 4 years and being part of my PhD committee.

Many thanks also to Prof. Dr. Markus Affolter and Prof. Dr. Klaus Schulze-Osthoff for being part of my PhD committee, for giving me valuable input and support during this time and of course for evaluating this work.

I would like to give a special thanks to my collaborators Rahel Fitzel and Estelle Erkner for their help and their willingness to listen whenever I needed it. Without their help, much of this project would not have been possible. I would also like to thank our collaborators and patients at the Women's Hospital in Tübingen for providing the cord blood samples that were essential for my experiments.

I would also like to thank all the members, namely Chris, Pauline, Alain, Melane, Sonika, Sarah, Janine, Sarah and Chiara, of the Lengerke group who came and went during my stay, as well as the people, Elsa, Marlon, Luca, Minh, Hilde, Taylor, Katharina and Lea, who are still part of the lab, for supporting me during this time. In particular, I would like to thank both Saskia and Anna for their expertise and support for my PhD project and Saskia for proofreading the entire thesis. Special thanks to Chiara, Elsa, Marlon Sonika, Melane and Luca for creating some nice moments and continuous support during this time.

Most importantly, I would like to thank my family and friends for their continuous support, which allowed me to keep my sanity during this time. I would especially like to thank Severina, Torsten, Sophie and Christin for their constant support and always having an open ear, allowing me to have some positive memories of the last 4 years.

Appendix

jove JOURNAL OF VISUALIZED EXPERIMENTS
1 Alewife Center #200
Cambridge, MA 02140
tel. 617.945.9051
www.jove.com

TITLE: (Instructions)

ABSENCE OF IMMUNE ACTIVATING NKG2D LIGANDS AS A TOOL TO IDENTIFY LEUKEMIC STEM CELLS

AUTHORS AND AFFILIATIONS: (Instructions)
Henrik Landerer[1], Marlon Arnone[1], Martina Konantz[1], Claudia Lengerke[1,2]

[1]University Hospital Basel and University of Basel, Department of Biomedicine, Basel Switzerland
[2]University Hospital Basel and University of Basel, Division for Hematology, Basel, Switzerland

KEYWORDS: (Instructions)
NKG2DL, CD34, AML, Chimera protein, mRNA, FACS

SUMMARY: (Instructions)
Here we show different methods of staining for NKG2DL with either a chimera protein, recognizing all known NKG2DL, or a combination of multiple antibodies and compare the mRNA levels of the NKG2DL to their surface presence.

ABSTRACT: (Instructions)
Absence of NKG2D ligand (NKG2DL) surface expression can distinguish, within the same patient sample, human leukemic cells with stem cell properties from more differentiated counterpart leukemic cells that lack disease initiation properties[1]. NKG2DL are biochemically diverse proteins of the MIC or ULBP families. They are induced on the surface of target cells to make them amenable for immune clearance by NKG2D receptor expressing immune cells such as natural killer (NK) cells. NKG2DL can be induced by cellular stress (e.g. oncogenic transformation) or in the course of infection to trigger the immunologic clearance of damaged cells. They are commonly not expressed on healthy cells in steady-state, as these should not suffer immune attack. Interestingly, among malignant cells, stem cells possess specific abilities to suppress NKG2DL expression which in fact allow them to selectively evade NKG2D mediated immune surveillance. Here we present side-by-side analyses and provide detailed protocols for two different investigation methods for NKG2DL surface expression in cancer cells: a method involving pan-ligand recognition and a method involving staining with antibodies against multiple single ligand stainings. These methods can be used to separate viable NKG2DL positive from NKG2DL negative cellular subpopulations with putative cancer stem cell properties.

INTRODUCTION: (Instructions)
Natural killer (NK) cells are a part of both the innate and the adaptive immune response, which respond to various diseases of the human body, such as virus infections or tumor formation[2].While NK cells do not necessarily require antibodies or the major histocompatibility complex (MHC) to detect and kill stressed or malignant cells[3], they employ immune receptors, such as NKG2D to detect target cells[4]. NKG2Ds are expressed on NK cells, but also on CD4- and CD8 T-cells and are activating immune receptors that recognize self-induced NKG2D ligand (NKG2DL) proteins[5].
There is a total of eight NKG2DL, which comprise the two MHC I Chain-related molecules A and

B (MICA and MICB)[6] and cytomegalovirus UL16-binding proteins 1-6 (ULBP1-6)[7]. The expression of NKG2DL is regulated on transcriptional, post-transcriptional as well as the post-translational levels[8]. Interestingly, although NKG2DL are usually not expressed on the surface of healthy cells to prevent an auto immune reaction NKG2DL mRNA[9] as well as intracellular protein expression has been reported in healthy tissues. On the cell surface instead, NKG2DL are only rarely observed in healthy cells, and the functional relevance of such expression, in the absence of pathogenic events, remains to be defined[10].

The mechanistic regulation of NKG2DL expression in cancer cells is a fascinating area of investigation. Pathways known to be involved in either cellular stress e.g. the heat shock stress pathway[8], or DNA damage associated pathways, such as the ataxia telangiectasia mutated (ATM) and ATM and Rad3 related (ATR) pathway[11], as well as viral or bacterial infections have been directly linked to the induction of NKG2DL expression[12]. However, even if surface expression of NKG2DL has been effectively induced, this expression can be again lost by proteolytic-mediated shedding, a mechanism for example demonstrated to mediate immune escape in some cancer cells[13]. Consistently, shedding in tumor cells has been associated with poor disease prognosis[14].

The absence of cell surface NKG2DL also plays a vital role in acute myeloid leukemia (AML). In AML, patients often achieve remission through intensive chemotherapy, but relapse from surviving chemotherapy-resistant leukemic stem cells (LSC) routinely occurs. As we recently showed, LSC also evade the immune response of NK cells through the absence of NKG2DL on their cell surface, facilitating the reinitiating of leukemia. Inhibition of poly-ADP-ribose polymerase 1 (PARP) can partly induce NKG2DL surface expression in LSC in some AML, thereby making these leukemia-initiating cells amenable to the detection and lysis by NK cells[1].

As the presence of NKG2DL on the cell surface plays an important role in AML LSC identification and biology, we here analyze different methods for NKG2DL expression analysis, among, which a method for pan-ligand surface recognition and staining with individual single (or pooled) antibodies recognizing specific NKG2DL.

PROTOCOL: (Instructions)

1. Staining of the fusion protein

1.1. Biotinylation of the NKG2D chimera protein

Note: This step of the protocol has to be performed at least 24 hours prior to the staining. The biotinylated NKG2D chimera protein can be stored at -20 °C for future usage.

1.1.1. Slowly thaw both the biotin, as well as the NKG2DL fusion protein tubes to room temperature

1.1.2. Transfer both tubes to the laminar flow hood and use 70-80 % ethanol to sterilize the tubes

1.1.3. Add 100 µL of the NKG2DL fusion protein to the biotin tube to obtain a final concentration of 10 µg/mL

1.1.4. Mix the solution thoroughly by continuous resuspending with a micropipette

1.1.5. Incubate the antibody/biotin solution at a controlled room temperature for 24 h

1.2. Thawing of primary AML cells

1.2.1. Transfer 45 mL of RPMI medium containing 10 % FCS to a 50 mL falcon and pre heat the medium to 37 °C using a water bath

1.2.2. Thaw the vial of the primary AML cells using a 37 °C water bath until 80 % of the cells remain frozen

1.2.3. Transfer frozen cells into the falcon containing the medium, rinse the vial once using medium and incubate the cells 2 hours at room temperature without moving the cells
Note: To save time, cells can also be transferred into 9 mL of medium, the vial rinsed once with medium and directly centrifuged

1.2.4. Centrifuge the cells at 300 x g for 10 minutes and discard the supernatant

1.2.5. Wash the cells once with 5 mL RPMI medium containing +10% FCS and determine the cell number.

1.2.6. Centrifuge the cells at 300 x g for 10 minutes and discard the supernatant

1.3. Staining of primary AML cells using the biotinylated NKG2DL chimera protein

1.3.1. Add MACS-Blocking Buffer to the cell pellet to a final concentration of 0.5 x 10^7 cells/ mL and resuspend with a micropipette
Note: Depending on the sample this step is not mandatory, but reduced unspecific binding.

1.3.2. Incubate the cells for 30 minutes at room temperature

1.3.3. Centrifuge the cell suspension at 300 x g for 10 minutes and discard the supernatant avoiding the pellet

1.3.4. Add PBS to cell pellet to a final concentration of 0.5 x 10^7 cells/ mL and resuspend with a micropipette

1.3.5. Add 1:10 of the total volume NKG2DL biotinylated fusion protein (resulting in a total concentration of 10 µg/ mL) to the cell suspension and resuspend until fully mixed with a micropipette

1.3.6. Centrifuge the cell suspension at 300 x g for 10 minutes and discard the supernatant avoiding the pellet

1.3.7. Wash twice with 200 µL MACS buffer at 4 °C

1.3.8. Add PBS to cell pellet to a final concentration of 0.5 x 10^7 cells/ mL and resuspend with a micropipette

1.3.9. Dilute the secondary antibody streptavidin-PE 1:100 in MACS buffer and add 100 µL of the solution to the cell suspension and mix thoroughly by resuspending with a micropipette

1.3.10. Incubate the cell-antibody suspension for 15 minutes at room temperature or 30 minutes at 4°C in the absence of light

1.3.11. Wash twice with 200 µL MACS buffer at 4 °C

1.3.12. Resuspend the cells in FACS buffer containing 7-AAD (1:1000) (or any other marker for live cell/dead cell discrimination) and incubate for 10 minutes at room temperature in the absence of light

1.3.13. Analyze or sort the cells using flow cytometry

2. Staining of single NKG2DL-Antibodies

2.1. Harvest cells and centrifuge at 300 x g for 10 minutes and discard the supernatant avoiding the pellet

2.2. Add FACS-Blocking Buffer at 4 °C containing 1 µg/ mL human IgG-Blocking Buffer to the cell pellet for a final concentration of 0.5 x10^7 cells/ml and block the cells for 30 minutes at room temperature

2.3. Transfer 100 µL of the cell suspension to a 96 well plate and centrifuge the plate at 450 x g for 2 minutes and discard the supernatant

2.4. Add 50 µL FACS buffer containing 10 µg/ mL of each specific antibody, or all antibodies and incubate for 25 minutes at room temperature. Use fluorescence minus one (FMO) controls for proper controls[15]

2.5. Centrifuge the cell suspension at 300 x g for 10 minutes and discard the supernatant avoiding the pellet

2.6. Wash twice with 200 µL FACS buffer at 4 °C

2.7. Add 50 µL FACS buffer containing 4 µg/ mL of the correlating secondary antibody and incubate for 15 minutes at room temperature or 30 minutes at 4 °C in the absence of light

2.8. Centrifuge the cell suspension at 300 x g for 10 minutes and discard the supernatant avoiding the pellet

2.9. Wash twice with 200 µL FACS buffer at 4 °C

2.10. Resuspend the cells in 100 µL FACS buffer containing 7-AAD (1:1000) (or any other marker for live cell/death cell discrimination) to the cell suspension and incubate for 10 minutes

2.11. Analyze or sort the cells using flow cytometry

REPRESENTATIVE RESULTS: (Instructions)

Leukemic stem cells can be isolated based on their cell surface markers using the currently available cell-sorting technologies. Once isolated, these cells can be analyzed as any other type of cancer cell to understand specific mutations and pathways. Previous studies showed that LSCs can be identified by using a multitude of markers such as TIM3, CD44, CD123, CD33, and many others[16]. Here, we analyzed an AML patient sample using FACS technology based on NKG2DL surface expression using either pan-ligand recognition as well as multiple single ligand staining Samples were first gated on their relative size and complexity using forward and side scatter gating followed by gating for singularity based on the side scatter area to side scatter height and cell viability employing 7AAD as a marker to exclude dead cells in our analysis (Figure 1A). NKG2DL surface expression was first analyzed on bulk AML based on the fluorochrome signal for NKG2DL-Fc (PE) or the single or pooled ligands (Alexa Fluor 488) (Figure 1B).
We also used combined gating based on the stem cell marker CD34 (APC) and NKG2DL to further refine AML LSCs (Figure 1C). To confirm the success of the staining we used unstained cells as a control for analysis (Figure 1D).

Cells stained with the NKG2DL-Fc chimera protein did not show a signal for the single ligands (Figure 2A and 2B) and vice versa (Figure 2C and 2D), indicating that there is minimal leakage into each other's channel. The value of positive events for single ligands ranges from 1 to 19%, but does not exceed the percentage of positive cells for cells stained with the pooled antibodies. Cells stained with all pooled antibodies can be positive for one or more NKG2DL. Therefore, cells stained with single antibodies can be positive for the same number of cells as cells stained with all antibodies, but cannot exceed it. Importantly, the percentage of NKG2DL-positive cells is approximately the same using both the Fc chimera ore the combined single ligands (Figure 2A and C).

Overall, both methods worked well and provided similar results, indicating, that both methods are equally sufficient for the analysis of NKG2DL surface presence.

Next, we stained AML cells for both the known stem cell marker CD34[17] and NKG2DL either using the NKG2DL-Fc (PE) or single ligands (Alexa Fluor 488). AML cells positive for CD34+ generally showed a lower surface expression of NKG2DL. This data was consistent for both methods. Interestingly, we were able to identify CD34+NKG2DL- as well as CD34+NKG2DL+ and CD34-NKG2DL- cells. Further analyses are needed to investigate which of these populations contain the real LSCs.

FIGURE AND TABLE LEGENDS: (Instructions)

Figure 1: (A) Cells were gated based on their morphology (y-axis: SSC-A, x-axis: FSC-A), on their singularity (y-axis SSC-H, x-axis: SSC-A) and on their viability (7AAD). (B) Samples not stained with CD34 were gated for NKG2DL-Fc (PE) or (combined) single ligands (Alexa Fluor 488). (C) Cells also were analyzed for both NKG2DL and CD34 simultaneously. (D) Histogram of cells positive for either NKG2DL-Fc (left) or single ligands (right) compared to the signal of unstained cells

Figure 2: Flow cytometric analyses of cells stained with either NKG2DL-Fc or single ligands. (A) AML cells stained and gated for NKG2DL-Fc (PE). (B) FACS-Blot gated for NKG2DL-Fc (PE) or (combined) single ligands (Alexa Fluor 488) (y-axis: FITC-A, x-axis: PE-A), (C) AML cells stained and gated for single ligands (Alexa Fluor 488)(D) FACS-Blot gated for NKG2DL-Fc (PE) or (combined) single ligands (Alexa Fluor 488) (y-axis: FITC-A, x-axis: PE-A

Figure 3: NKG2DL presence on CD34 positive or negative AML cells
(A) AML cells gated on CD34 (APC). (B) AML cells gated first on CD34 and then on NKG2DL-Fc (PE). (C) AML cells gated first on CD34 and then on single ligands

DISCUSSION: (Instructions)

The method we presented here focuses on the staining of NKG2DL on human primary AML cells. These cells are fragile and have to be treated with caution. The thawing of cells requires the user to precisely carry out the protocol described in this manuscript to ensure a sufficient viability of the cells.

We analyzed one primary patient sample from a patient suffering from AML which is a highly heterogenous disease. Results can therefore be vastly different depending on the genotype of the patient. For the protocol presented here, we analyzed a limited number of surface markers, which can be extended according to the user's needs, such as for example CD33 or other potential leukemic stem cell markers[16].

With this protocol, we demonstrate the effectiveness of the NKG2DL-Fc chimera protein, which detects all known NKG2DL as well as potentially unknown NKG2DL and compare it to the effectiveness of a staining with pooled antibodies detecting specific NKG2DL. Both methods appear effective and feasible and the NKG2DL-Fc chimera protein detects NKG2DL with the same efficacy as the pooled antibodies, while being easier and faster to handle, thus reducing the

probability of human error, as well as reducing the number of required reagents.

While providing insight into the surface presence of NKG2DL, this method does not provide information on the intracellular levels of NKG2DL, their trafficking, or regulation.

ACKNOWLEDGMENTS: (Instructions)
This study was supported by grants from the Swiss National Science Foundation (179239), the Foundation for Fight Against Cancer (Zürich) and the Novartis Foundation for medical-biological research to C.L. We thank Elsa Görsch for experimental assistance and the Flow Cytometry Facility in Basel for support.

DISCLOSURES: (Instructions)
The authors have nothing to disclose.

REFERENCES: (Instructions)

1 Paczulla, A. M. *et al.* Absence of NKG2D ligands defines leukaemia stem cells and mediates their immune evasion. *Nature.* **572** (7768), 254-259, doi:10.1038/s41586-019-1410-1, (2019).
2 Vivier, E. *et al.* Innate or adaptive immunity? The example of natural killer cells. *Science.* **331** (6013), 44-49, doi:10.1126/science.1198687, (2011).
3 López-Soto, A., Gonzalez, S., Smyth, M. J. & Galluzzi, L. Control of Metastasis by NK Cells. *Cancer Cell.* **32** (2), 135-154, doi:10.1016/j.ccell.2017.06.009, (2017).
4 Long, E. O., Kim, H. S., Liu, D., Peterson, M. E. & Rajagopalan, S. Controlling natural killer cell responses: integration of signals for activation and inhibition. *Annu Rev Immunol.* **31** 227-258, doi:10.1146/annurev-immunol-020711-075005, (2013).
5 Raulet, D. H. Roles of the NKG2D immunoreceptor and its ligands. *Nat Rev Immunol.* **3** (10), 781-790, doi:10.1038/nri1199, (2003).
6 Eagle, R. A. & Trowsdale, J. Promiscuity and the single receptor: NKG2D. *Nat Rev Immunol.* **7** (9), 737-744, doi:10.1038/nri2144, (2007).
7 El-Gazzar, A., Groh, V. & Spies, T. Immunobiology and conflicting roles of the human NKG2D lymphocyte receptor and its ligands in cancer. *J Immunol.* **191** (4), 1509-1515, doi:10.4049/jimmunol.1301071, (2013).
8 Venkataraman, G. M., Suciu, D., Groh, V., Boss, J. M. & Spies, T. Promoter region architecture and transcriptional regulation of the genes for the MHC class I-related chain A and B ligands of NKG2D. *J Immunol.* **178** (2), 961-969, doi:10.4049/jimmunol.178.2.961, (2007).
9 Long, E. O. Negative signaling by inhibitory receptors: the NK cell paradigm. *Immunol Rev.* **224** 70-84, doi:10.1111/j.1600-065X.2008.00660.x, (2008).
10 Hüe, S. *et al.* A direct role for NKG2D/MICA interaction in villous atrophy during celiac disease. *Immunity.* **21** (3), 367-377, doi:10.1016/j.immuni.2004.06.018, (2004).
11 Gasser, S. & Raulet, D. H. Activation and self-tolerance of natural killer cells. *Immunol Rev.* **214** 130-142, doi:10.1111/j.1600-065X.2006.00460.x, (2006).

12 Groh, V. *et al.* Cell stress-regulated human major histocompatibility complex class I gene expressed in gastrointestinal epithelium. *Proc Natl Acad Sci U S A.* **93** (22), 12445-12450, doi:10.1073/pnas.93.22.12445, (1996).
13 Maurer, S. *et al.* Platelet-mediated shedding of NKG2D ligands impairs NK cell immune-surveillance of tumor cells. *Oncoimmunology.* **7** (2), e1364827, doi:10.1080/2162402x.2017.1364827, (2018).
14 Li, K. *et al.* Clinical significance of the NKG2D ligands, MICA/B and ULBP2 in ovarian cancer: high expression of ULBP2 is an indicator of poor prognosis. *Cancer Immunol Immunother.* **58** (5), 641-652, doi:10.1007/s00262-008-0585-3, (2009).
15 Tung, J. W. *et al.* Modern flow cytometry: a practical approach. *Clin Lab Med.* **27** (3), 453-468, v, doi:10.1016/j.cll.2007.05.001, (2007).
16 Zhou, J. & Chng, W. J. Identification and targeting leukemia stem cells: The path to the cure for acute myeloid leukemia. *World J Stem Cells.* **6** (4), 473-484, doi:10.4252/wjsc.v6.i4.473, (2014).
17 Bonnet, D. & Dick, J. E. Human acute myeloid leukemia is organized as a hierarchy that originates from a primitive hematopoietic cell. *Nat Med.* **3** (7), 730-737, doi:10.1038/nm0797-730, (1997).